

AIMS AND SCOPE

The Defence S&T Technical Bulletin (*Buletin Teknikal S&T Pertahanan*) is the official technical bulletin of the Science & Technology Research Institute for Defence (STRIDE). It contains articles on research findings in various fields of defence science & technology. The primary purpose of this bulletin is to act as a channel for the publication of defence-based research work undertaken by researchers both within and outside the country.

WRITING FOR THE DEFENCE S&T TECHNICAL BULLETIN

Contributions to the journal should be based on original research in areas related to defence science & technology. All contributions should be in British English or Bahasa Melayu.

PUBLICATION

The editors' decision with regard to publication of any item is final. A paper is accepted on the understanding that it is an original piece of work which has not been accepted for publication elsewhere. Contributors will receive one complimentary copy of the issue in which their work appears.

PRESENTATIONS OF MANUSCRIPTS

The format of the manuscript is as below:

- a) Page size B5 (JIS).
- b) MS Word format.
- c) Single space.
- d) Justified.
- e) In Times New Roman 11-point font.
- f) Should not exceed 15 pages, including references.
- g) Margin should be 2 1/2 cm or 1 inch an all sides.
- h) Texts in charts and tables should be in 10-point font.

Please e-mail the manuscript to :

- 1) Dr. Zalini bt Yunus (zalini.yunus@stride.gov.my)
- 2) Dinesh Sathyamoorthy (dinesh.sathyamoorthy@stride.gov.my)

The next edition of the bulletin is expected to be published in April 2011. The due date for submissions is 9th March 2011. **It is strongly iterated that authors are solely responsible for taking the necessary steps to ensure that the submitted manuscripts do not contain confidential or sensitive material.**

The template of the manuscript is as follows:

TITLE OF MANUSCRIPT

Name(s) of author(s)

Affiliation(s)

E-mail:

ABSTRACT

Contents of abstract.

Keywords: *Keyword 1; keyword 2; keyword 3.*

1 TOPIC

Paragraph 1.

Paragraph 2.

1.1 Sub Topic 1

Paragraph 1.

Paragraph 2.

2 TOPIC 2

Paragraph 1.

Paragraph 2.



Figure 1: Title of figure.

Table 1: Title of table.

Content	Content	Content
Content	Content	Content
Content	Content	Content
Content	Content	Content

$$\begin{array}{ll} \text{Equation 1} & (1) \\ \text{Equation 2} & (2) \end{array}$$

REFERENCES

Long lists of notes of bibliographical references are generally not required. The method of citing references in the text is ‘name date’ style, e.g. ‘Hanis (1993) claimed that...’, or ‘...including the lack of interoperability (Bohara *et al.*, 2003)’. End references should be in alphabetical order. The following reference style is to be adhered to:

Books

Serra, J. (1982). *Image Analysis and Mathematical Morphology*. Academic Press, London.

Book Chapters

Goodchild, M.F. & Quattrochi, D.A. (1997). Scale, multiscaling, remote sensing and GIS. In Quattrochi, D.A. and Goodchild, M.F. (Eds.), *Scale in Remote Sensing and GIS*. Lewis Publishers, Boca Raton, Florida, pp. 1-11.

Journals/ Serials

Jang, B.K. & Chin, R.T. (1990). Analysis of thinning algorithms using mathematical morphology. *IEEE T. Pattern Anal.*, **12**: 541-550.

Online Sources

GTOPO30 (1996). *GTOPO30: Global 30 Arc Second Elevation Data Set*. Available online at: <http://edcwww.cr.usgs.gov/landdaac/gtopo30/gtopo30.html> (Last access date: 1st June 2009)

Unpublished Materials (e.g. theses, reports and documents)

Wood, J. (1996). *The Geomorphological Characterization of Digital Elevation Models*. PhD Thesis, Department of Geography, University of Leicester, Leicester.

FAILURE ANALYSIS OF BOLTS ON AN END PLATE OF A PROPELLER HUB

Mahdi Che Isa^{1*}, Mohd Subhi Din Yati¹, Mohd Moesli Muhammad¹,
Syed Rosli Sayd Bakar² & Irwan Mohd Noor¹

¹Maritime Technology Division (BTM), Science & Technology Research Institute for Defence (STRIDE), Ministry of Defence, Malaysia

²Mechanical & Aerospace Technology Division (BTJA), Science & Technology Research Institute for Defence (STRIDE), Ministry of Defence, Malaysia

*Email: mahdicheisa@gmail.com

ABSTRACT

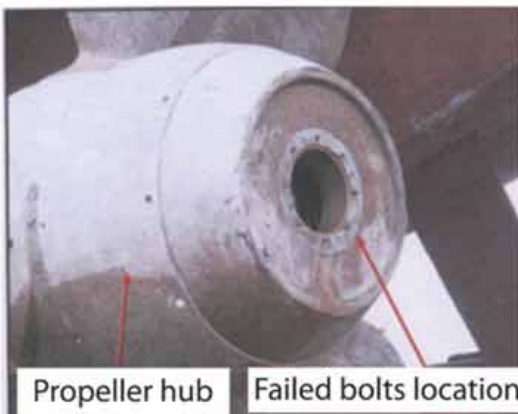
This paper provides a case study on the failure of bolts on an end plate of a ship's propeller hub. The possible causes of the fracture, which occurred at the threaded zone of the bolts, were assessed. The fracture surface was examined using both an optical stereomicroscope and a scanning electron microscope in order to determine the failure initiation and mode. It was discovered that the fracture initiated at the thread zone and propagated towards the inner parts of the bolt before being completely broken due to overloading. Microscopic observation also showed that the microstructure of the bolt contains internal defects or discontinuities. These bolts were also found to be unsuitable for its specific application based on strength and type of materials used.

Keywords: failure analysis; scanning electron microscope (SEM); microstructure; ductile; bolt.

1. INTRODUCTION

Threaded bolts are widely used in engineering and utilised throughout industries to hold two or more mechanical parts together. The failure of threaded bolts can lead to catastrophic failure of structures. In the case of this study (Figure 1), it was reported that a number of bolts had failed when the ship propeller was in 0 % pitch while preparing for sea trials. The particular bolts were sent to the Ships Technology Branch, Science & Technology Research Institute for Defence (STRIDE), for failure investigation. Figure 2 shows the as-received condition of the bolts; none of the bolts had nuts attached and the bolts were completely broken. A total of seven bolts had been removed from the end plate propeller hub of the ship and all the nuts from the bolts were lost. The samples were then labelled as S1 to S7. Samples S1 to S6 showed clear observations of being broken bolts. Each of these bolts had been found broken into two separate pieces. Bolt S7 showed a major deformation on the alignment as well as irregular shape of worn or damaged thread. The goals of this failure investigation were to get an understanding of how and

when failure initiated in the bolts, and to determine whether the mechanical properties of the material were insufficient for the intended operation of the bolts.



Propeller hub Failed bolts location



Figure 1: Ship propeller without cone. Figure 2: The as-received failed bolts.

2. INVESTIGATION

According to the design specification, the system of the propeller hub and end plate fittings should be safe under normal operation conditions. However, the failure still occurred, indicating that there were some important factors that were not considered during the maintenance works. The following investigations were aimed at identifying the cause of the failure from different considerations (ASM, 1986, 1992, 1993). The failed bolts were inspected visually, and then, micro- and macroscopically using a light microscope (Zeiss Axioplan) complete with special software. Throughout the process, care was taken to avoid damage to the fractured surfaces. The fractured surfaces were ultrasonically cleaned and examined using a scanning electron microscope (SEM) equipped with energy dispersive x-ray (EDX) capability for semi-quantitative analysis. The fracture surface morphologies of the failed bolts were then observed under a SEM (Leo VP 1480). A confocal laser scanning microscope (CLSM) (LSM 5 Pascal) was used for surface topographic study. The hardness of each bolt was measured using a Rockwell hardness tester (Affri DRMC 250) at ten different locations.

3. RESULTS & DISCUSSION

3.1 Macroscopic Examination

Figures 2-4 show fracture surfaces of the broken bolts with signs of major damages and spiral fracture surfaces. The fracture surface on each bolt clearly shows signs of fibrous surfaces, radial marks or patterns, as well as a very clear rupture zone. Visual examination clearly shows that the fracture surfaces of samples S1 to S6 exhibit cup-cone features together with the presence of radial marks as shown by the arrows. For each bolt, the radial marks pattern propagates towards the initiation

point of the failure. The fracture surface of each failed bolt exhibits a clear crack initiation site, spiral fracture surfaces, and the final fracture region. The surface area of the final fracture was calculated, with approximately not less than 60% of the total fine fracture surface, suggesting that the bolt was overloaded (Chen *et al.*, 2006; Osman, 2006).

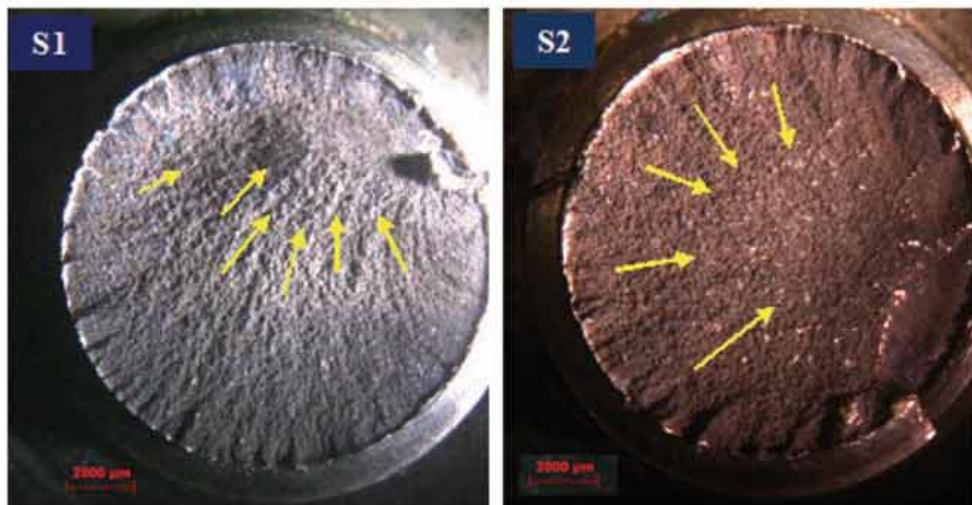


Figure 2: Macrographs of fracture surfaces for samples S1 and S2 indicate the presence of radial marks.

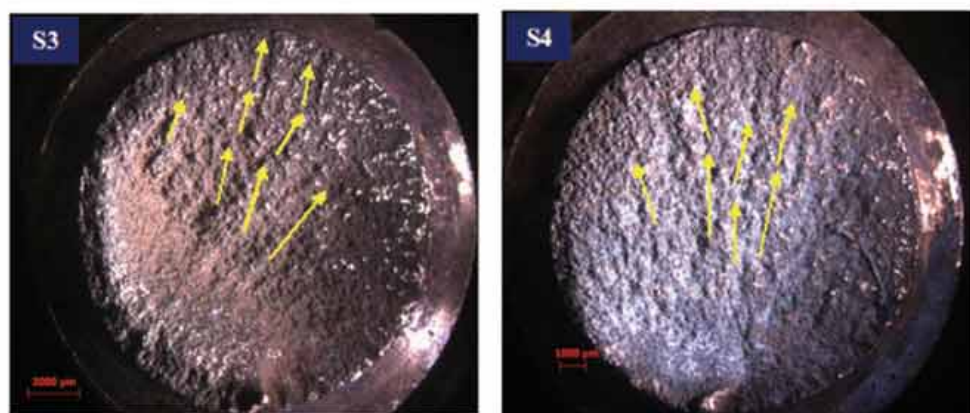


Figure 3: Macrographs of fracture surfaces for samples S3 and S4 with fibrous surfaces.

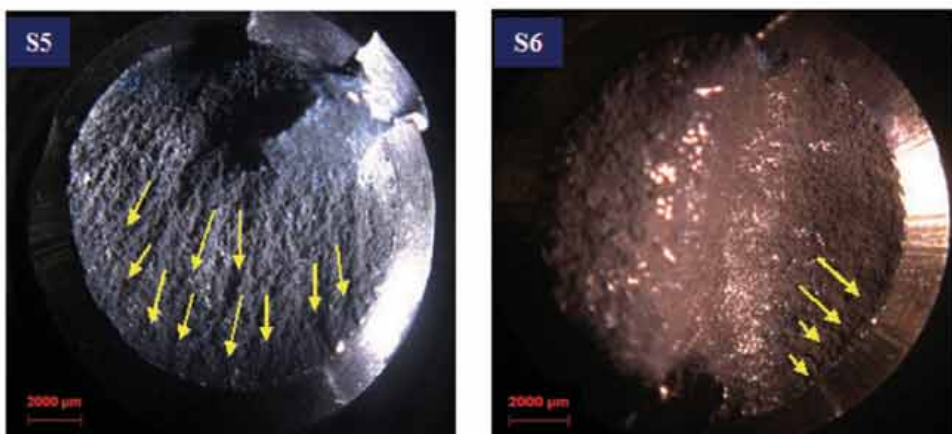


Figure 4: Combination of fibrous surfaces and radial marks on samples S5 and S6.

The fracture surfaces of samples were further examined using a stereo microscope. The bolts' fracture surfaces reveal the same radial failure pattern, with an example being shown in Figure 5. It was strongly believed that extremely high stress concentrations had contributed to the crack initiation, which originated in the vicinity of the thread root as shown in Figure 6. From the macrograph, it can be observed that cracks have initiated from more than one point. The presence of radial patterns or marks, and cup-cone features on sample S2, which can be clearly seen on the fracture surfaces in Figures 5 and 6, was a strong indicator that a ductile failure had occurred (ASM, 1993; Chen *et al.*, 2006; Krishnaraj, 2003).

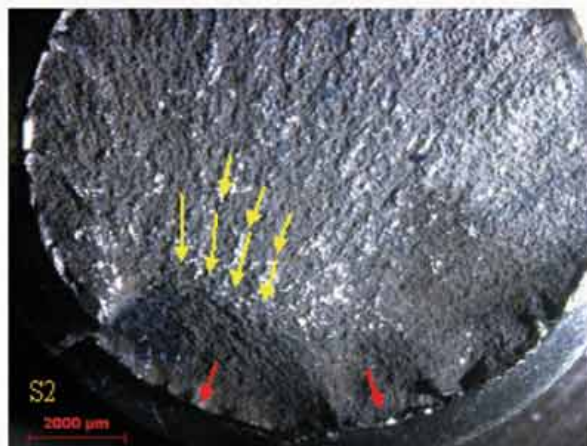


Figure 5: Stereo macrograph showing the radial pattern (yellow arrows) on the fracture surface of sample S2.

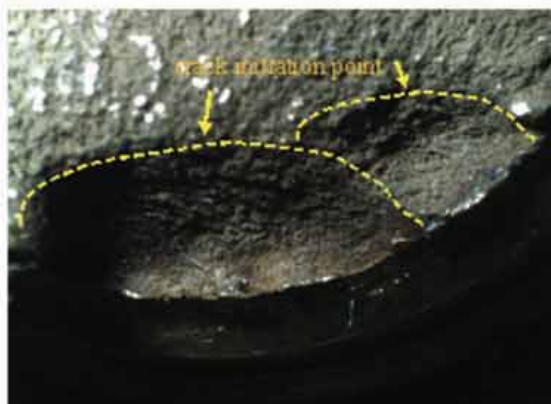


Figure 6: Fracture surface showing the crack initiation region on sample S2.

3.2 Microscopic Examinations

The microstructure of the failed bolt is shown in Figure 7. The orientation of the grains was found to be in one direction as indicated by the arrows in Figures 7(a) and 7(b). This phenomenon can be attributed to the fabrication process of alloy in order to produce a bolt. The part of the alloy that has been cut-off or machined can give an adverse effect to the strength of the bolt. Based on the grain orientation in the micrographs in Figure 7, we strongly believe that the failed bolt was produced by the thread cutting process. The thread cutting resulted in a non-uniform thread profile with undulations and sharp thread root radii. Such imperfections nucleate wear and can serve as starting points for failure to occur. Figure 8 clearly shows non-uniformities and discontinuities in the size and shape of grains as well as bulk properties in the failed bolt. At the microscopic level, any discontinuities can contribute to mechanical stress risers and, at the same time, act as the most vulnerable point for failure to occur (Gao & Cheng, 2008).

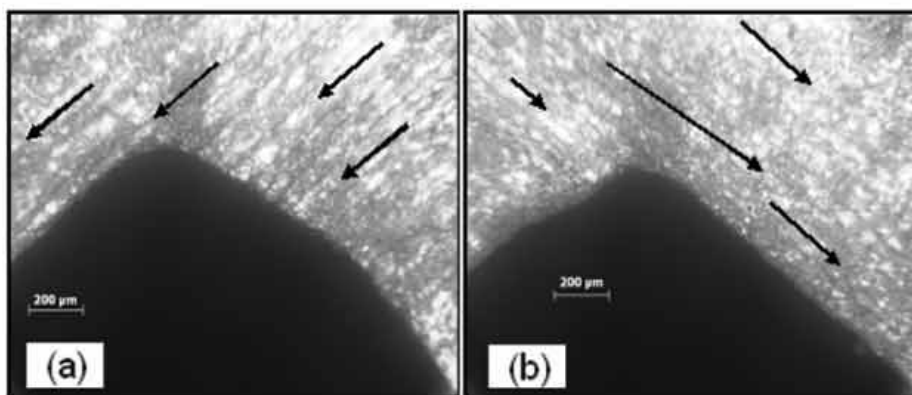


Figure 7: Bolt microstructure of near thread area.

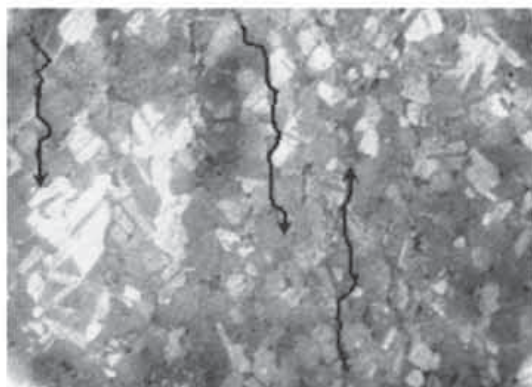


Figure 8: Microstructure with internal discontinuities (200 x).

The etched samples were subsequently further studied using a CLSM. It is important to quantitatively describe the changes in the surface structure in three-dimensional (3D) topography and to digitize the image for further computer analysis (Gjønnes, 1996; Liu *et al.*, 2006; Udupa *et al.*, 2000). Figure 9 clearly reveals the presence of internal microstructural defects inside the grain structure of the bolt based on 2D images from the CLSM. The line scan images across the bolt surface in Figure 10 shows 3D and “cross-sectional” views of the grooves and peaks on the surface. From the line scan, topographic parameters, such as mean surface depth and length of the grooves in the alloy, were measured. The mean depth of the surface grooves in the alloy was approximately 6 μm , while the mean groove length was approximately from 20 to 80 μm .

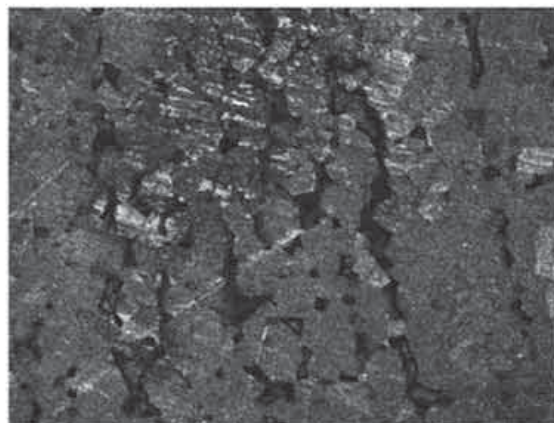


Figure 9: CLSM image showing an inter-crystalline defect in an etched surface bolt from sample S2 (200 x).

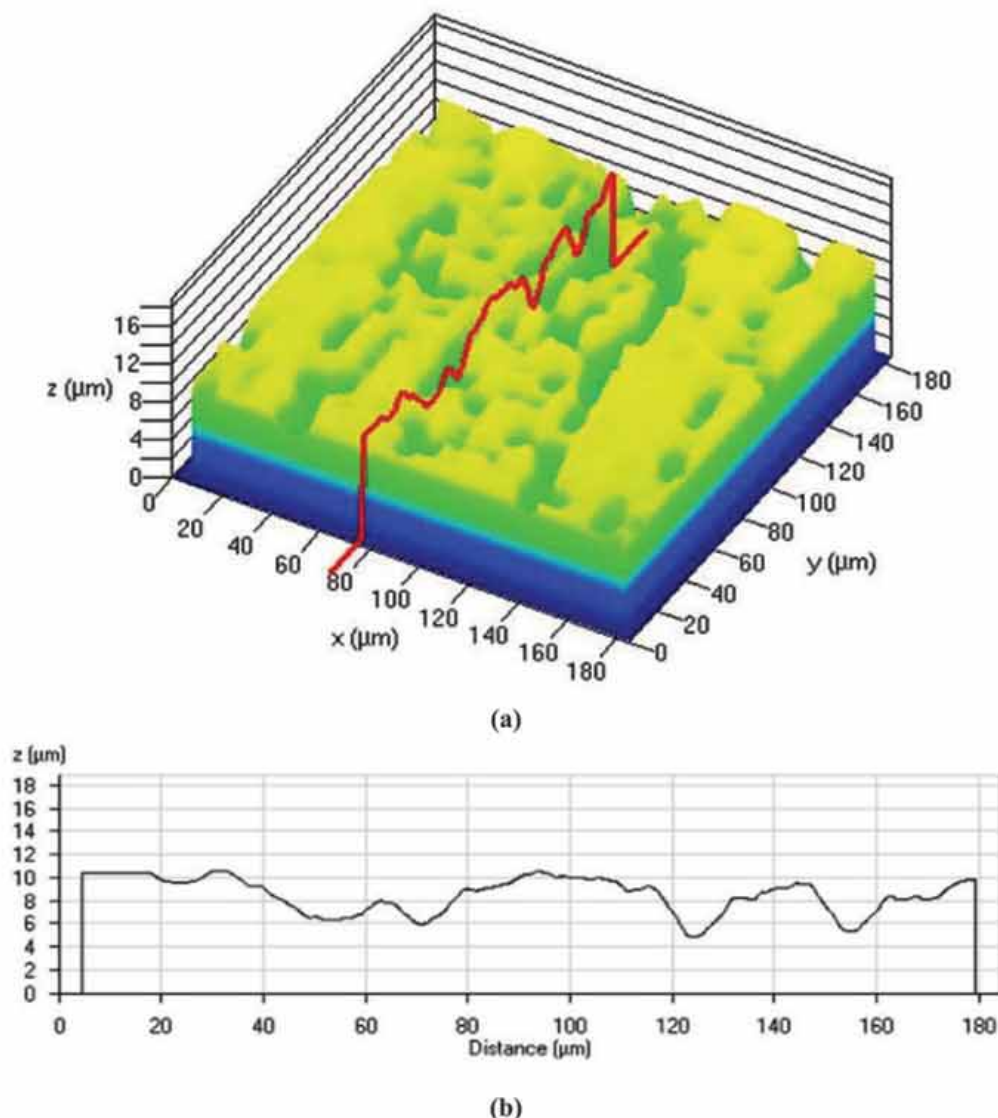


Figure 10: Line scan image of the failed bolt surface: (a) 3D CLSM topographical image and line scan on the failed bolt; (b) "Cross-sectional" view of the grooves and peaks on the surface.

Each failure mode or type of failure has a certain characteristic on fractographic features. Closer examination by the aid of SEM showed that the fracture surface of sample S2 was composed of shear ductile dimple morphology. The rough microstructure and multiple dimples on the surface, as shown in Figure 11, denote the occurrence of ductile and sudden overload failure in the sample (ASM, 1992). The presence of dimples is indicative of a ductile overload failure. Dimples indicate that the loads applied to cause the failure of the component are in excess of the tensile strength of the material, and that the material has ductility or the ability to

deform. The presence of discontinuities or other defects such as inclusions (Figure 12) in S2 sample also contribute to the lower performance of the bolt (Al-Hashem & Riad, 2002; Krishnaraj, 2003; Osman, 2006). When dimple features, inclusions and microvoids are present and ductile overload has occurred, the component typically shows early signs of deformation, such as bending (Figure 1 – sample S7).

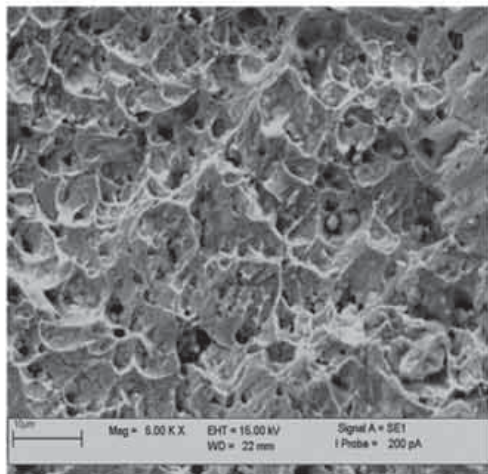


Figure 11: SEM micrograph of shear dimples on the fracture surface of the failed bolt.

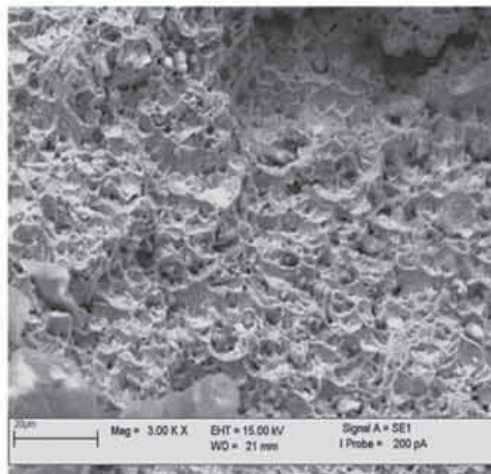


Figure 12: SEM micrograph of the failed bolt with shear dimples and inclusion.

3.3 Materials Properties

Semi-quantitative chemical analysis on the fracture surface of the failed bolt was carried out by EDX to qualitatively determine the elemental composition, and to identify elements or any contaminants present in the alloy (sample S2). Based on EDX analysis (Figure 13), the bolt was found to contain a high percentage of Cu and Zn elements as shown by the presence of major peaks in the EDS spectrum. For quantitative and accurate results, chemical analysis using an atomic absorption spectrophotometer (AAS) was carried out, and the results are given in Table 1. For comparison, the typical composition of aluminum bronze alloys (bolts) is also included in Table 1. The chemical composition of sample S2 is not the same as that of a typical aluminum bronze alloy bolt which is usually used for the same application (Kudashov *et al.*, 2008; Fonlupt *et al.*, 2005).

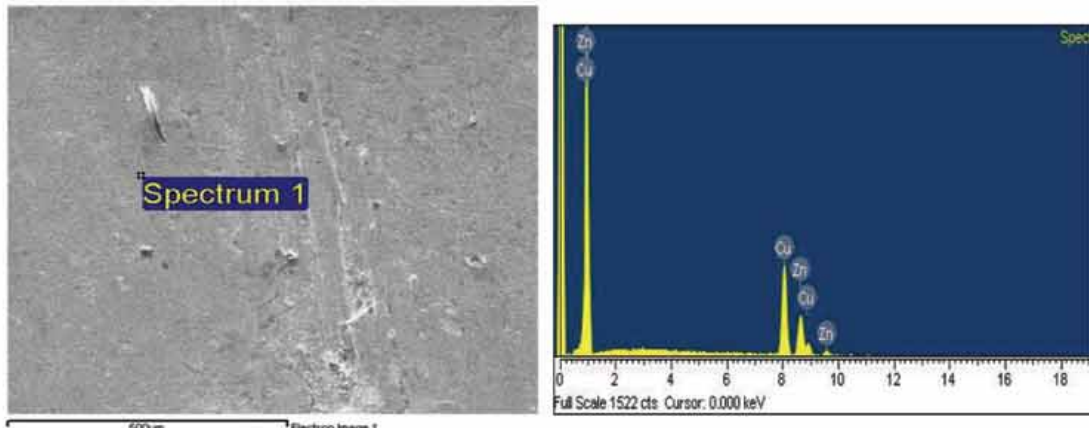


Figure 13: Semi-quantitative EDX analysis of sample S2.

Table 1: Chemical composition of the sample S2 analysed by AAS.

Elements	Failed Bolt	Typical Al Bronze (Bolt)
Aluminium, %Al	Trace	9 – 12
Iron, %Fe	Trace	1.5 – 6
Nickel, %Ni	Trace	0 – 6
Manganese, %Mn	Trace	0 – 3
Zinc, %Zn	35.5	0 – 0.5
Copper, %Cu	64.5	Remainder

The hardness of the failed bolts was measured using Rockwell hardness scale B, and the results are presented in Table 2. The average hardness values recorded are in the range of 72 to 76 HRB. On the other hand, the hardness value for aluminum bronze has been reported to be not less than 85 HRB and this value increases with additional alloying and thermal treatment (Yasar & Altunpak, 2008).

Table 2: Hardness values of failed bolts.

Bolt samples	S1	S2	S3	S4	S5	S6	S7
Average Hardness Value (Rockwell B Scale (HRB))	73.18	76.35	73.30	73.88	73.02	72.08	72.25

4. CONCLUSIONS

This investigation was conducted on the failed bolts that were used to fix the end plate of a ship's propeller hub. Visual examination on the fracture surfaces of all the failed bolts showed dimple or cup-cone appearances along with fibrous surfaces and radial marks. Macroscopic examination showed that the direction of radial marks is propagating towards the failure initiation site. Microscopic studies showed that the condition of internal grain microstructures was not good due to the presence of voids and internal crystalline defects. Crack initiation occurred at the stress concentration points and propagated towards the end point area with an indication of ductile failure due to overloading. The bolt failures were caused by a cumulative effect of high stress concentrations at the thread and the additional stress concentration imposed by the presence of machining defect at the surface. Different rupture areas were found in the failed samples indicating that the amount of loads received by the bolts were different before they totally failed. Based on material analysis and hardness testing results, it can be concluded that the material of the failed bolts was Cu-Zn alloy (brass) with lower hardness, and not Cu-Al alloy (aluminum bronze) as specified by the requirement.

ACKNOWLEDGEMENT

The authors would like to thank the officers and technical staff from various laboratories in STRIDE Kajang and Lumut for their comments, technical support and help during the investigation works and writing.

REFERENCES

- Al-Hashem, A. & Riad, W. (2002). The role of microstructure of nickel-aluminum-bronze alloy on its cavitation corrosion behavior in natural seawater. *Mat. Charac.*, **48**: 37-41.
- American Society for Metals (ASM) (1986). *ASM Metals Handbook, Volume 11: Failure Analysis and Prevention*. American Society for Metals (ASM), Russell Township, Ohio.
- American Society for Metals (ASM) (1992). *ASM Handbook of Case Histories in Failure Analysis, Vol. 1 and Vol. 2*. American Society for Metals (ASM), Russell Township, Ohio.
- American Society for Metals (ASM) (1993). *Handbook of Case Histories in Failure Analysis, Vol. 2*. American Society for Metals (ASM), Russell Township, Ohio.
- Chen, H.S., Tseng, P.T. & Hwang, S.F. (2006). Failure analysis of bolts on an end flange of a steam pipe. *Eng. Failure Anal.*, **13**: 656-668
- Fonlupt, S., Bayle, B., Delafosse, D. & Heuze, J.L. (2005). Role of second phases in the stress corrosion cracking of a nickel-aluminum bronze in saline water. *Corr. Sci.*, **47**: 2792-2806

- Gao, L. & Cheng, X. (2008). Microstructure & mechanical properties of Cu-10%Al-4%Fe alloy produced by equal channel angular extrusion. *Mat. & Design*, **29**: 904-908
- Krishnaraj, N., Bala Srinivasan, P. & Muthupandi, V. (2003). Investigation of a mounting bolt failure in an automobile air brake assembly. *J. of Failure Anal. & Prev.*, **3**: 69-72
- Kudashov, D.V., Zauter, R. & Muller, H.R. (2008). Spray-formed high-aluminum bronzes. *Mat. Sci. Eng. A*, **477**: 43-49.
- Liu, S., Faisal Anwar, A.H.M., Kim, B.C. & Ichikawa, Y. (2006). Observation of microcracks in granite using a confocal laser scanning microscope. *Int. J. of Rock Mech. & Mining Sci.*, **43**: 1293-1305
- Gjønnes, L. (1996). Quantitative characterization of the surface topography of rolled sheets by laser scanning microscopy and fourier transformation. *Metall. Mat. Trans A*, **27**: 2338-2346.
- Osman, A. (2006). Failure of a stud bolt in a ring spinning frame textile machine. *Eng. Failure Anal.*, **13**: 963-970.
- Udupa, G., Singaperumal, M., Sirohi, R.S. & Kothiya, M.P. (2000). Characterization of surface topography by confocal microscopy: I. Principles and the measurement system. *Meas. Sci. Tech.*, **11**: 305-310
- Yasar, M. & Altunpak, Y. (2008). The effect of ageing heat treatment on the sliding wear behavior of Cu-Al-Fe alloys. *Mat. & Design*, **30**: 878-884.

FAILURE ANALYSIS OF A DIESEL ENGINE ROCKER ARM

Mohd Moesli Muhammad¹, Mahdi Che Isa¹, Mohd Subhi Din Yati¹,
Syed Rosli Sayd Bakar² & Irwan Mohd Noor¹

¹Maritime Technology Division (BTM), Science & Technology Research Institute for Defence (STRIDE), Ministry of Defence, Malaysia

²Mechanical & Aerospace Technology Division (BTJA), Science & Technology Research Institute for Defence (STRIDE), Ministry of Defence, Malaysia

*Email: moesli.muhammad@stride.gov.my

ABSTRACT

This paper presents the failure analysis of a diesel engine rocker arm, used in ships and boats, which failed in service. The fracture occurred at the threaded part of the rocker arm. A detailed metallurgical investigation was conducted to identify the mode of failure and the point at which the crack was initiated. The failure was dominated by fatigue due to the appearance of beach mark patterns on the fracture surface. The fractographic study showed the presence of metal particles and scratches adjacent to the crack region which contributed to stress localisation, resulting in the crack being initiated and propagated.

Keywords: Failure analysis; fatigue; stress localisation; rocker arm; beach mark.

1. INTRODUCTION

Failure analysis is a broad discipline that includes metallurgy and mechanical engineering. There are numerous failure mechanisms that might occur, some appear more often than others, which include various types of corrosion or wear by itself, corrosion in combination with wear, and compression to name a few. Failure of engineered products and structures can occur by cyclic application of stresses (or strains), the magnitude of which would be insufficient to cause failure when applied singularly. Structural and mechanical components subjected to fluctuating service stress (or more appropriately, strain) are susceptible to failure by fatigue (Lee *et al.*, 2008). Fatigue is considered as one of the most common causes of structural and machinery component failures which are frequently found in engineering services (Gagg & Lewis, 2009).

Fatigue failure is localised structural damage that occurs when a material is subjected to variable cyclic stresses. These stresses are much lower than the ultimate tensile stress limit when under the application of a single static stress (Suresh, 2001). In the case of this study (Figure 1), the failure of a diesel engine rocker arm was reported to have occurred during normal engine operation, with the engine running at 3,000 running hours, and the failed sample was sent to the Ships Technology Branch, Science & Technology Research Institute for Defence

(STRIDE), for failure investigation. The failure occurred at the first cylinder of a marine diesel engine with 6 cylinders. The failed rocker arm was broken into two separate pieces, as shown in Figure 2. This paper describes the detailed metallurgical investigation and fractographic study conducted to assess the possible causes of failure.



Figure 1: The failed rocker arm.

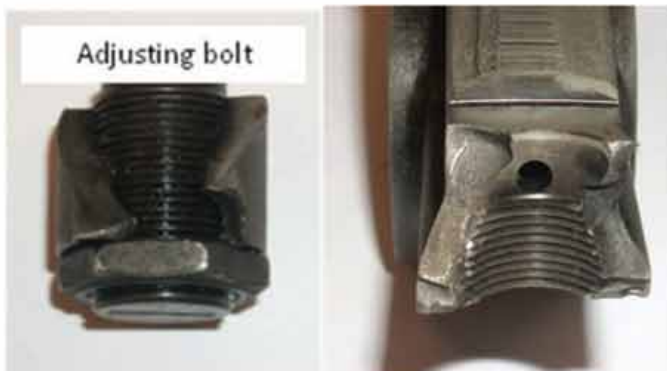


Figure 2: The as-received failed rocker arm.

2. INVESTIGATION

The rocker arm is a part of the engine component that is located on the valve for controlling intake and exhaust of airflow and fuel to the cylinder head (Figure 3). However, due to fluctuating loads applied, any defects in the manufacturing process will expose the rocker arm to fatigue failure (Gagg & Lewis, 2009). In order to counter the possibility of fatigue failure, most of the rocker arms are fabricated through forging, which can improve strength and reduce the manufacturing process defects (Nisbett, 2005; Smith, 1996). However, in certain cases, failure of rocker arms still occurs (ASM, 1986, 1992, 1993). The main purpose of this investigation

is to identify the causes of failure of the rocker arm, including possible factors attributed from the maintenance works during the service periods. The failed rocker arm was examined using an optical stereo microscope for macroscopic examination. In order to verify the failure mode, the fracture surface of the rocker arm was ultrasonically cleaned and further examined with the aid of a scanning electron microscope (SEM) associated with energy dispersive x-ray (EDX) for chemical composition determination.



Figure 3: Rocker arm of a marine diesel engine.

3. RESULTS & DISCUSSION

3.1 Macroscopic Examination

Figure 4 shows the fracture surface of the broken rocker arm which reveals the presence of a crack initiation point, beach marks and striations. From the beach marks' orientation, the location of the crack initiation point can be determined. It is strongly believed that the crack started at that point due to material inhomogeneities, such as notches, grooves, surface discontinuities, flaws and other material defects. These inhomogeneities or initiation points act as stress raisers where the applied stress concentrates until it exceeds the local strength of the material and produces a crack. From the macroscopic observation in Figure 4, it can be concluded that the cracks started from the inner threaded part and propagated towards the sidewall. The presence of beach marks, which can be clearly seen on the fracture surface, is a strong indicator that a fatigue failure had occurred (Yu & Zu, 2006; Jones, 2001).

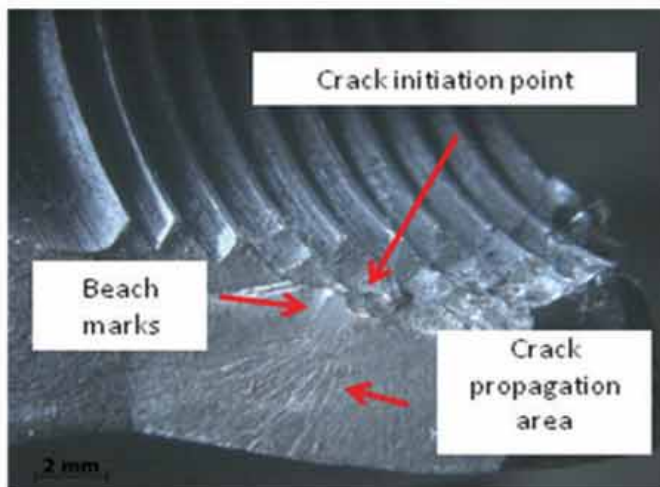


Figure 4: Optical micrograph of the fractured surface of the rocker arm.

3.2 Fractographic Investigation

The fractographic examination was performed using a variable pressure SEM (Joel VPSEM 1480) to reveal fracture features. The SEM micrograph in Figure 5 clearly shows the presence of metal particles and scratches on the surface of the failed sample. The presence of scratches on the thread surface can be attributed to heavy contaminants, such as metal particles or metal debris as shown in Figure 5(a). Such deformations can contribute to the formation of stress concentration zones at the surface of thread region of the rocker arm and can be the potential point of failure. Detailed investigation by SEM showed the presence of fatigue striation marks (Figure 6) on the fracture surface. The fatigue striation marks appear within the crack propagation zone which is located adjacent to the crack initiation point. Furthermore, fluctuating loads applied during engine operation made the stresses much higher and localised. Thus, the crack was initiated and propagated until the fracture toughness of the material was exceeded and the final fracture occurred (Chung & Kim, 2010).

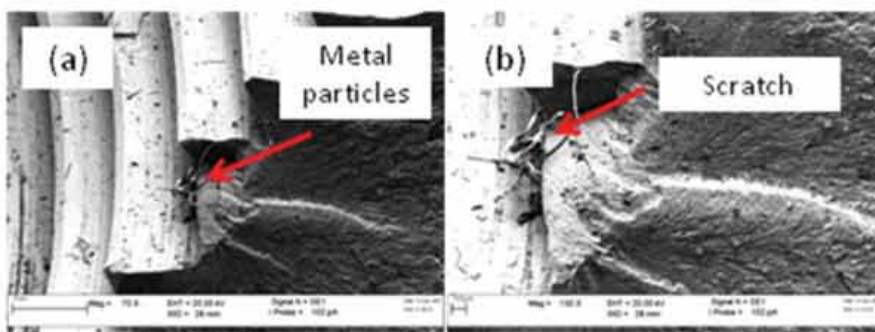


Figure 5: SEM fractography on the thread surface. (a) Metal particles. (b) Scratch marks.

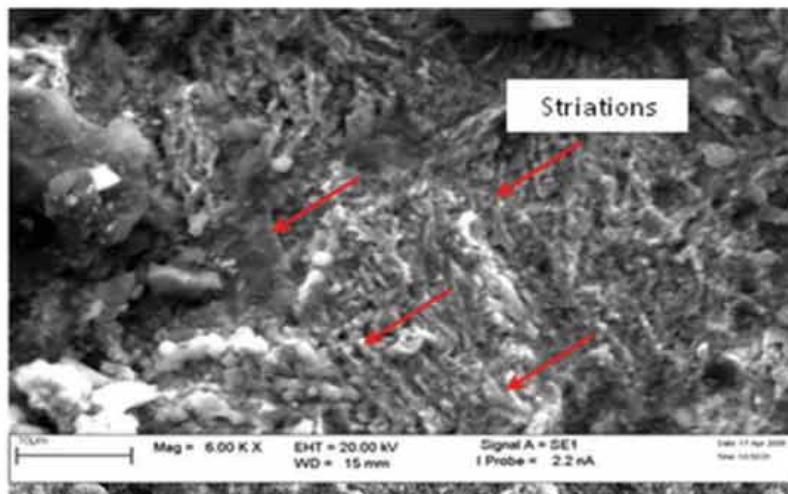


Figure 6: SEM fractography of the crack showing striations direction (the arrows show the striation marks).

3.3 Material Composition

The material composition of the failed rocker arm is determined using the EDX machine, and the spectrum obtained is shown in Figure 7. The peaks show that the major element of the rocker arm is Fe, with alloying elements Mn and Cr. The semi-quantitative results in Table 1 show that Fe is the main constituent (97.7%), while the concentrations of Cr and Mn were 1.09 % and 1.13 % respectively. It can be seen that the composition of the materials corresponds to the typical composition range for the same products. The high content of Cr and Mn in steel alloys is aimed at improving hardenability and wear resistance, and to increase the strength of the rocker arm at high temperatures (Smith, 1996). Hence, it can be concluded that the elements in the material are suitable for use in the rocker arm application and were not a cause of the failure.

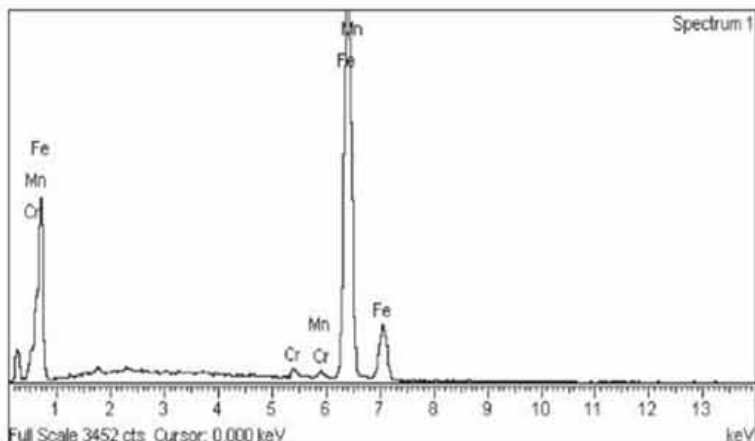


Figure 7: EDX spectrum of the failed rocker arm.

Table 1: Chemical composition of the failed rocker arm.

Element	Composition (%)
Cr	1.09
Mn	1.13
Fe	97.78

4. CONCLUSION

The metallurgical examination showed the presence of beach marks, and from its orientation, it was clear that the crack started at an initiation site, which is from the inner threaded part, and propagated towards the final zone at the sidewall. Further examination by SEM revealed the presence of scratches and metal particles adjacent to the crack region. It is strongly believed that these scratches and metal particles contributed to the high concentration stress region, which under cyclic and localised loads applied on the structure can create the initial crack point. Based on these observations, the laboratory generated data and the reference literature, it can be concluded that the failure of the rocker arm was due to fatigue failure. In order to prevent further rocker arm failures, it is recommended that all components should be subjected to a thorough cleaning and inspection before being placed into service.

ACKNOWLEDGEMENT

The authors are grateful to the officers and staff of the STRIDE's Ships Technology (in Lumut) and Structural & Mechanical (in Kajang) Branches for their technical support and help during the investigation works.

REFERENCES

- American Society for Metals (ASM) (1986). *ASM Metals Handbook, Volume 11: Failure Analysis and Prevention*. American Society for Metals (ASM), Russell Township, Ohio.
- American Society for Metals (ASM) (1992). *ASM Handbook of Case Histories in Failure Analysis, Vol. 1 and Vol. 2*. American Society for Metals (ASM), Russell Township, Ohio.
- American Society for Metals (ASM) (1993). *Handbook of Case Histories in Failure Analysis, Vol. 2*. American Society for Metals (ASM), Russell Township, Ohio.
- Chung, C.S. & Kim, H.K. (2010). Safety evaluation of the rocker arm of a diesel engine. *J. Matl. Dsgn* **31**: 940-945.
- Gagg, C.R. & Lewis, P.R. (2009). In-service fatigue failure of engineered products and structures-Case study review. *Eng. Fail. Anal.*, **16**: 1775-1793.

- Nisbett, E.G. (2005). *Steel forgings: Design, Production, Selection, Testing, and Application*. ASTM International, Pennsylvania.
- Jones, D.R.H. (2001). *Failure Analysis Case Study II*. Elsevier Science Ltd., Oxford.
- Lee, D.W., Cho, S.S. & Joo, W.K. (2008). An estimation of failure stress condition in rocker arm shaft through FEA and microscopic fractography. *J. Mech. Sc. Tech.* **22**: 2056-2061.
- Suresh, S. (2001). *Fatigue of Materials*. Press Syndicate of the University of Cambridge, Cambridge.
- Smith, W.F. (1996). *Principles of Material Science and Engineering*. McGraw-Hill Inc., New York.
- Yu, Z.W. & Xu, X.L. (2006). Failure analysis of diesel engine rocker arms. *Eng. Fail. Anal.*, **13**: 598-605.

DESIGN OPTIMISATION OF STITCHED FABRIC ARMOURS

Ridwan Yahaya^{1*}, Risby Mohd Sohaimi² & Megat Mohamad Hamdan Megat Ahmad²

¹Protection and Biophysical Technology Division, Science and Technology Research Institute for Defence (STRIDE), Ministry of Defence, Malaysia

²Faculty of Engineering, National Defence University of Malaysia (UPNM), Malaysia

*Email: ridwan.yahaya@stride.gov.my

ABSTRACT

A full factorial experimental investigation has been carried out in order to study the factors that affect energy absorption of stitched fabric armours. The ballistic testing procedures were conducted with reference to the National Institute of Justice Ballistic Test Standard for Body Armor Testing (NIJ-0108.01). A total of five factors were studied; fabric areal density (represents the number of plies of fabric), stitched area, stitch density, sewing thread strength, and bullet velocity. The factors' variables and their ranges were; areal density, $2.03\text{-}8.02 \text{ kg/m}^2$; stitched area, $6.45\times 10^{-4}\text{-}5.8\times 10^{-3} \text{ m}^2$; stitched density, 3-13 stitches per 2.5 cm; sewing thread strength, 26.5-42.8 N; and bullet velocity, 250-420 m/s. Energy absorption was measured as the response to the experimental design. The model showed that fabric areal density, stitch density and bullet velocity have the most influence on the stitched fabric's energy absorption capabilities. Areal density and stitch density values of 3.78 kg/m^2 and 13 stitches per 2.5 cm respectively were found to be the desired optimised settings of the stitched fabric panel which is statistically predicted to absorb the highest impact energy from a 9 mm bullet at 437 m/s. A statistical model for energy absorption of stitched fabric panels was successfully developed and validated. The error was recorded to be within 3-9 %. This study has highlighted the combinations of factors that would be of most importance for fabric armour manufacturers to consider.

Keywords: *fabric armour; stitched fabric; energy absorption; ballistic impact; Design of Experiments (DOE).*

1. INTRODUCTION

In recent years, ballistic resistant materials formed from high tensile strength fibres, such as aramid fabrics or polyethylene fabrics, have been in common use. These fabrics have been used to design flexible fabric-based bullet defeating vests. These ballistic resistant materials typically have the advantages of greater tensile strength and less weight per unit area as compared to other materials. Multiple layers of aramid fabric are used in single bullet proof vests as a single layer is insufficient to

stop a ballistic projectile. Attaching multiple plies of fabric still leaves the vest lighter and more flexible as compared to metal.

Experimental studies on ballistic impacts can be time and cost intensive. High costs and restricted sources of high performance fabric raw materials have limited research activities in this area. Thus, a technique to minimise the number of experiment samples without losing accuracy would save a lot of cost and reduce time. Design of Experiments (DOE) provides a systematic technique to serve this purpose. DOE is an experimental approach in which more than one factor is changed simultaneously. By systematically varying the levels of the variables and by applying statistics to the experimental process (if there exists an optimal experimental distribution of tests which minimises the variance of the responses), more factors and the interactions among them can be studied with less runs. This is better than the alternative of looking at each variable individually in a series of separate experiments, since a more complete understanding of the features of the system and how they interact may be gained. Factorial designs are widely used in experiments involving several factors where it is necessary to study the joint effect of these factors on certain responses (Hassan, 2009; Montogomery *et al.*, 1982).

The ballistic properties of a fabric armour depend on energy absorption and propagation ability of the fibres and yarns forming the armour. Factors such as fibre and yarn properties, fabric construction, fabric weight per unit area, and ply number were studied actively by other researchers (Shim *et al.*, 2001; Chocron-Benloulo *et al.*, 1997; Lim *et al.*, 2002; Smith *et al.*, 1960). The effect of stitching on fabric armours was studied by Karahan *et al.* (2008), Mazelsky (1996) and Ahmad *et al.* (2008).

From the literature review conducted, the effect of influencing parameters of energy absorption depends largely on several factors, such as type of material, fabric structure, boundary condition, interface friction, impact velocity and number of plies. This paper will, therefore, examine experimental studies focused on fabric areal density, sewing thread strength, stitch density and bullet velocity.

2. MATERIALS AND METHODS

2.1 Material

Kevlar 129 Type 802F was selected for this study based on its common use in the industry and availability in the market. The preparation of these test specimens was based on meeting specific areal density values of 2.03 and 8.12 kg/m² as selected in the DOE. The materials were cut into 25.4 x 25.4 cm pieces using an electric cutter and weighed to determine the number of plies required to meet the areal density values. The samples were stitched together using through-the-thickness stitching thread by an industrial sewing machine (JUKI DU-1181N). The lockstitch was used to stitch the samples in this study.

2.2 Ballistic Test

Ballistic testing was performed primarily to determine the energy absorption of the fabric armour panels. The experimental setup (Figure 1) was designed according to the guidelines given in the National Institute of Justice Ballistic Test Standard for Body Armor Testing (NIJ-0108.01).

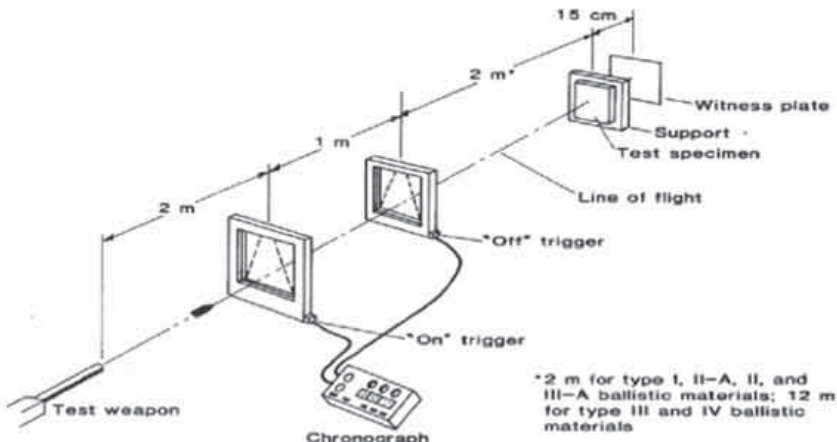


Figure 1: Schematic of ballistic test setup following the NIJ-0108.01 standard.

2.3 Test Weapon

The universal test gun (PROTOTYPA) was used in this test. It is a 9 mm test gun consisting of a fixed mounted gun with interchangeable test barrel and breech unit. The 9 mm calibre test barrel was used to shoot the standard military ball projectiles.

2.4 Projectile

A standard 9 mm Full Metal Jacketed Round Nose (FMJ RN) projectile with a nominal round-nose lead mass of 7.45 g and a copper outer coating (jacket) was chosen. The 9 mm projectile velocity is controlled by altering the weight of propellant. The 9 mm projectile was chosen because it is sufficient for soft fabric armours.

2.5 Portable Velocity Chronograph

The projectile velocity measurement system used in this operation was a portable velocity chronograph as shown in Figure 2. This equipment can perform a system scan within an accuracy of 0.1 %, and record velocities from as low as 10 m/s to in excess of 1000 m/s.



Figure 2: Portable velocity chronograph.

2.6 Ballistic Panel

The ballistic panels were constructed based on the DOE standard configuration, and each panel was impacted with four projectiles. The locations for projectile impact were chosen to minimise the effects of previous impact damage and of boundary conditions. Figure 3 shows a sample fixed in a steel target holder using a G-clamp.

2.7 Full Factorial Designs

The experimental design was determined using the Design Expert software, version 7 (State-Ease Inc., Minneapolis, USA). A 2^5 full factorial was used for 2 independent factors leading to a total of 32 sets of experiments. This can allow for the study of main and joint effects of five different factors (Table 1), namely areal density of the fabric, stitched area, stitched density, sewing thread strength and bullet velocity each at 2 levels. Low and high factor settings were coded as -1 and +1 respectively, as shown in Table 2. A total of 32 samples were stitched according to the design matrix in Table 3.

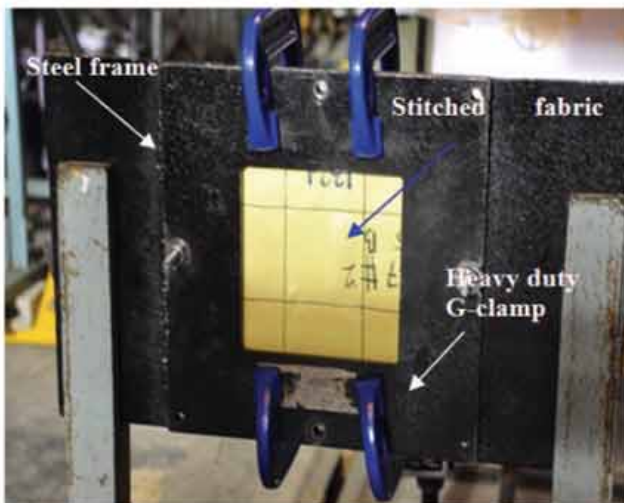


Figure 3: Stitched Kevlar panel ($\text{stitching area} = 5.8 \times 10^{-3} \text{ m}^2$) clamped at the target holder.

Table 1: Input factors and output responses for the full factorial experimentation.

Parameter (DOE Factor)	Unit	Responses	Unit
Areal density (A)	kg/m^2	Energy absorbed	J
Stitching area (B)	cm^2		
Sewing thread strength (C)	N		
Stitch density (D)	n		
Bullet velocity (E)	m/s		

Table 2: Input factors' levels for the full factorial experimentation.

Parameter (DOE Factor)	Unit	Low Level Value (-1)	High Level Value (+1)
Areal density (A)	kg/m^2	2.03	8.12
Stitching area (B)	m^2	6.45×10^{-4}	5.8×10^{-3}
Stitching density (C)	N	26.5	42.8
Sewing thread strength (D)	n	3	13
Bullet velocity (E)	m/s	250	420

2.8 Determination of Energy Absorption of Samples

The velocity of the bullet was measured using the ProChrono Digital chronograph. The energy absorption of a bullet E_{abs} with weight m travelling at partial penetration velocity v_1 and residual velocity v_2 is calculated as follows:

$$E_{abs} = \frac{1}{2} m_p (v_1^2 - v_2^2) \quad (1)$$

The energy expended by the projectiles in perforating the panels is regarded as the energy absorbed by the fabric. It is found by subtracting the residual energy of the projectile from its initial impact energy.

3. RESULTS AND DISCUSSION

3.1 Energy Absorption

The energy absorption was reported as in Table 3. Using Design Expert, a half normal probability plot (Figure 4) was used to determine factors that are significant for the energy absorption. The plot shows the absolute value of the term effects (horizontal axis) that was tested against a half normal probability scale (vertical axis). Insignificant terms fall on the straight line.

Terms that depart from the line are initially modelled and tested for significance. In analysing the half normal plot for energy absorption, several factors, including main effects and their interactions, were shown to potentially affect energy absorption. These factors and interactions are:

- a. Factors A (areal density) and E (bullet velocity)
- b. Interaction of factors A and E
- c. Interaction of factors C (stitch density) and E
- d. Interaction of factors A, C and E.

3.2 Analysis of Variance (ANOVA)

The ANOVA results for energy absorption are as shown in Table 4. From this table, a “low p-value” is shown for the overall model signifying the model to be significant. The “p-value” uses the data to test the hypothesis showing the significance of the factors. A “p-value” less than 0.05 is generally said to be significant. The results also show the main effects A (areal density), E (bullet velocity), AE (areal density and bullet velocity) to be significant with “p-value” < 0.05.

Table 3: Design matrix for the 32 runs and the responses recorded.

Standard	Factor					Response Energy absorption (J)
	A Areal density (kg/m ²)	B Stitched area (m ²)	C Stitched density (per 2.5cm)	D Thread strength (N)	E Bullet velocity (m/s)	
2	1	-1	-1	-1	-1	261.59
31	-1	1	1	1	1	196.19
24	1	1	1	-1	1	666.51
28	1	1	-1	1	1	688.75
16	1	1	1	1	-1	234.68
18	1	-1	-1	-1	1	685.55
25	-1	-1	-1	1	1	55.38
9	-1	-1	-1	1	-1	63.33
17	-1	-1	-1	-1	1	25.09
13	-1	-1	1	1	-1	73.36
7	-1	1	1	-1	-1	56.98
11	-1	1	-1	1	-1	230.95
22	1	-1	1	-1	1	711.36
1	-1	-1	-1	-1	-1	58.51
8	1	1	1	-1	-1	230.95
30	1	-1	1	1	1	695.17
26	1	-1	-1	1	1	685.55
3	-1	1	-1	-1	-1	197.80
21	-1	-1	1	-1	1	80.77
19	-1	1	-1	-1	1	54.98
23	-1	1	1	-1	1	81.94
6	1	-1	1	-1	-1	221.77
5	-1	-1	1	-1	-1	57.65
14	1	-1	1	1	-1	277.62
27	-1	1	-1	1	1	65.00
20	1	1	-1	-1	1	698.40
4	1	1	-1	-1	-1	257.65
10	1	-1	-1	1	-1	240.32
29	-1	-1	1	1	1	182.30
12	1	1	-1	1	-1	205.71
15	-1	1	1	1	-1	70.48
32	1	1	1	1	1	695.17

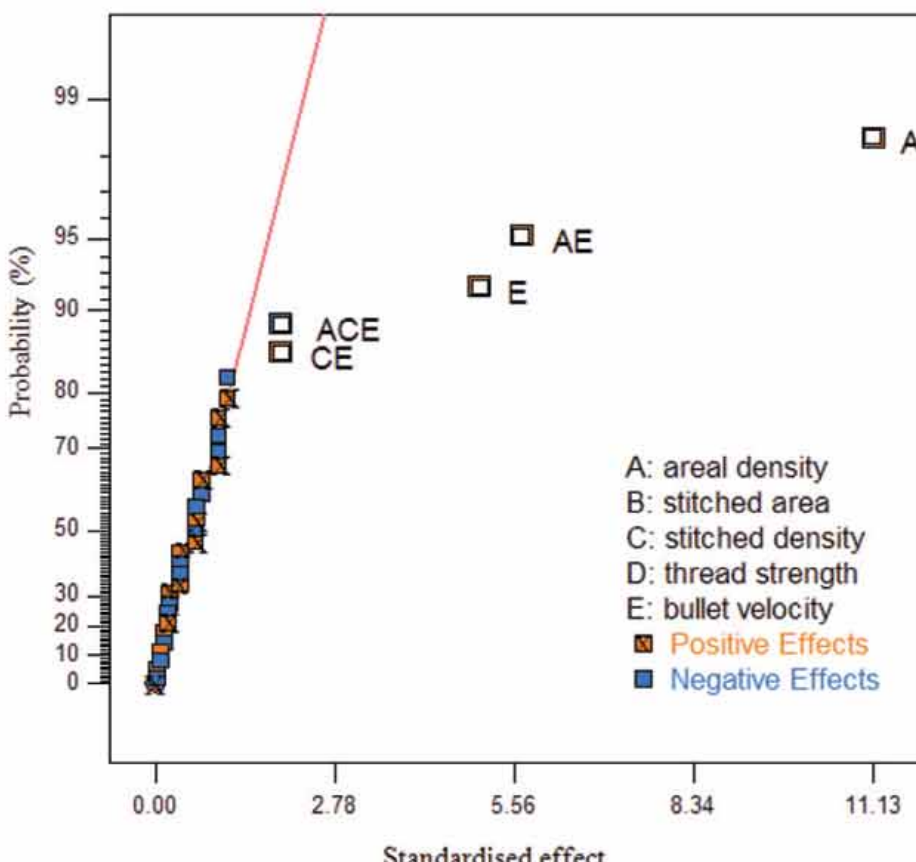


Figure 4: Half normal probability plot of the major effects for energy absorption.

The “F-value” is the ratio of the model Sum of Square to Residual Sum of Square. The model F-value of 72.57 implies that the model is significant. This as a large number indicates more of the variance being explained by the model; a small number says the variance maybe more due to noise. There is only a 0.01% chance that a “Model F-Value” this large could occur due to noise. Values of “Prob > F” less than 0.0500 indicate model terms that are significant, whereas values greater than 0.1000 indicate the model terms that are not significant. In this case, A, E, and interactions of AE, CE and ACE are significant model terms.

Table 4: ANOVA for the energy absorption analysis as calculated using Design Expert.

Source	Sum of squares	Mean square	F value	p-value Prob>F	Remark
Model	1586.47	226.64	72.57	< 0.0001	Significant
A-area density	986.27	986.27	315.82	< 0.0001	
C-stitched density	0.38	0.38	0.12	0.7308	
E-bullet velocity	201.91	201.91	64.66	< 0.0001	
AC	0.38	0.38	0.12	0.9308	
AE	256.62	256.62	82.18	< 0.0001	
CE	30.09	30.09	9.64	0.0048	
ACE	30.09	30.09	9.64	0.0048	
Residual	74.95	3.12			
Cor Total	1661.42				
R ²	0.9549				
Adj R-Squared	0.9417				
Pred R-Squared	0.9190				
Adeq Precision	22.443				

The adjusted and predicted R² were found to be 0.9417 and 0.9190 respectively, with the difference between these two being 0.022, which is less than 0.2. This indicates that the model adequately fits the experimental data. The final statistical model for energy absorption is given in Equation 2 in terms of coded factors:

$$\text{Energy absorption (J)} = [14.94 + 5.56A + 0.11C + 2.90E - 0.11AC + 3.27AE + 1.12CE - 1.12ACE]^2 \quad (2)$$

Figure 5 shows the plot of predicted energy absorption vs. actual energy absorption. It is a good fit as the data points lie close to the diagonal line.

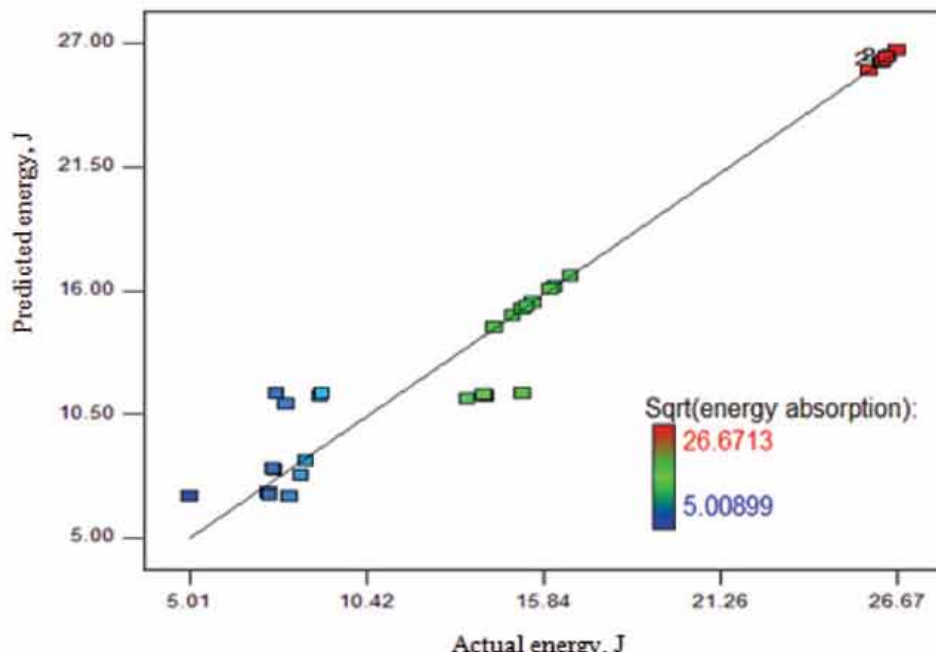


Figure 5: Predicted energy absorption vs. actual energy absorption.

3.4 Model Graphs

The effect of each factor on energy absorption of stitched fabrics is shown in the model graphs in Figures 6 - 8. As shown in Figure 6, an increase in areal density, which represents the number of fabric plies in a stitch fabric panel, will increase energy absorption. This is consistent with the findings of Shockley *et al.* (2004) and Roylance *et al.* (1979). It is observed in Figure 7 that the interaction of areal density and stitch density is predicted to increase energy absorption of stitched fabrics.

Figure 8 shows the effect of stitch density on energy absorption of stitched fabrics. It was found that the change in stitched area from $6.45 \times 10^{-4} \text{ m}^2$ to $5.8 \times 10^{-3} \text{ m}^2$ resulted in an increase in energy absorption. In this model, stitched area acts in interaction with bullet velocity. The impact velocity of a projectile will affect the performance of fabrics. According to Cheeseman & Bogetti (2003), during low-impact velocities, the yarn does not fail during the initial stress rise. Therefore, the transverse deflection of the fabric has time to propagate to the edge of the panel, which allows the fabric to absorb more energy. With a high-velocity impact, the damage is localised and the yarn fails before significant transverse deflection can develop.

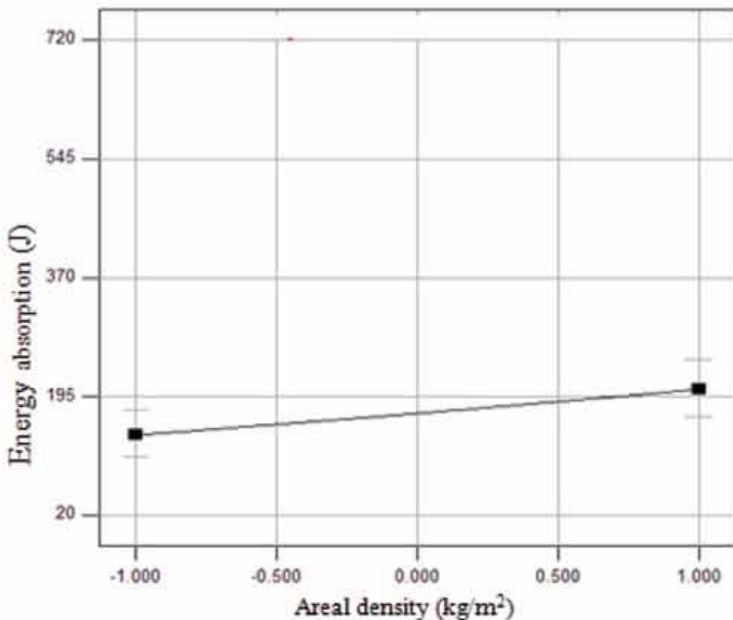


Figure 6: Relation of areal density and energy absorption of stitched fabrics.

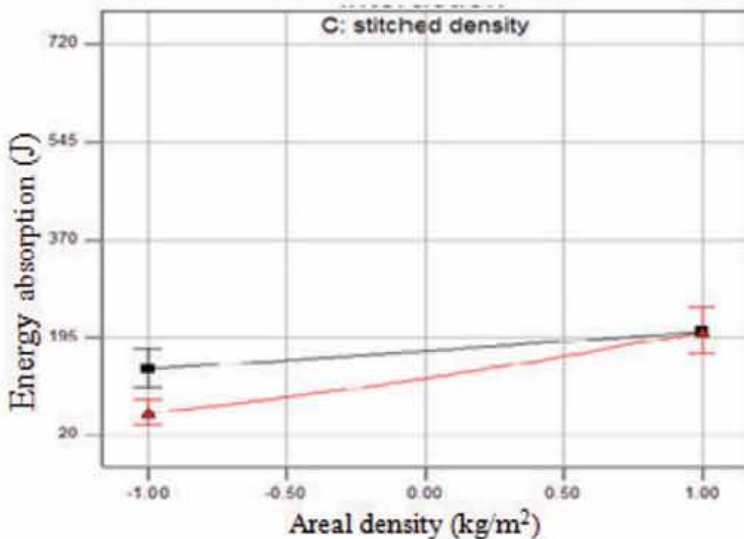


Figure 7: Interaction effect of areal density and stitch density on energy absorption.

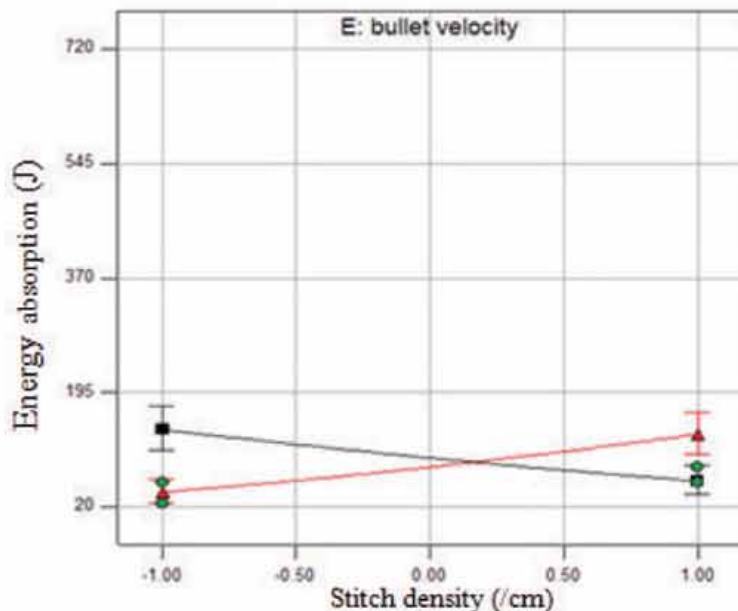


Figure 8: Interaction effect of stitch density and bullet velocity on energy absorption.

3.5 Validation

Using Equation 3, the model was validated for its accuracy. For the developed model, a verification process was done by performing additional experiments with different factors' values. The outcomes of these runs are predicted before the samples were tested and compared with the actual test results. The percentages of error were calculated based on Equation 3. The validation results of the responses (Table 5) show that the regression model's percentage of error is between 3 to 9 %.

$$\% \text{ Error} = \frac{\text{Predicted}-\text{Actual}}{\text{Actual}} \times 100 \quad (3)$$

Table 5: Results of the validation test.

Samples	Factors					Responses		% Error
	A (kg/m ²)	B (m ²)	C (n)	D (N)	E (m/s)	Energy (J) (Actual)	Energy (J) (Predicted)	
I	8.12	5.8x10 ⁻³	13	26.5	420	711.36	691.9	2.73
II	2.03	5.8x10 ⁻³	13	42.8	250	70.48	64.4	8.62
III	4.14	2.0x10 ⁻³	3	26.5	395	168.13	181.24	7.80
IV	6.36	6.45x10 ⁻⁴	3	26.5	252	236.5	219.48	7.22

3.6 Optimisation of Factors

Design Expert was used to determine values of factors required to obtain the maximum energy absorption. The factors' levels and responses were set at the desired goal using Design Expert's Numerical Optimization feature with desirability level set to one. The energy absorption lower limit was selected as 512 J (lowest energy absorption based on a 9 mm bullet with velocity of 358 m/s in NIJ Level II (NIJ-0108.01)), and the higher limit was selected as 100% (desired to be as high as possible), which is shown in Table 6. A prediction can be made using the regression model to predict the response of the panel by altering the factors' values in the selected ranges. By referring to the NIJ ballistic levels of threat, the energy absorption response is used to determine the capability of the panel to absorb the kinetic energy of the projectile in the optimal condition. In Design Expert, optimisation of the panel is done by using the NIJ Level IIA threat as an example.

Table 6: Targeted values.

Factor	Goal	Lower Limit	Upper Limit
Areal density (kg/m^2)	minimise	2.03	8.12
Stitched area (m^2)	in range	0.000645	0.0058
Stitched density (n)	in range	3	13
Thread strength (N)	in range	26.5	42.8
Bullet velocity (m/s)	maximise	235	437
Energy absorption (J)	maximise	512	711.36

Table 7 shows the solutions for the targeted values. Based on the solutions, in order to maximise the energy absorption of a 9 mm bullet travelling at 437 m/s, the fabric panel should have areal density of $3.78 \text{ kg}/\text{m}^2$ (about 9 plies of Kevlar fabric) and stitched area of $1.37 \times 10^{-3} \text{ m}^2$. Desirability is an objective function that ranges from zero outside of the limits to one at the goal. The desirability value for optimised soft armour design is recorded as 0.709.

Table 7: Solutions for the targeted values.

No.	Areal Density (kg/m^2)	Stitched Area (m^2)	Stitch Density (n/cm)	Thread Strength (N)	Bullet Velocity (m/s)	Energy Absorption (J)	Desirability
1.	3.78	1.37×10^{-3}	13.00	28.94	437.00	250.907	0.709
2.	3.78	1.55×10^{-3}	13.00	42.49	437.00	250.864	0.709
3.	3.78	5.28×10^{-3}	13.00	32.49	437.00	250.939	0.709

4. CONCLUSION

The Design of Experiments (DOE) technique was demonstrated to be capable of modelling factors contributing to energy absorption of stitched fabric armours. From the ANOVA test, it was found that areal density and bullet velocity had the greatest effect on fabric armour energy absorption. A statistical model for energy absorption of stitched fabric panels was successfully developed and validated. The model can be used to predict the energy absorption at the selected parameter settings with 3 - 9 % error, and can be used as a guideline for manufacturers in designing optimised stitched fabric armours.

ACKNOWLEDGEMENTS

The authors would like to thank the Director and personnel of the Weapons Technology Division, Science & Technology Research Institute of Defence (STRIDE), Ministry of Defence, Malaysia, for their technical assistance in ballistic testing.

REFERENCES

- Ahmad, M.R, Wan Ahmad, W.Y, Salleh, J. & Samsuri, A. (2008). Effect of fabric stitching on ballistic impact resistance of natural rubber coated fabric systems. *Mater. Design*, **29**: 1353-1358.
- Cheeseman, B.A. & Bogetti, T.A (2003). Ballistic impact into fabric and compliant composite laminates. *Compos. Struct.*, **61**: 161-173.
- Chocron-Benloulo, I.S., Rodriguez, Martinez, J.M.A. & Galvez, V.S. (1997). Dynamic tensile testing of aramid and polyethylene fiber composites. *Int. J. Impact Eng.*, **19**: 135-146.
- Hassan, S. (2009). *Design of Experiment Analysis of High Velocity Oxy-Fuel Coating of Hydroxyapatite*. MEng Thesis, Dublin City University.
- Karahan, M., Abdil Kus, A. & Eren, R. (2008). An investigation into ballistic performance and energy absorption capabilities of woven aramid fabrics. *Int. J. Impact Eng.*, **35**: 499-510.
- Lim, C.T., Tan, V.B.C. & Cheong, C.H. (2002). Perforation of high-strength double-ply fabric system by varying shaped projectiles, *Int. J. Impact Eng.*, **27**: 577-591.
- Mazelsky, B. (1996). *Armor with Breakaway Sewing*. U.S. Patent No. 5512348.
- Montgomery, T.G., Grady, P.L. & Tomasino, C. (1982). The effects of projectile geometry on the performance of ballistic fabrics, *Text. Res. J.*, **52**: 442-450.
- Roylance, D. & Wang, S.S. (1979). *Penetration Mechanics of Textile Structures*. Technical Report.

- Natick/TR-80/021, United States Army Natick Research and Development Command, 1-154.
- Shim, V.P.W., Lim, C.T. & Foo, K.J. (2001). Dynamic mechanical properties of fabric armour. *Int. J. Impact Eng.*, **25** (1):1-15.
- Shockley, D.A., Erlich, D.C. & Simons, J.W. (2004). *Improved Barriers to Turbine Engine Fragments*. Interim Report III, Report No. DOT/FAA/AR-99/8, III.
- Smith, J.C., Blanfort, J.M. & Schiefer, H.F. (1960). Stress-strain relationships in yarns subjected to rapid loading. Part VI; velocities of strain waves resulting from impact, *Text. Res. J.*, **30**: 752-760.

EVALUATION OF THE EFFECT OF RADIO FREQUENCY INTERFERENCE (RFI) ON GLOBAL POSITIONING SYSTEM (GPS) ACCURACY

Dinesh Sathyamoorthy*, Wan Mustafa Wan Hanafi, Mohd Faudzi Muhammad, Kamarulzaman Mustapa, Hasniza Hambali, Nor Irza Shakhira Bakthir, Siti Robiah Abdul, Shalini Shafii, Jamilah Jaafar, Aliah Ismail, Lim Bak Tiang, Zainal Fitry M. Amin, Mohd Rizal Ahmad Kamal, Siti Zainun Ali & Mohd Hasrol Hisam M Yusoff

Instrumentation and Electronics Technology Division (BTIE), Science & Technology Research Institute for Defence (STRIDE), Ministry of Defence, Malaysia

*E-mail: dinsat60@hotmail.com

ABSTRACT

In order to study the effect of radio frequency interference (RFI) on the global positioning system (GPS) L1 coarse acquisition (C/A) signal, the Instrumentation & Electronics Technology Division (BTIE), Science & Technology Research Institute for Defence (STRIDE), conducted a series of tests specifically aimed at evaluating the minimum interference signal power levels required to jam various GPS receivers. However, interference signals with power levels below the minimum jamming threshold could still severely distort GPS accuracy, rendering it useless for applications requiring high precision. BTIE conducted a test on 8th April 2010 to evaluate the effect of RFI on the accuracy of a Garmin GPSmap 60CSx handheld receiver, which employs the GPS L1 C/A signal. As expected, the probable error values of the location fixes increased as the transmitted interference signal power level was increased, until the GPS receiver was completely jammed. The amount of increase of probable error values and the minimum jamming power levels varied significantly based on GPS coverage and various error parameters, including ionospheric and tropospheric delays, and satellite clock, ephemeris and multipath errors. On the whole, this test has demonstrated the disadvantages of field global navigation satellite system (GNSS) evaluations; without the ability to control the various GNSS error parameters, it is difficult to effectively study the effect of any particular error parameter, in the case of this test, interference, on GNSS accuracy. This highlights the importance of using a GNSS simulator for such tests, whereby the tests could be done under repeatable user-controlled conditions.

Keywords: global positioning system (GPS) accuracy; radio frequency interference (RFI); position dilution of precision (PDOP); GPS L1 coarse acquisition (C/A) signal; signal power level.

1. INTRODUCTION

There is a steady growth in the entrenchment of global navigation satellite systems (GNSS) in current and upcoming markets, having penetrated various consumer products, such as cell phones, personal navigation devices (PNDs), cameras and assimilation with radio-frequency identification (RFID) tags, for various applications, including navigation, surveying, timing reference and location based services (LBS). While the global positioning system (GPS), operated by the US Air Force (USAF), is the primarily used GNSS system worldwide, the upcoming Galileo and Compass systems, and the imminent conversion of *Global'naya Navigatsionnaya Sputnikovaya Sistema* (GLONASS) signals from frequency division multiple access (FDMA) to code division multiple access (CDMA) look set to make multi-satellite GNSS configurations the positioning, navigation & timing (PNT) standard for the future.

However, many GNSS users are still not fully aware of the vulnerabilities of GNSS systems to various error parameters, such as ionospheric and tropospheric delays, satellite clock, ephemeris and multipath errors, satellite positioning and geometry, and unintentional signal interferences and obstructions. These error parameters can severely affect the accuracy of GNSS readings, and in a number of cases, disrupt GNSS signals (Volpe, 2001; Harding, 2001; Adams, 2001; Forssell, 2005; Kaplan & Hegarty, 2006; Gakstatter, 2008; Last, 2008, 2009, 2010; IDA, 2009; GAO, 2009; Dinesh, 2009; Schwartz, 2010; Palmer, 2010; Gibbons, 2010).

In his keynote speech during the Tuft University Institute for Foreign Policy Analysis (IFPA) Fletcher Conference on National Security Strategy and Policy, the USAF Chief of Staff, Gen. Norton Schwartz, pointed out that "*Another widely-known dependence that creates an exploitable vulnerability is that of GPS. It seems critical to me that the Joint Force should reduce its dependence on GPS-aided precision navigation and timing, allowing it to ultimately become less vulnerable, yet equally precise, and more resilient. The global value of GPS will endure, but our forces must be able to operate in GPS-denied environments in the future*" (Schwartz, 2010). Given these vulnerabilities, various recommendations have been provided on the application of PNT backups, including inertial navigation systems (INS), enhanced long range navigation (eLORAN), VHF omnidirectional range distance measuring equipment (VOR/DME), and internet time services and network time protocols (Volpe, 2001; Lilley *et al.*, 2006; Last, 2008, 2009, 2010; Grant *et al.*, 2009; IDA, 2009; IALA, 2009; Dinesh, 2009; Schwartz, 2010; Groves, 2010).

One particular vulnerability that has received significant attention is jamming. Since GNSS satellites, powered by photocells, are approximately 20,200 km above the Earth surface, GNSS signals that reach the Earth have very low power (10^{-16} - 10^{-13} W = -160 --130 dBm), rendering them highly susceptible to jamming (Pinker & Smith, 2000; Adams, 2001; Johnston & Warner, 2004; Papadimitratos and Jovanovic, 2008; Last, 2008, 2009, 2010; IDA, 2009; Dinesh, 2009; Schwartz, 2010; Palmer, 2010). Jamming is defined as the broadcasting of a strong signal that overrides or obscures the signal being jammed (DOA, 2009; JCS, 2007; Poisel, 2002). Given the various incidents of intentional and unintentional jamming of GNSS signals, including military GNSS signals (Adams, 2001; Williams, 2006; Jewell, 2007), the development of various GNSS anti-jamming technologies has

received significant attention (Casabona & Rosen, 1999; Gustafon *et al.*, 2000; Deshpande, 2004; Loegering, 2006; Meng *et al.*, 2008; Zhuang *et al.*, 2009; Wilde & Willems, 2010). In addition, many current GNSS receiver evaluations concentrate on radio frequency interference (RFI) operability (FAA, 1996; ION, 1997; Rash, 1997; Gautier, 2003; Agilent, 2008; Weinstein *et al.*, 2009).

In order to study the effect of RFI on the GPS L1 coarse acquisition (C/A) signal, the Instrumentation & Electronics Technology Division (BTIE), Science & Technology Research Institute for Defence (STRIDE), conducted a series of tests specifically aimed at evaluating the minimum interference signal power levels required to jam various GPS receivers (STRIDE, 2009a,b, 2010a,b,c; Dinesh *et al.*, 2009a, 2010a,b). However, interference signals with power levels below the minimum jamming threshold could still severely distort GPS accuracy, rendering it useless for applications requiring high precision.

BTIE conducted a test on 8th April 2010 to evaluate the effect of RFI on the accuracy of a Garmin GPSmap 60CSx handheld receiver (Garmin, 2007) (Figure 1), which employs the GPS L1 C/A signal (STRIDE, 2010d). The test was conducted at the STRIDE Kajang Block B car park (Figure 2). This article is aimed at discussing the procedure employed during the test, and the overall conclusions observed from its results.



Figure 1: A Garmin GPSmap 60CSx handheld receiver.



Figure 2: Test area located at N 2° 58' 3.4" E 101° 48' 35.2" (Screen capture from Google Earth).

2. MEASUREMENT OF GNSS ACCURACY

GNSS accuracy can be assessed using various methods. In this paper, it is measured via probable error, which is a function of dilution of precision (DOP) and user equivalent ranging error (UERE) (DOD, 2001; USACE, 2003; Kaplan & Hegarty, 2006).

DOP is a measure of satellite geometry, which represents the geometry of GNSS satellites as tracked by the receiver. High GNSS accuracy is obtained with good satellite geometry, which is obtained when the satellites are spread out in the sky. In general, the more spread out the satellites are, the better the satellite geometry will be, and vice versa (DOD, 2001; USACE, 2003; Kaplan & Hegarty, 2006; Huihui *et al.*, 2008).

Figure 3 demonstrates the effect of satellite geometry on GNSS accuracy using two satellites. The receiver is located at the intersection of two arcs of circles, each having a radius equal to the receiver-satellite distance and centred at the satellite itself. The measurement of the receiver-satellite distance will not be exact due to measurement errors, and an uncertainty region on both sides of the estimated distance will be present. As shown in Figure 3(a), if the two satellites are spread out, the size of the uncertainty area will be small, resulting in good satellite geometry. On the other hand, if the satellites are close to each other (Figure 3(b)), the size of the uncertainty area will be large, resulting in poor satellite geometry.

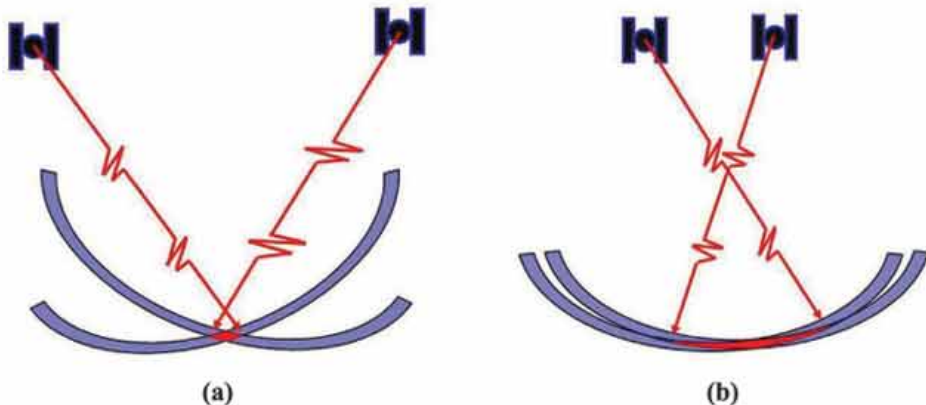


Figure 3: Examples of (a) good and (b) bad satellite geometries (Leonard, 2002).

The DOP value is computed based on relative receiver-satellite geometry at any instance. Low DOP values indicate good satellite geometry, and vice versa. As a result of relative motion of the satellites and the receiver, the DOP value will change over time. However, these changes will generally be slow, except in cases of (DOD, 2001; USACE, 2003; Kaplan & Hegarty, 2006; Huihui *et al.*, 2008):

- a. Satellites rising or falling, as tracked by the receiver
- b. Obstructions between the receiver and the satellite (such as passing through a tunnel).

There are various DOP forms, depending on the user's requirements. Position dilution of precision (PDOP), the most commonly used DOP to determine GNSS accuracy, represents the effect of satellite geometry on 3D positioning precision. PDOP can be broken into two components; horizontal dilution of precision (HDOP) and vertical dilution of precision (VDOP). HDOP and VDOP represent the effect of satellite geometry on the horizontal and vertical components, respectively, of positioning precision. As GNSS receivers can only track satellites above the horizon, VDOP will always be larger than HDOP. Hence, the GNSS height solution is expected to be less precise than the horizontal solution (DOD, 2001; USACE, 2003; Kaplan & Hegarty, 2006; Huihui *et al.*, 2008).

A PDOP value of 1 is associated with an ideal arrangement of the satellite constellation. To ensure high-precision GPS positioning, a PDOP value of 5 or less is usually recommended. In practice, the actual PDOP value is usually much less than 5, with a typical average value in the neighbourhood of 2. GNSS performances for HDOP and VDOP are normally in the 2-3 and 3-4 ranges respectively. In most cases, VDOP values will closely resemble PDOP values (DOD, 2001; USACE, 2003; Kaplan & Hegarty, 2006; Huihui *et al.*, 2008).

UERE is the total expected magnitude of position errors due to measurement uncertainties from the various error components for a particular receiver. UERE is divided into two components; user range error (URE) and user equipment error (UEE). URE is the sum of satellite-dependent errors, including ionospheric and tropospheric delays, and satellite clock and ephemeris errors. UEE is the sum of receiver-dependent errors, including receiver noise, multipath and antenna orientation (DOD, 2001; USACE, 2003; Kaplan & Hegarty, 2006; Worley, 2007).

Estimate probable error (EPE), horizontal probable error (HPE) and vertical probable error (VPE) are computed by multiplying PDOP, HDOP and VDOP, respectively, with UERE. EPE gives a 3D confidence ellipsoid that depicts uncertainties in all three coordinates, while HPE and VPE give the accuracy of the horizontal and height solutions respectively. Given the continuously changing DOP values, due to varying satellite geometry, GPS accuracy is time / location dependent (DOD, 2001; USACE, 2003; Kaplan & Hegarty, 2006).

3. METHODOLOGY

3.1 Preliminary Preparation

The Trimble Planning software (Trimble, 2009) was employed to estimate the GPS satellite coverage in the test area on 8th April 2010. It was observed that the period of the test, 0900 – 1100, coincided with a period of good GPS coverage (Figure 4), with high satellite visibility (9-12 satellites), and low HDOP (0.67-0.87), VDOP (1.34-1.56) and PDOP (1.48-1.78) values. Nevertheless, Trimble Planning only takes into account estimated satellite positions and geometry, and does not consider other sources of GNSS errors, including ionospheric and tropospheric delays, satellite clock, ephemeris and multipath errors, and unintentional signal interferences and obstructions. Furthermore, the parameters of elevation cutoff and

obstacles were estimated from 30 m resolution terrain models, which do not take into consideration man-made structures, and thereby, are subject to errors.

It should also be noted that the DOP values provided by Trimble Planning are best case estimates of GNSS coverage in a particular region. The actual DOP values obtained by a particular GNSS receiver are dependent on its sensitivity and the strength of GNSS signals received.

3.2 Test Procedure

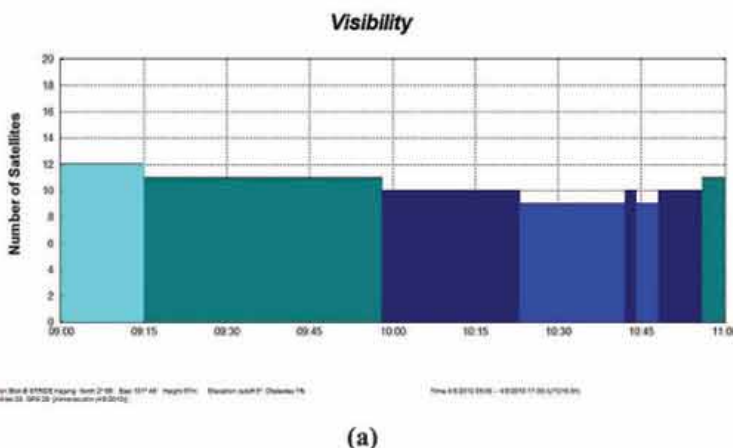
The apparatus used in the test were an Advantest U3751 spectrum analyser (Advantest, 2009), an IFR 2023B signal generator (IFR, 1999), a Hyperlog 60180 directional antenna (Aaronia, 2009), a notebook running GPS Diagnostics v1.05 (CNET, 2004) and a Garmin GPSmap 60CS handheld receiver (Garmin, 2004) (used as a reference). The test setup employed is an in Figure 5.

The signals in the frequency range of 1,560 - 1,590 MHz are measured. A location fix is obtained using the reference and evaluated GPS receivers, and the corresponding HPE, VPE and EPE values are recorded.

The antenna is placed 3 m away from the GPS receivers. An FM signal is transmitted with:

- Carrier wave frequency: 1,575.42 MHz
- Peak deviation: 1 MHz
- Information frequency: 5 kHz

Transmission is started at power level of -70 dBm. The corresponding HPE, VPE and EPE values are recorded. The step is repeated for power levels in the range of -70 to -30 dBm (increments of 1 dBm). The test is then repeated four times.



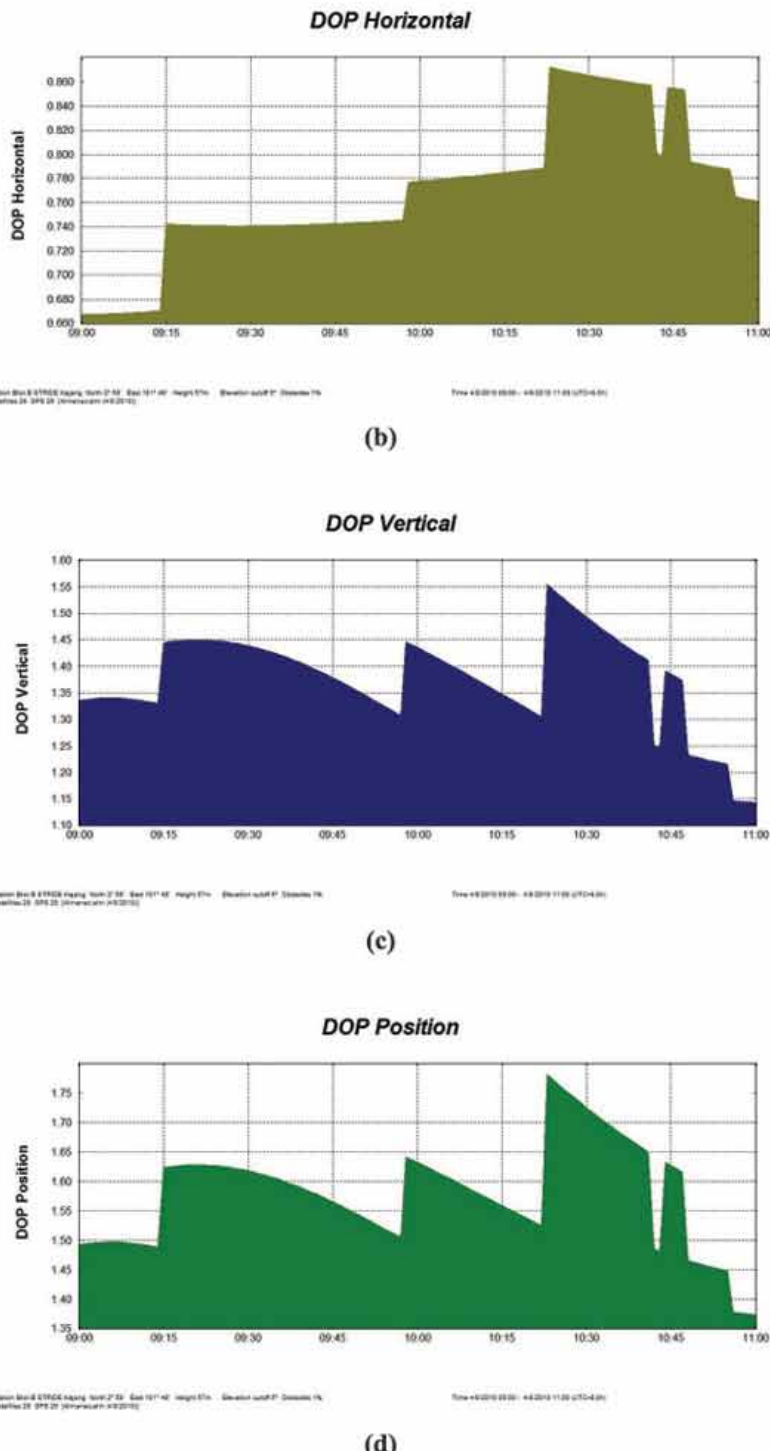


Figure 4: GPS coverage in the test area during the test period (8th April 2010, 0900 - 1100): (a) Satellite visibility (b) HDOP (c) VDOP (d) PDOP
(Screen captures from the Trimble Planning software).

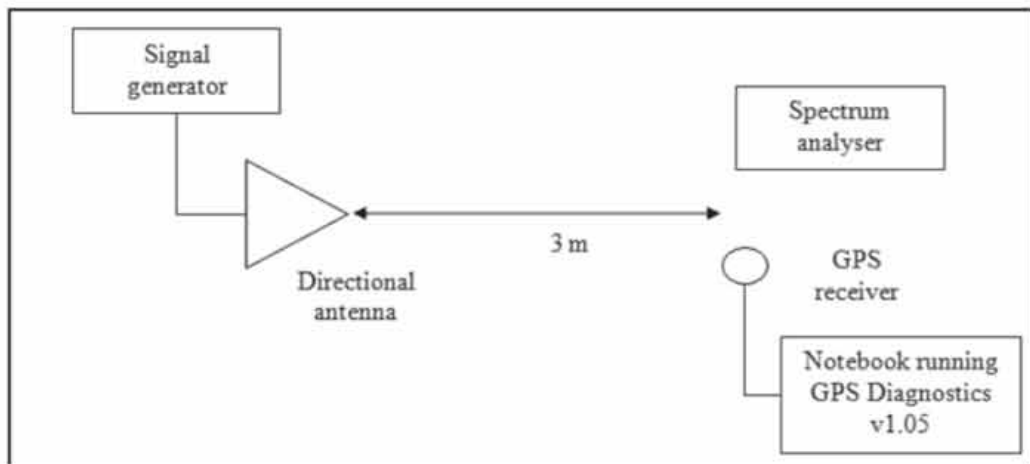


Figure 5: The test setup.

4. RESULTS

No discernible signals were observed in the range of 1,560 - 1,590 MHz (Figure 6(a)). However, it should be noted that the spectrum analyser was only able to measure received signals above -80 dBm, well over the minimum power levels required to jam GNSS signals. It is unknown if there are any unwanted interference signals below this threshold.

For the transmitted signal, at power level of 13 dBm, the received signal at distance of 3 m is shown in Figure 6(b). The measured signal is used to estimate received power levels which were too low to be measured with the spectrum analyser (appendix).

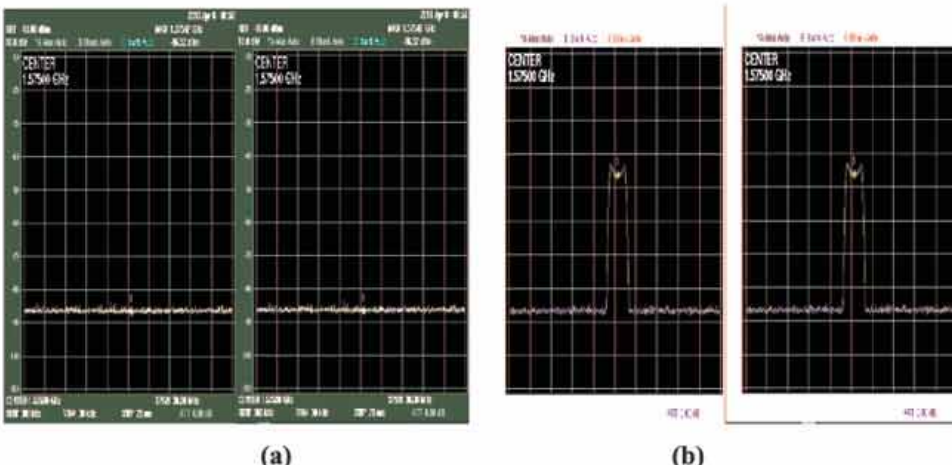


Figure 6: Advantest U3751 spectrum analyser readouts: (a) Frequency range of 1,560 - 1,590 MHz (no signals transmitted). (b) Received signal, at a distance of 3 m, for interference signals transmitted at power level of 13 dBm.

Prior to transmission of interference signals, the evaluated GPS receiver recorded lower probable error values compared to the reference GPS receiver (Table 1). This occurred as the evaluated GPS receiver has higher receiver sensitivity, and hence, was able to obtain lower PDOP values. In addition, it has lower receiver noise, reducing the value of its UERE. It is observed that the corresponding initial probable error values differed for each reading due to varying GPS coverage.

In general, it is expected that higher values of PDOP will result in higher values of probable errors. For the first four readings in Table 1, having PDOP values within the range of 0.07, the probable error values were mixed. While Readings 3 and 4 had almost similar PDOP values, Reading 4 recorded much higher probable error values. Reading 5, having the highest PDOP value, recorded the highest probable error values.

Table 1: HPE, VPE and EPE values prior to transmission of interference signal.

Reading	Start time	PDOP	Probable error (m)					
			Evaluated GPS			Reference GPS		
			HPE	VPE	EPE	HPE	VPE	EPE
1	0857	1.49	3.0	4.6	5.5	9.6	13.5	16.6
2	0915	1.48	4.0	5.6	6.9	13	14.2	19.3
3	0944	1.57	3.0	4.6	5.5	7.8	11.1	13.6
4	1011	1.56	5.1	7.3	8.9	15.3	22.5	27.2
5	1023	1.78	5.7	10.6	12.0	12.7	33.5	35.8

It is important to reiterate that the estimated PDOP values were based on 30 m resolution terrain models, which do not contain man-made structures or trees. The Block B building and trees in the vicinity of the test area could have resulted in the actual PDOP values being significantly different from the estimate values. Furthermore, other GNSS error parameters, including ionospheric and tropospheric delays, and satellite clock, ephemeris and multipath errors could have affected the location fix accuracy.

For the interference signal power levels evaluated in the test, the recorded probable error values are shown in Figures 7 and 8.

5. DISCUSSION

For both GPS receivers, as expected, the probable error values increased as the interference power level was increased, until the GPS receiver was completely jammed. The jamming threshold was different for the five readings due to varying GPS coverage, which also caused slight fluctuations in the trend of plots.

As shown in Table 2, as expected, the evaluated GPS receiver, having higher receiver sensitivity, required higher interference power levels for it to be jammed, as compared to the reference GPS receiver (Readings 1-4). However, for Reading 5, there was a discrepancy; the reference GPS required higher interference power level to be jammed compared to the evaluated GPS receiver. This could be due to improving GPS coverage during the period of the reading (Figure 2(d), 1023-1040). No clear correlation is observed between the minimum jamming power levels and the PDOP values, as the former is also a function of the various other error parameters.

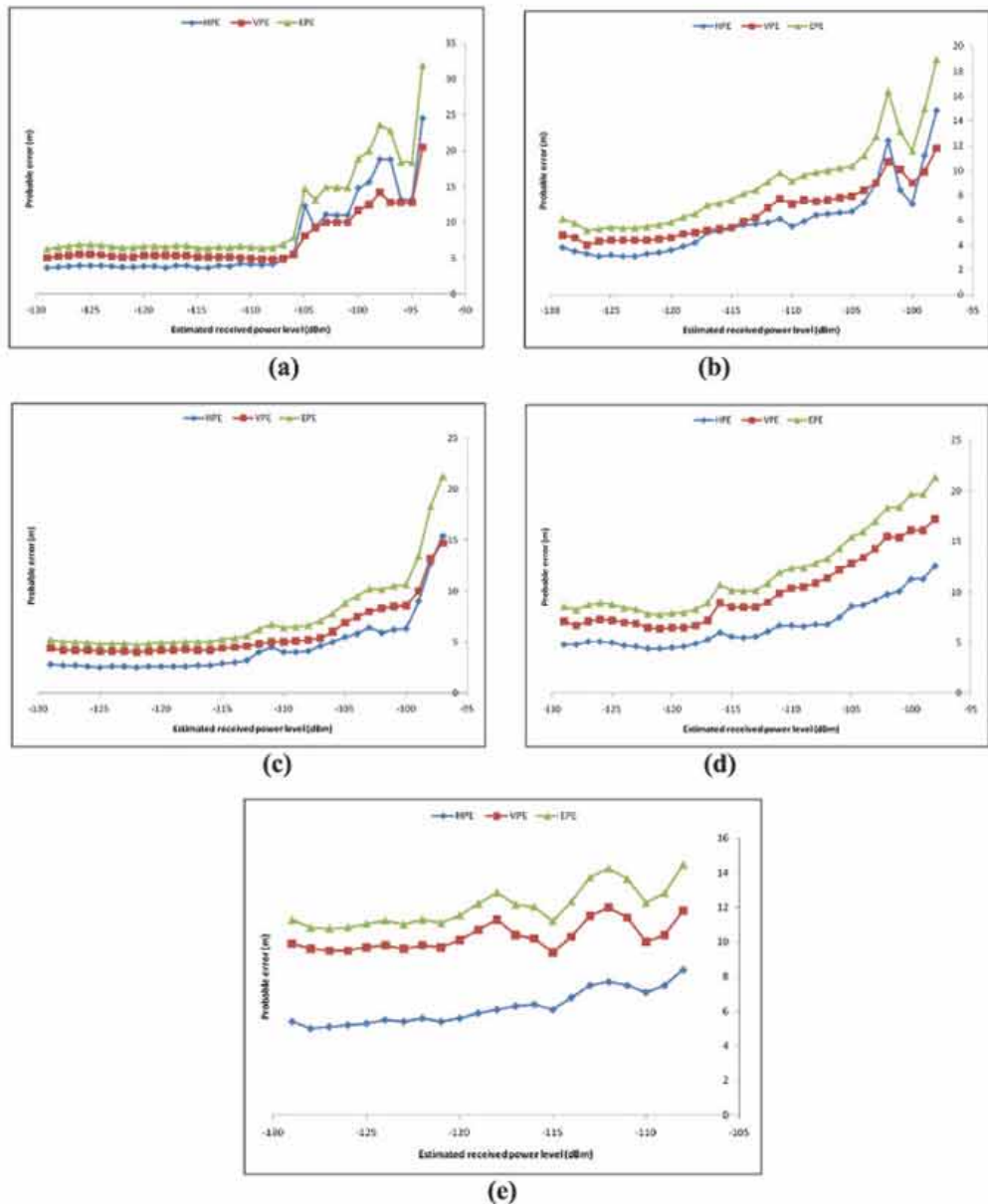


Figure 7: Measured probable error values for the evaluated GPS receiver. (a) Reading 1 (b) Reading 2 (c) Reading 3 (d) Reading 4 (e) Reading 5.

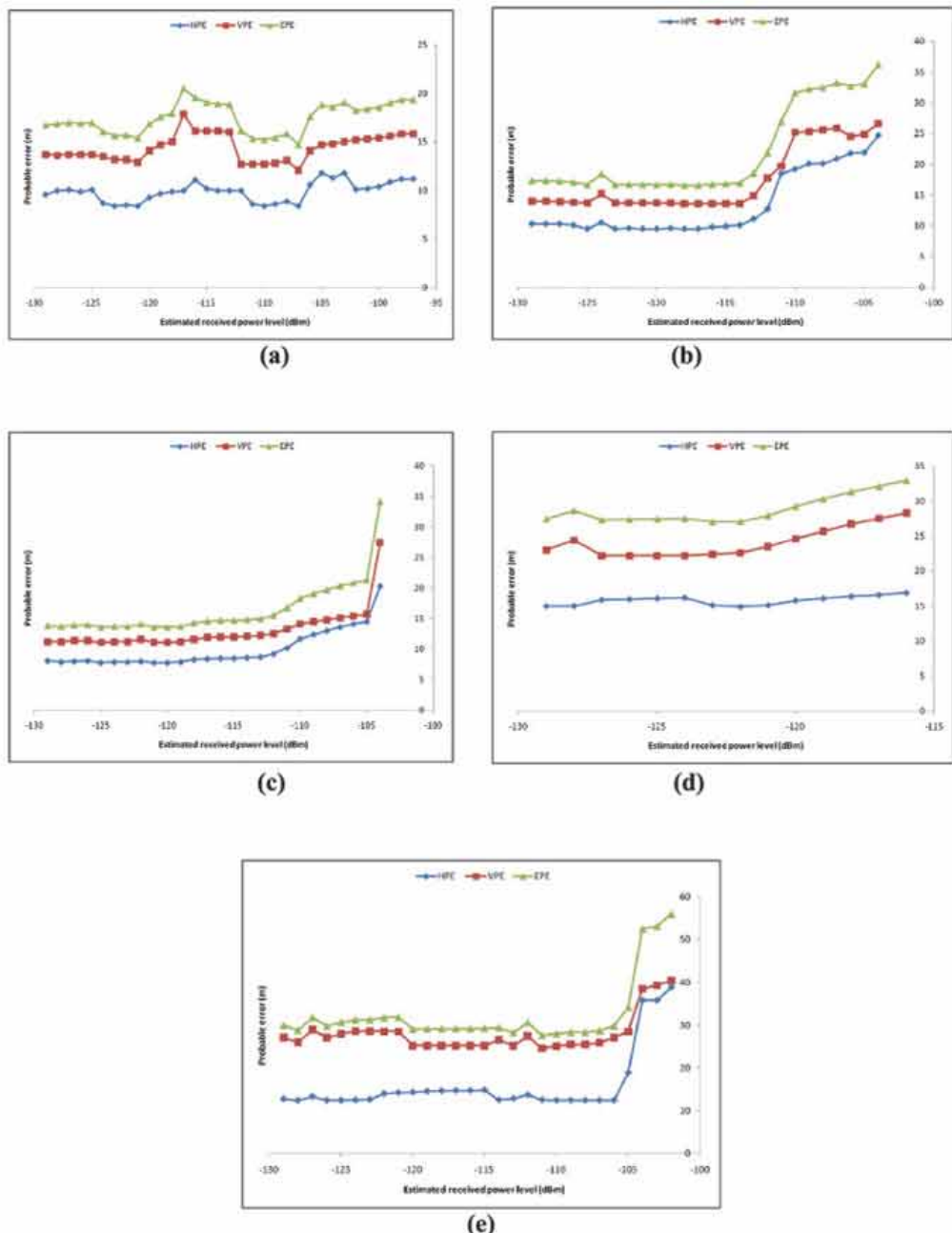


Figure 8: Measured probable error values for the referee GPS receiver. (a) Reading 1 (b) Reading 2 (c) Reading 3 (d) Reading 4 (e) Reading 5.

Table 2: Minimum received interference power levels required to jam the GPS receivers.

Reading	Start time	PDOP	Power level (dBm)	
			Evaluated GPS	Reference GPS
1	0857	1.49	-93.99	-96.99
2	0915	1.48	-97.99	-103.99
3	0944	1.57	-96.99	-103.99
4	1011	1.56	-97.99	-115.99
5	1023	1.78	-107.99	-101.99

The maximum probable errors prior to location fix loss (Table 3) and increases of probable error values (Table 4) also varied significantly with each reading. It is expected that higher PDOP values would result in higher maximum probable error values, and hence, higher increases of probable error values.

For the reference GPS receiver, the lowest maximum probable error values were obtained for the reading with one the lowest PDOP values (Reading 1), while the highest maximum probable error values were obtained for one of the highest PDOP values (Reading 5).

However, significant discrepancies were observed for the evaluated GPS receiver; the highest maximum probable error values were obtained for the reading with one the lowest PDOP values (Reading 1), while the lowest maximum probable error values were obtained for one of the highest PDOP values (Reading 5). This could be due to the varying GPS coverage while the readings were being taken, in addition to the various error parameters.

Table 3: Maximum probable errors for the GPS receivers prior to location fix loss.

Reading	Start time	PDOP	Probable error (m)					
			Evaluated GPS			Reference GPS		
			HPE	VPE	EPE	HPE	VPE	EPE
1	0857	1.49	24.5	20.5	31.9	11.2	15.8	19.4
2	0915	1.48	14.8	11.8	18.9	24.7	26.6	36.3
3	0944	1.57	15.4	14.7	21.3	20.3	27.5	34.2
4	1011	1.56	12.6	17.2	21.3	16.9	28.3	33.0
5	1023	1.78	8.4	11.8	14.5	38.9	40.4	56.1

Table 4: Differences between the initial and pre-location fix loss probable errors for each reading for the GPS receivers.

Reading	Start time	PDOP	Probable error (m)					
			Evaluated GPS			Reference GPS		
			HPE	VPE	EPE	HPE	VPE	EPE
1	0857	1.49	21.5	15.9	26.4	1.6	2.3	2.8
2	0915	1.48	10.8	6.2	12.0	11.7	12.4	17
3	0944	1.57	12.4	10.1	15.8	12.5	16.4	20.6
4	1011	1.56	7.5	9.9	12.4	1.6	5.8	5.8
5	1023	1.78	2.7	1.2	2.5	26.2	6.9	20.3

There was a fundamental difference observed in the plots of the evaluated and reference GPS receivers. For the reference receiver, the VPE values were always significantly higher than the HPE values. For the evaluated receiver, the VPE and HPE values were much closer, with a number of occurrences where the HPE values were larger than the VPE values. The reference GPS receiver, having lower receiver sensitivity, had much better horizontal component accuracy as compared to the vertical component. For the evaluated receiver, with higher receiver sensitivity, while the horizontal accuracy is still higher, the difference with vertical component is much smaller. During the jamming test, at some points, depending on GPS coverage, the horizontal component accuracy became lower than the vertical component.

On the whole, this test has demonstrated the disadvantages of field GNSS evaluations. Without the ability to control the various GNSS error parameters, it is difficult to effectively study the effect of any particular error parameter, in the case of this test, interference, on GNSS accuracy. This highlights the importance of using a GNSS simulator for such tests, whereby the tests could be done under repeatable user-controlled conditions. The advantages of GNSS simulators, as compared to field evaluations, are discussed in Dinesh *et al.* (2009b) and Petrovski *et al.* (2010).

6. CONCLUSION

The results of this test have demonstrated that interference signals that are insufficient to jam a GPS receiver can still cause significant reduction in GPS accuracy. Increase in transmitted interference signal power level results in increase in probable error values of the location fixes, until the GPS receiver is completely jammed. The amount of increase of probable error values, and the minimum jamming power levels vary significantly based on GPS coverage and various error parameters, including ionospheric and tropospheric delays, and satellite clock, ephemeris and multipath errors. Due to the disadvantages of field GNSS evaluations, this test should be repeated using a GNSS simulator to ensure that more accurate results are obtained.

ACKNOWLEDGEMENT

The authors are grateful to Dr. Mahdi Che Isa, Head of the Ships Technology Branch, Science & Technology Research Institute for Defence (STRIDE), Ministry of Defence, Malaysia, for his suggestions that have helped improved this manuscript.

REFERENCES

- Aaronia, (2009). *Precompliance Test Antenna Series HyperLOG® 60xxx: Span 680 MHz to 18 GHz*. Aaronia AG, Strickscheid, Germany.
- Adams, T.K. (2001). GPS Vulnerabilities. *Mil. Rev.*, **1**: 10-16.
- Advantest (2009). *U3741/3751 Spectrum Analyzers*. Advantest Corporation, Chiyoda-ku, Tokyo
- Agilent (2008). *Typical GPS Receiver Verification Tests Using a GPS Signal Simulator*. Agilent Technologies, Santa Clara, California.
- Casabona, M.M. & Rosen, M.W. (1999). Discussion of GPS anti-jam technology. *GPS Sol.*, **2**: 18-23.
- CNET (2004). GPSDiag 1.0. Available online at: http://download.cnet.com/GPSDiag/3000-2130_4-4951103.html (Last access date: 31st January 2010).
- Department of Army (DOA) (2009). *Electronic Warfare in Operations*. Army Field Manual 3-36, Department of Army, Washington D.C.
- Department of Defence (DOD) (2001). *Global Positioning System Standard Positioning Service Performance Standard. Command, Control, Communications, and Intelligence*. Department of Defence (DOD), Washington D.C.
- Deshpande, S.M. (2004). *Study of Interference Effects on GPS Signal Acquisition*. Masters thesis, University of Calgary, Calgary, Alberta.
- Dinesh, S. (2009). Vulnerabilities of civilian Global Navigation Satellite Systems (GNSS) signals: A review. *Defence S&T Tech. Bull.*, **2**: 100-114.
- Dinesh , S., Wan Mustafa, W.H., Mohd Faudzi., M., Kamarulzaman, M., Nor Irza Shakhira, B., Siti Robiah, A., Norhayaty, Z., Aliah, I., Lim, B.T., Arumugam, P., Zainal Fitry, M.A., Mohd. Rizal, A.K., Azlina, B. & Mohd. Hasrol, H.M.Y. (2009a). Evaluation of the effect of radio frequency interference (RFI) on Global Positioning System (GPS) Receivers. *Defence S&T Tech. Bull.*, **2**: 115-129.
- Dinesh , S., Wan Mustafa, W.H., Mohd Faudzi., M., Kamarulzaman, M., Nor Irza Shakhira, B., Siti Robiah, A., Norhayaty, Z., Aliah, I., Lim, B.T., Arumugam, P., Zainal Fitry, M.A., Mohd. Rizal, A.K., Azlina, B. & Mohd. Hasrol, H.M.Y. (2009b). The advantages of Global Navigation Satellite Systems (GNSS) receiver evaluation using GNSS simulators. *BUDI*, **2009**: 6-10.

- Dinesh , S., Wan Mustafa, W.H., Mohd Faudzi, M., Kamarulzaman, M., Nor Irza Shakhira, B., Siti Robiah, A., Norhayaty, Z., Aliah, I., Lim, B.T., Arumugam, P., Zainal Fitry, M.A., Mohd. Rizal, A.K., Azlina, B. & Mohd. Hasrol, H.M.Y. (2010a). *MRSS 6th International Remote Sensing & GIS Conference & Exhibition*, 28th-29th April 2010, Putra World Trade Center (PWTC), Kuala Lumpur.
- Dinesh , S., Wan Mustafa, W.H., Mohd Faudzi, M., Kamarulzaman, M., Hasniza, H., Nor Irza Shakhira, B., Siti Robiah, A., Shalini, S., Jamilah, J., Aliah, I., Lim, B.T., Zainal Fitry, M.A., Mohd. Rizal, A.K., Azlina, B. & Mohd. Hasrol, H.M.Y. (2010b). Evaluation of Power Levels Required by Interference Signals at Various Distances to Jam the Global Positioning System (GPS) L1 Coarse Acquisition (C/A) Signal. *Defence S&T Tech. Bull.*, 3: 14-28.
- Federal Aviation Administration (FAA) (1996). *Airborne Supplemental Navigation Equipment Using the Global Positioning System (GPS)*. Technical Standard Order (TSO) C129a, Federal Aviation Administration (FAA), Department of Transport, Washington D.C.
- Forssell, B. (2005). GPS/GNSS indoors: Possibilities and limitations. *GPS/GNSS Seminar of the Swedish National Survey*, March 2005, Gävle, Sweden.
- Gakstatter, E. (2008). Introduction to GNSS. *GNSS Technology Workshop*, 10th-12th December 2008, Institut Tanah Dan Ukur Negara (INSTUN), Behrang, Perak.
- Garmin (2004). *GPSmap 60CS Owner's Manual*. Garmin International Inc., Olathe, Kansas.
- Garmin (2007). *GPSmap 60CSx Owner's Manual*. Garmin International Inc., Olathe, Kansas.
- Gautier, J. (2003). *GPS/INS Generalized Evaluation Tool (GIGET) for the Design and Testing of Integrated Navigation Systems*. PhD thesis, Stanford University, Palo Alto, California.
- Gibbons, G. (2010). Service and security: The vulnerability of our timing and transportation infrastructure. *Inside GNSS*, 5: 8.
- Government Accountability Office (GAO) (2009). *Global Positioning System: Significant Challenges in Sustaining and Upgrading Widely Used Capabilities*. Report to the Subcommittee on National Security and Foreign Affairs, Committee on Oversight and Government Reform, House of Representatives, Government Accountability Office (GAO), U.S.
- Grant, A., Williams, P., Ward, N. and Basker, S. (2009). GPS jamming and the impact on maritime navigation. *J. Navigation*, 62: 173-187.
- Groves, P.D. (2010). Positioning, navigation and timing without using GNSS. *GPS Jamming & Interference: A Clear and Present Danger*, 23rd February 2010, National Physics Laboratory, Teddington.
- Gustafson, D., Dowdle, J. and Flueckiger, K. (2000). A high anti-jam GPS-based navigator. *Proceedings of the Institute of Navigation*, 28th-30th June 2000, Cambridge, Massachusetts.

- Harding, S.J. (2001). *Vulnerability Assessment of the Transport Infrastructure Relying on the Global Positioning System*. QinetiQ Group, Buckingham Gate, London.
- Huihui, W., Xingqun, Z. & Yanhua, Z. (2008). Geometric dilution of precision for GPS single-point positioning based on four satellites. *J. Syst. Eng. Electr.*, **19**: 1058-1063.
- IFR (1999). *2023A/B, 2025 Signal Generators*. IFR Americas Inc., Wichita, Kansas
- Institute for Defense Analyses (IDA) (2009). *Independent Assessment Team (IAT): Summary of Initial Findings on eLoran*. Institute for Defense Analyses (IDA), Alexandria, Virginia.
- Institute of Navigation (ION) (1997). *Institute of Navigation Standard 101 (ION STD 101): Recommended Test Procedures for GPS Receivers, Revision C*. Institute of Navigation (ION), Manassas, Virginia.
- International Association of Marine Aids to Navigation and Lighthouse Authorities (IALA) (2009). *IALA World Wide Radio Navigation Plan*. International Association of Marine Aids to Navigation and Lighthouse Authorities (IALA), Saint Germain en Laye, France.
- Jewell, J. (2007). *GPS Insights*. Available online at: <http://www.gpsworld.com/defense/gps-insights-april-2007-8428> (Last access date: 17th November 2009).
- Johnston, R.G. & Warner, J.S. (2004). Think GPS offers high security? Think again! *Business Contingency Planning Conference*, 23rd-27th May 2004, Las Vegas, Nevada.
- Joint Chief of Staffs (JCS) (2007). *Geospatial Electronic Warfare*. Joint Publication 3-13.1, Joint Chief of Staffs, USA.
- Gautier, J. (2003). *GPS/INS Generalized Evaluation Tool (GIGET) for the Design and Testing of Integrated Navigation Systems*. PhD thesis, Stanford University, Palo Alto, California.
- Gibbons, G. (2010). *Service and security: The vulnerability of our timing and transportation infrastructure*. Inside GNSS, **5**: 8.
- Government Accountability Office (GAO) (2009). *Global Positioning System: Significant Challenges in Sustaining and Upgrading Widely Used Capabilities*. Report to the Subcommittee on National Security and Foreign Affairs, Committee on Oversight and Government Reform, House of Representatives, Government Accountability Office (GAO), U.S.
- Grant, A., Williams, P., Ward, N. and Basker, S. (2009). GPS jamming and the impact on maritime navigation. *J. Navigation*, **62**: 173-187.
- Groves, P.D. (2010). Positioning, navigation and timing without using GNSS. *GPS Jamming & Interference: A Clear and Present Danger*, 23rd February 2010, National Physics Laboratory, Teddington.
- Gustafson, D., Dowdle, J. and Flueckiger, K. (2000). A high anti-jam GPS-based navigator. *Proceedings of the Institute of Navigation*, 28th-30th June 2000, Cambridge, Massachusetts.

- Palmer, J. (2010). *Sat-nav Systems Under Increasing Threat from 'Jammers'*. Available online at: <http://news.bbc.co.uk/2/hi/science/nature/8533157.stm> (Last access date: 24th February 2010).
- Pinker, A. and Smith, C. (2000). Vulnerability of GPS signal to jamming. *GPS Sol.*, 3: 19-27.
- Petrovski, I., Townsend, B. & Ebinuma, T. (2010). Testing multi-GNSS equipment: Systems, simulators and the production pyramid. *Inside GNSS*, 5: 52-61.
- Poisel, A.R. (2002). *Introduction to Communication Electronic Warfare Systems*. Artech House, Boston.
- Rash, G.D. (1997). *GPS Jamming in a Laboratory Environment*. Naval Air Warfare Center Weapons Division (NAWCWPNS), China Lake, California.
- Schwartz, N. (2010). The United States as an aerospace nation: Challenges and opportunities. *Tuft University Institute for Foreign Policy Analysis (IFPA) Fletcher Conference on National Security Strategy and Policy*, 20th-21st January 2010, The Ronald Reagan Building and International Trade Center, Washington, D.C.
- Science & Technology Research Institute for Defence (STRIDE) (2009a). *Evaluation of the Effect of Radio Frequency Interference (RFI) on the GPS L1 C/A Signal*. Science & Technology Research Institute for Defence (STRIDE), Ministry of Defence, Malaysia.
- Science & Technology Research Institute for Defence (STRIDE) (2009b). *Evaluation of Power Levels of Interference Signals Required to Jam the GPS L1 C/A Signal*. Science & Technology Research Institute for Defence (STRIDE), Ministry of Defence, Malaysia.
- Science & Technology Research Institute for Defence (STRIDE) (2010a). *Evaluation of Minimum Distances Required by Interference Signals of Various Power Levels to Jam the GPS L1 C/A Signal*. Science & Technology Research Institute for Defence (STRIDE), Ministry of Defence, Malaysia.
- Science & Technology Research Institute for Defence (STRIDE) (2010b). *Evaluation of Power Levels Required by Interference Signals at Various Distances to Jam the GPS L1 C/A Signal*. Science & Technology Research Institute for Defence (STRIDE), Ministry of Defence, Malaysia.
- Science & Technology Research Institute for Defence (STRIDE) (2010c). *Evaluation of Effective GPS Jamming Radiiuses for Interference Signals of Various Power Levels*. Science & Technology Research Institute for Defence (STRIDE), Ministry of Defence, Malaysia.
- Science & Technology Research Institute for Defence (STRIDE) (2010d). *Evaluation of the Effect of Radio Frequency Interference (RFI) on GPS Accuracy*. Science & Technology Research Institute for Defence (STRIDE), Ministry of Defence, Malaysia.
- US Army Corps of Engineers (USACE) (2003). *NAVSTAR Global Positioning System Surveying. Engineer Manual*. EM 1110-1-1003, US Army Corps of Engineers (USACE), Washington D.C.

- Trimble (2009). *Trimble's Planning Software*. Available online at: <http://www.trimble.com/planningsoftware.shtml> (Last access date: 17th November 2009).
- Weinstein, B., Akos, D., Vinande, E. and Chu, T. (2009). *GNSS Receiver Evaluation: Record-and-Playback Test Methods*. Available online at: <http://www.gpsworld.com/transportation/gnss-receiver-evaluation-9302> (Last access date: 6th March 2010).
- Wilde, W.D. and Willems, T. (2010). Designing GNSS receivers to mitigate against interference. *GPS Jamming & Interference: A Clear and Present Danger*, 23rd February 2010, National Physics Laboratory, Teddington.
- Williams, S.F. (2006). *Radar'd Out: GPS Vulnerable to High-Power Microwaves*. Available online at: <http://mg.gpsworld.com/gpsmg/article/articleDetail.jsp?id=320030> (Last access date: 17th November 2009).
- Worley, S. (2007). *GPS Errors & Estimating Your Receiver's Accuracy*. Available online at: http://edu-observatory.org/gps/gps_accuracy.html (Last access date: 29th January 2010).
- Zhuang, X., Cui, X., Lu, M. & Feng, Z. (2009). Reduced-rank space-time processing for anti-jamming GPS receivers. *Tsinghua Sci. Tech.*, **14**: 189-195.

APPENDIX

Estimation of received power:

P_T	:	Transmitter power
P_R	:	Receiver power
G_T	:	Transmitter gain
G_R	:	Receiver gain
L	:	Free-space path loss
L_E	:	External losses
R	:	Distance (km)
F	:	Frequency (MHz)
δ	:	FM signal peak deviation

$$P_R = P_T + G_T + G_R - L - L_E \quad (A1)$$

$$L = 32.44 + 20 \log R + 20 \log f \quad (A2)$$

Effective transmitted power $P_{T_{eff}}$:

$$P_{T_{eff}} = P_T + G_T \quad (A3)$$

Effective received power $P_{R_{eff}}$:

$$P_{R_{eff}} = P_R - G_R \quad (A4)$$

With L_E , R and f being constant:

$$P_{R_{eff}} = P_{T_{eff}} - L_O - G_R \quad (A5)$$

where:

$$L_O = 32.44 + 20 \log R + \log f + L_E \quad (A6)$$

For the directional antenna, $G_T = 5$ dBi.

For receiving antenna, $G_R = 1$ dBi.

For FM signal with bandwidth of 2 MHz, $P_{T_{eff}} = 18$ dBm and $P_R = -45.46$ dBm.

$$L_O = 18 - (-45.46) - 1 = 62.99 \text{ dBm} \quad (A7)$$

INVESTIGATION OF CARBON MONOXIDE (CO) LEVELS IN THE MAIN BATTLE TANK (MBT) PT-91M PENDEKAR DURING FIRING OF MAIN AND SMALL GUNS

Adam bin Hj Gani^{1*}, Abdul Hamid bin Hassan² & Shamsul Akmar Ab Aziz²

¹Acceptance of Samples & Inspections of Equipment Branch (CT&P), Procurement Division, Ministry of Defence, Malaysia

²Vehicle Branch, Technology and Aerospace Division, Science & Technology Research Institute for Defence (STRIDE), Ministry of Defence, Malaysia

*Email: ag_stride@yahoo.com

ABSTRACT

The firing of the Main Battle Tank (MBT) PT-91M Pendekar's main and small guns can cause the emission of carbon monoxide (CO) which can damage the crew members' health. This was highlighted in the incident that occurred in Poland on 23rd March 2008, in which two Malaysian Armed Forces (MAF) tank crew members fainted due to overexposure to CO during the firing of the main and small guns of the PT-91M. Hence, as a precautionary measure, the STRIDE Vehicle Branch was assigned to investigate CO levels in the tanks during a firing test which was conducted in the Gemas Army Camp for the fourth batch of delivery of PT91Ms. The Oldham MX21 Plus gas and flame detection analyser was used to measure the CO levels. A total of seven MBTs were monitored, with each vehicle firing nine bullets from the main gun continuously over two rounds of firing; six in the first and three in the second. The time was recorded and CO emission was checked. There was a dramatic increase of CO level after the first firing took place. The accumulation rate of CO was higher in the tanks compared to the removal rate of gas from the tank through the ventilation system. Further investigation is needed to improve the condition of the ventilation system.

Keywords: Carbon monoxide (CO); Main Battle Tank (MBT) PT91M Pendekar; tank firing test; armoured vehicle; CO effects.

1. INTRODUCTION

According to Koren & Bisesi (2002), the occupational environment can be simply defined as any place, indoors or outdoors, where people work in return for financial or other remuneration. The environmental hazards include chemical, physical, biological, ergonomic, mechanical, electrical, and psychological agents. Chemical hazards may become airborne in the form of dusts, mists, fibres, fumes, smoke, gases and vapours. A number of gases, such as carbon monoxide (CO), arsine (AsH_3) and chlorine trifluoride (ClF_3), are toxic and can cause death.

CO poisoning is dangerous not just within the home and office, but also inside vehicles. Up until the 1970s, CO pollution from automobiles was a big problem. However, in the 1970s, automobile manufacturers began to develop sophisticated systems that could reduce CO emission, cutting up to eight percent of pollution from cars and other vehicles (Silent-Shadow, 2000).

The issue of CO in tanks is not new; World War II experiences with CO were dominated by problems associated with large numbers of soldiers fighting in armoured fighting vehicle (AFVs) (Cleator, 1967; Bean, 1968; Weyandt & Ridgeley, 1993). For example, Nelson *et al.* (1944) reported that the peak levels of CO recorded after the firing of five rounds from the 75 mm gun of the M3A4 tank was found to have increased rapidly to 0.718% within 1 minute. This shows that CO levels in tanks is critical and needs to be monitored.

Due to the increasing numbers of deployments of military personnel in AFVs, problems related to CO exposure remains an important issue (Weyandt & Ridgeley, 1993). Geddie (1984) reported on unusual exposure to CO during the operational test of the M1E1 tank. The firing portion of the exercise included the firing of 13 main gun rounds and approximately 100 coaxial machine gun rounds. After performing the exercise, the tank's commander and loader experienced physical distress and had to be taken to a hospital. The carboxyhemoglobin levels of the tank's crew members were obtained during the subsequent medical evaluation. The tank's commander and loader had very high levels of carboxyhemoglobin; 27.8 % and 33 % respectively.

In the Main Battle Tank (MBT) PT-91M Pendekar, CO is emitted by the engine through the exhaust and from the burning process during gun firings. The main concern here is that the burning fumes are disbursed into the crew compartment creating an accumulation of gases inside the vehicle. This will expose the crew members to hazardous gases such as CO. In an incident which occurred in Poland on 23rd March 2008, two Malaysian Armed Forces (MAF) tank crew members fainted due to overexposure to CO during the firing of the main and small guns of the PT-91M (Abdullah, 2008).

Consequently, the Vehicle Branch, Science & Technology Research Institute for Defence (STRIDE) was requested to investigate the levels of CO inside the tank during a firing test which was conducted in the Gemas Army Camp. The results of the investigation would then be used for further action on improvements by the manufacturer.

2. CARBON MONOXIDE (CO)

CO is a poisonous, colourless, odourless, and tasteless gas. Due to its high inherent toxicity and extensive exposure potential, CO has historically been considered not only the most widespread poison known but also the most significant toxic gas in the workplace (Weyandt & Ridgeley, 1993). CO poisoning is a common industrial hazard which results from the incomplete burning of natural gases and any other material containing carbon, such as gasoline, kerosene, oil, propane, coal and wood. While forges, blast furnaces and coke ovens emit CO, one of the most common

sources of CO exposure in the workplace is internal combustion engines (USDOL, 2002). Koren & Bisesi (2002) stated that a major source of carbon monoxide is motor vehicles that burn fuel inefficiently during start up, idling or moving slowly in congested traffic.

CO inhibits the blood's ability to carry oxygen to body tissues, including vital organs such as the heart and brain. When CO is inhaled, it combines with the oxygen-carrying hemoglobins of the blood to form carboxyhemoglobin (COHb). These hemoglobins will no longer be able to transport oxygen, depriving the heart, brain and other vital organs of oxygen. The rate of COHb build-up is dependent on the concentration of CO being inhaled (measured in parts per million or ppm) and the duration of the exposure. Compounding the effects of the exposure is the long half-life of COHb in the blood. Half-life is a measure of time required for hemoglobin levels to return to normal. The half-life of COHb is approximately five hours. This means that for a given exposure level, it will take about five hours for the level of COHb in the blood to drop to half its current level after the exposure is terminated (Brandon, 1995).

The initial symptoms of CO poisoning may include headache, fatigue, dizziness, drowsiness and nausea. During prolonged or high exposures, the symptoms may worsen and include vomiting and confusion, and in addition to loss of consciousness, suffocation and muscle weakness (USDOL, 2002). These symptoms are summarised in Table 1.

Table 1: Symptoms of CO exposure (Brandon, 1995)

CO Concentration (PPM)	Time	Symptoms
35	8 hours	Maximum exposure allowed by OSHA in the workplace over an eight hour period.
200	2-3 hours	Mild headache, fatigue, nausea and dizziness.
400	1-2 hours	Serious headache; other symptoms intensify. Life threatening after 3 hours.
800	45 minutes	Dizziness, nausea and convulsions. Unconscious within 2 hours. Death within 2-3 hours.
1600	20 minutes	Headache, dizziness and nausea. Death within 1 hour.
3200	5-10 minutes	Headache, dizziness and nausea. Death within 1 hour.
6400	1-2 minutes	Headache, dizziness and nausea. Death within 25-30 minutes.

3. METHODOLOGY

A total of seven MBTs were monitored, with each vehicle firing nine bullets from the main gun continuously over two rounds of firing; six in the first and three in the second. The Oldham MX21 Plus gas and flame detection analyser was used to measure the CO levels in the tank. For the purpose of comparison, tanks ZC393, ZC395 and ZC399 were measured with open hatches, while tanks ZC403, ZC396, ZC402 and ZC394 were measured with closed hatches.

The Oldham gas detector was placed at the gunner compartment and was monitored by the gunner. The equipment was switched on at least one minute before the firings take place. The level of CO emission was recorded.

During the measurement, three approaches were used to identify the differences of CO level in varying firing conditions. In the first approach, the equipment was placed for a period of five hours inside three tanks, ZC393, ZC399 and ZC403. The hatch of ZC403 was closed. During that period of time, the firing of 6 bullets from the main gun was carried out.

The second approach was carried out by measuring the level of CO during the firing of 6 bullets from the main gun within 10 minutes on four vehicles, ZC396, ZC 402, ZC395 and ZC 394. All hatches of the tanks were closed, except for ZC395. The third approach was to measure the level of CO inside the four tanks during the firing of 3 bullets from the small gun within 5 minutes.

4. RESULTS & DISCUSSION

From the results shown in Table 2, for all three approaches of firing, the tanks with closed hatches had significantly higher levels of CO as compared to tanks with opened hatches. This occurred as the closed hatch disallows the burning fume from the firings to escape from the tank, resulting in accumulation of CO, and hence, an increase in the CO level.

The results also show that, when the hatch is closed, accumulation of CO increases when a longer time is taken for the firing. The gases were trapped due to the poor ventilation system which was unable to neutralise the air in the tank. The ventilation system needs to be improved in order to increase its efficiency.

5. CONCLUSION

The concentration of CO when the hatch is closed shows that the ventilation inside the tank is not enough when high rates of released CO is disbursed into the tank compartment during firing. Further investigations need to be carried out to study the capacity of the ventilation system in sucking out the accumulated CO. Some modifications need to be made immediately if the ventilation system is found to be not working properly. This is very important because exposure to more than 400 ppm of CO may result in death. The results can also be used to provide recommendations to the MAF on solutions to overcome the problem, and also on awareness on safety and health practices. Engineering control methods, such as

appropriate process design, automation, guarding, shielding, grounding and ventilation (Koren & Bisesi, 2002), must be taken into consideration to overcome the problem.

Table 2: Accumulative CO in the tanks.

MBT Tank PT91	Carbon Monoxide (CO) Level (PPM)		
	Firing 6 bullets from main gun within 5 hours	Firing 6 bullets from main gun within 10 minutes	Firing 3 bullets from small gun within 5 minutes
ZC393 (Opened Hatch)	51	-	-
ZC399 (Opened Hatch)	67	-	-
ZC395 (Opened hatch)	-	82	45
ZC403 (Closed Hatch)	417	-	-
ZC396 (Closed Hatch)	-	140	72
ZC402 (Closed Hatch)	-	113	61
ZC394 (Closed Hatch)	-	167	58

ACKNOWLEDGEMENT

This research was conducted when the first author was with the Science & Technology Research Institute for Defence (STRIDE).

REFERENCES

- Abdullah, L.C. (2008). First author's interview with the PT-91M tank Project Leader on the PT-91M tank accident.
- Bean, W.B. (1968). The ecology of the soldier in World War II. *Trans. Am. Clin. Climatol. Assoc.*, 79: 1-12.
- Brandon, H. (1995). *About Carbon Monoxide*. Available online at: <http://www.aboutcarbonmonoxide.com/articles/volunteerfd.htm> (Last access date: 1st June, 2009).
- Cleator, P.E. (1967). *Weapons of War*. Robert Hale, London.

- Geddie, J.C. (1984). *MIE1 Carbon Monoxide Exposure Incident*. US Army Human Engineering Laboratory, Liaison Office (TCATA), Fort Hood, Texas.
- Koren, H. & Bisesi, M.S. (2002). *Handbook of Environmental Health*. Lewis Publishers Boca Raton.
- United States Department of Labor (USDOL) (2002). *Carbon Monoxide Poisoning*. Available online at: http://www.osha.gov/OshDoc/data_General_Facts/carbonmonoxide-factsheet.pdf (Last access date: 28th May, 2009)
- Nelson, N., Walpole, R.H. & Swigert, T.C. (1944). *Carbon Monoxide Hazard from Exhaust Gases in Tanks That Are in Tow*. Armored Medical Research Laboratory Fort Knox, Kentucky.
- Silent-Shadow (2000). *Carbon Monoxide in Your Vehicle*. Available online at: <http://www.silentshadow.org/carbon-monoxide-in-your-car.html>. (Last access date: 29th May 2009).
- Weyandt, T.B. & Ridgeley, C.D. (1993). Carbon monoxide. In Deeter, D.P. & Gaydos, J.C. (Eds.), *Occupational Health: The Soldier and the Industrial Base*. Office of the Surgeon General, U.S. Department of the Army, Falls Church, Virginia, pp. 397-427.

SIMULATION

Nor Hafizah Mohamed

Research and Strategic Studies Branch, Human Resources and Technical Support Division, Science & Technology Research Institute for Defence (STRIDE), Ministry of Defence, Malaysia

Email: norhafizah.mohamed@stride.gov.my

ABSTRACT

Simulation is one of the most powerful tools available to decision-makers responsible for the design and operation of complex processes and systems. The purpose of this paper is to discuss the concept and approach of simulation as a problem solving tool. Simulation involves building a mathematical model that attempts to describe a real world situation. The goal of the model is to incorporate important variables and their interrelationships in such a way that we can study the impact of managerial changes upon the total system. The approach has many advantages over other management science techniques and is especially useful when a problem is too complex or difficult to be solved by other means. Simulation is a procedure in which random numbers are generated according to probabilities assumed to be associated with a source of uncertainty. Outcomes associated with these random drawings are then analysed to determine the likely results and the associated risk. This technique is oftentimes called Monte Carlo simulation, being named for the city of Monte Carlo. The Monte Carlo method, as it is understood today, encompasses any technique of statistical sampling employed to approximate solutions to quantitative problems. The Monte Carlo method simulation is developed through the use of probability distributions and random numbers. Random number intervals are established to represent possible outcomes for each probabilistic variable in the model. Random numbers are then either selected from a random number table or generated by computer to simulate variable outcomes. Monte Carlo simulation is illustrated by hands on problems of inventory, queuing and machine maintenance. Many of the applications of simulation are in the areas of education and training, military, medical, manufacturing, entertainment, and many others.

Keywords: *Simulation; management science; Monte Carlo; random number.*

1. INTRODUCTION

The history of military simulation began 5,000 years ago with Chinese war games, called *weich'i*, and continued through the 1780s, when the Prussians used the games to help train their army. Since then, all major military powers have used war games to test military strategies under simulated environments. From military or

operational gaming, a new concept, Monte Carlo simulation, was developed as a quantitative technique by the great mathematician, John Von Neumann, in 1940, during World War II. Working with neutrons at the Los Alamos Scientific Laboratory, Von Neumann used simulation to solve physics problems that were too complex or expensive to analyse by hand or by using a physical model. The random nature of the neutrons suggested the use of a roulette wheel in dealing with probabilities. Von Neumann used this method to study the random actions of neutrons and the effectiveness of aircraft bombing missions. This method was first used in industries to determine the maximum potential productivity of factories. Due to the method's gaming nature, Von Neumann called it the Monte Carlo model of studying laws of chance (Render & Stair, 1992).

Simulation has been significantly used for aircraft design since World War II. Boeing, the Douglas Aircraft Company^I and Lockheed^{II}, for example, commonly built simulation models of their proposed jet aircrafts, and then, tested the aerodynamic properties of the models. At the beginning of World War II, 80 percent of airplanes in the commercial service were DC-3s. During the war, the DC-3 served as a personnel carrier, and in other design variations such as the B-18 bomber and the C-47 transport. Over 10,000 DC-3s of various configurations were built for service with the Army Air Corps. Douglas also produced a number of attack planes for the military, the A-20 Havoc and the SBD Dauntless among them. A squadron of Dauntless airplanes was instrumental in the defeat of the Japanese Navy at the battle of Midway Island (4th-7th June 1942) (St. James Press, 2000).

The US Army simulates enemy attacks and defence strategies in war games played on computers. In addition, thousands of business, government and service organisations develop simulation models to assist in making decisions concerning inventory controls, maintenance scheduling, plant layouts, investments and sales forecasting.

Simulation technology is currently being used by many manufacturing companies in developed countries, such as the US and many European countries, with much success. The opportunities to cut costs and to improve service levels in this sector are tremendous by applying this technology. It has become the main agenda of the manufacturing sector to produce cost effective products so as to remain competitive. In today's highly competitive marketplace, manufacturers use the latest technologies to reduce time off production cycles, ramp up production and speed up time to market. One way companies can save time and cost is by using factory-simulation software, which enable the testing of production line activities prior to implementation (Evans & Leemis, 2000).

The design of new manufacturing systems or improving the existing systems can be immensely supported by simulation as the designer is given an opportunity to assess the proposed system via properly designed experiments without the cost and time associated with physically building the system. A real-life system envitably contains

^I Merged with McDonnell Aircraft in 1967 to form McDonnell Douglas. Later merged with Boeing in 1997.

^{II} Merged with Martin Marietta in 1995 to form Lockheed Martin.

randomness or variability and simulation is able to closely mimic these characteristics (Banks, 1999).

There is a general impression that simulation may be the solution to all management problems. This is, unfortunately, by no means true. Nevertheless, it is one of the most flexible and fascinating management science techniques. The purpose of this paper is to discuss the process of designing a model of a real or imagined system and conducting experiments with that model, and to understand the behaviour of the system or evaluate strategies for the operation of the system. The applications of simulation are also discussed.

2. THE NATURE OF SIMULATION

Simulation is the discipline of designing a model of an actual or theoretical physical system, executing the model on a digital computer, and analysing the execution output. Simulation embodies the principle of "learning by doing"; to learn about the system, we must first build a model of some sort and then operate the model (Fishwick, 1995).

Simulation is the imitation of a real thing, state of affairs, or process. The act of simulating something generally entails representing certain key characteristics or behaviours of a selected physical or abstract system (Figure 1). Simulation is used in many contexts, including the modelling of natural or human systems in order to gain insight into their functions. Other contexts include simulation of technology for performance optimisation, safety engineering, testing, training and education. Simulation can be used to show the eventual real effects of alternative conditions and courses of action. Key issues in simulation include acquisition of valid source information about the relevant selection of key characteristics and behaviours, the use of simplifying approximations and assumptions within the simulation, and fidelity and validity of the simulation outcomes (Smith, 1998).



Figure 1: A modern simulator, circa 1930-1960.
(Source: Moore (2008))

However, problems of interest in the real world are usually much more complex than this. In fact, they may be so complex that a simple mathematical model cannot be constructed to represent them. In this case, the behaviour of the system must be

estimated with a simulation. Exact representation is seldom possible in a model, constraining us to approximations to a degree of fidelity that is acceptable for the purposes of the study. Models have been constructed for almost every system imaginable, to include factories, communications and computer networks, integrated circuits, highway systems, flight dynamics, national economies, social interactions, and imaginary worlds. In each of these environments, a model of the system has proved to be more cost effective, less dangerous, faster and more practical than experimenting with the real system (Smith, 1998).

The idea behind simulation is to imitate a real world situation mathematically, then to study its properties and operating characteristics, and finally to draw conclusions and make decisions based on the results of the simulation. In this way, the real-life system is not touched until the advantages and disadvantages of what may be major policy decisions are first measured on the system's model (Render & Stair, 1992).

The steps of simulation are (1) define a problem; (2) introduce the variables associated with the problem; (3) construct a numerical model; (4) set up possible courses of action for testing; (5) run the experiment; (6) consider the results (possibly deciding to modify the model or change data inputs); and (7) decide on the course of action to take. These steps are illustrated in Figure 2.

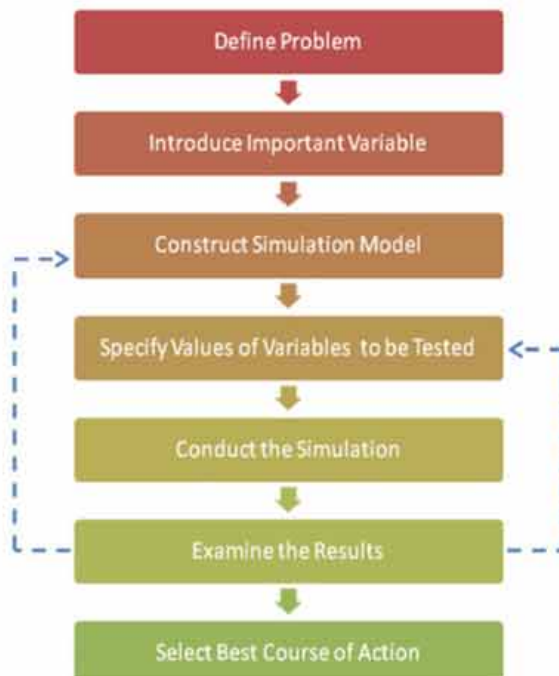


Figure 2: The process of simulation.
(Source: Render & Stair (1992))

A computer simulation (or "sim") is an attempt to model a real-life or hypothetical situation on a computer so that it can be studied to see how the system works. By changing variables, predictions may be made about the behaviour of the system (Smith, 1998).

Computer simulation has become a useful part of the modelling of many natural systems in physics, chemistry and biology, and human systems in economics and social science (the computational sociology), as well as in engineering to gain insight into the operation of these systems. A good example of the usefulness of using computers for simulation can be found in the field of network traffic simulation. In such simulations, the model behaviour will change each simulation according to the set of initial parameters assumed for the environment.

Several software packages exist for running computer-based simulation modelling (e.g. Monte Carlo simulation, stochastic modelling, multimethod modelling) that makes the modelling almost effortless. Modern usage of the term "computer simulation" may encompass virtually any computer-based representation (Figure 3).

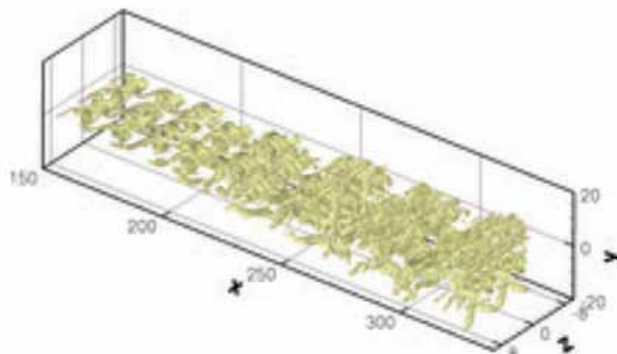


Figure 3: Visualization of a direct numerical simulation model (Smith, 1998).

3. ADVANTAGES AND DISADVANTAGES OF SIMULATION

Simulation is a tool that has become widely accepted by many users for several reasons. It has proven to be a useful and powerful tool for modelling operations in several types of areas. However, simulation does have certain limitations.

3.1 Advantages

Simulation is relatively straightforward and flexible, and can be used to analyse large and complex real world situations that cannot be solved by conventional management science models. For example, it may not be possible to build and solve a mathematical model of a city government system that incorporates important economic, social, environmental and political factors. Simulation has been

successfully used to model urban, hospitals and educational systems, national and state economies, and even world food systems.

Simulation allows for what-if questions. Managers like to know in advance what options are attractive. With computers, a manager can try out several policy decisions within a matter of minutes. Simulations do not interfere with the real world system. It may be too disruptive, for example, to actually experiment with new policies or ideas in a hospital, school or manufacturing plant. With simulation, experiments are done with the model, not on the system itself. Simulation allows for the study of the interactive effect of individual components or variables in order to determine which ones are important. "Time Compression" is possible with simulation. The effect of ordering, advertising or other policies over many months or years can be obtained by computer simulation in a short time. Simulation also allows for the inclusion of real world complications that most quantitative analysis models cannot permit. For example, some queuing models require exponential or Poisson distributions and some inventory and network models require normality. On the other hand, simulation can use any probability distribution that the user defines; it does not require standard distributions (Render & Stair, 1992).

3.2 Disadvantages

The main disadvantage of simulation is that good simulation models can be very expensive. It is often a long and complicated process to develop a model. A corporate planning model, for example, may take years to develop. Simulation does not generate optimal solutions to problems as do other management science techniques such as economic order quantity (EOQ), linear programming, or program evaluation and review technique (PERT). It is a trial and error approach that may produce different solutions in repeated runs. Managers must generate all of the conditions and constraints for solutions that they want to examine. The simulation model does not produce answers by itself. Each simulation model is unique, and hence, its solutions and inferences are not usually transferable to other problems (Render & Stair, 1992).

4. MONTE CARLO SIMULATION

Interestingly, Monte Carlo simulation methods do not always require truly random numbers to be useful, while for some applications, such as primality testing, unpredictability is vital (Davenport, 1992). Many of the most useful techniques use deterministic, pseudo-random sequences, making it easy to test and re-run simulations. The only quality usually necessary to make good simulations is for the pseudo-random sequence to appear "random enough" in a certain sense. What this means depends on the application, but typically they should pass a series of statistical tests. Testing that the numbers are uniformly distributed or follow another desired distribution when a large enough number of elements of the sequence are considered is the simplest and most common test (Smith, 1998).

4.1 The Monte Carlo Simulation Process

When a system contains elements that exhibit chance in their behaviour, the Monte Carlo method of simulation may be applied. The basis of Monte Carlo simulation is experimentation on the chance (or probabilistic) elements through random sampling. The technique can be broken down into five simple steps which are: (1) setting up a probability distribution for important variables; (2) building a cumulative probability distribution for each variable in step (1); (3) establishing an interval of random numbers for each variable; (4) generating random numbers; (5) actually simulating a series of trials (Render & Stair, 1992).

Step 1: Establishing Probability Distributions

The basic idea of Monte Carlo simulation is to generate values for the variables making up the model being studied. There are a lot of variables in real world systems that are probabilistic in nature and what we might want to simulate. One common way to establish a probability distribution for a given variable is to examine historical outcomes. The probability, or relative frequency, for each possible outcome of a variable is found by dividing the frequency of observation by the total number of observations. Probability distributions, we should note, need not be based solely on historical observations. Often, managerial estimates, based on judgment and experience, are used to create a distribution. The distributions themselves can be based on the commonly known normal, binomial, Poisson or exponential patterns.

Step 2: Building a Cumulative Probability Distribution for Each Variable

The conversion from a regular probability distribution, to a cumulative distribution is an easy job. Monte Carlo simulation is categorised as a sampling method because the inputs are randomly generated from probability distributions to simulate the process of sampling from an actual population. Hence, we try to choose a distribution for the inputs that most closely matches data we already have, or best represents our current state of knowledge. The data generated from the simulation can be represented as probability distributions (or histograms), or converted to error bars, reliability predictions, tolerance zones and confidence intervals (Wittwer, 2004). The cumulative probability is used in Step 3 to help assign random numbers.

Step 3: Setting Random Number Intervals

Once a cumulative probability distribution for each variable included in the simulation has been established, a set of numbers must be assigned to represent each possible value or outcome. These are referred to as random number intervals. Basically, a random number is a series of digits (say two digits from 01, 02,....., 99,00) that has been selected by a totally random process (Figure 4).

100 Random Numbers*

79 80 77 87 58 71 85 17 68 67 98 78 84 68 16 72 31 27 92 70 09 91 73 00 20 86 86 61 62 14 30 54 09
46 06 53 87 10 88 83 71 06 00 44 13 33 45 37 60 92 94 36 38 57 02 66 22 52 15 27 64 80 59 20 11 12
09 19 90 76 90 48 00 72 03 10 15 99 47 03 62 32 23 01 41 22 05 31 51 18 17 93 67 19 62 86 14 78 11
84

* This table of 100 random numbers was produced according to the following specifications: Numbers were randomly selected from within the range of 0 to 99. Duplicate numbers were allowed.

Figure 4: Table of random numbers.
(Source: Stat Trek (2009))

Step 5: Simulating the Experiment

The outcomes of an experiment are simulated by simply selecting random numbers from the random number table. If this simulation were repeated hundreds or thousands of times, it is much more likely that the average simulated demand would be nearly the same as expected demand. Naturally, it would be risky to draw any hard and fast conclusions regarding the operation of a firm using only a short simulation. It is also unlikely that anyone would actually want to go to the effort of simulating such a simple model containing only one variable. Simulation by hand does, however, demonstrate the important principles involved and may be useful in small scale studies. Computers can be a very helpful tool in carrying out tedious work in larger simulation under-takings (Render & Stair, 1992).

4.2 Other Types of Monte Carlo Simulation

Monte Carlo simulation is illustrated by hands-on problems of inventory control, queuing and machine maintenance.

4.2.1 Simulation of Inventory Analysis

In many real world inventory situations, though, demand and lead time are variables, and accurate analysis becomes extremely difficult to handle by any means other than simulation. Usually, the owner of a store would like to establish order quantity and reorder point decisions for a particular product that has probabilistic daily demand and reorder lead time. He wants to make a series of simulation runs, trying out various order quantities and reorder points, in order to minimise his total inventory cost for the item (Render & Stair, 1992).

4.2.2 Simulation of Queuing Problem

The assumptions required for solving queuing problems analytically are quite restrictive. For most realistic queuing systems, simulation may actually be the only approach available. The queuing system is the most typical problem in the discrete

event system. For example, computer, communication and transportation systems are all typical tangible or intangible queuing system. As a result of the widely used queuing system, the queuing character, and the queuing regulation, the service organisation become more and more complex so that the parsing method almost cannot be obtained. Computer simulation is quite an effective way to solve the queuing problem and to analyse the performances of the queuing system, which can construct a real system model with computer program, and attain the performances and the characters changing with time through computation. With computer simulation, the cost of the development of the system can be reduced, and enhance the safety of the experiment and the debugging, thus it will make the great society and economic effort worthwhile (Hong & Zhenkai, 2007).

4.2.3 Simulation of Maintenance Policy

Simulation is a valuable technique for analysing various maintenance policies before actually implementing them. For example, a firm can decide whether to add additional maintenance staff based on machine downtime costs and costs of additional labour. It can simulate replacing parts that have not yet failed as part of exploring ways to prevent future breakdowns. Many companies use computerised simulation models to decide if and when to shut down a whole plant for maintenance activities (Render & Stair, 1992).

5. APPLICATIONS OF SIMULATION MODELS

Simulation is a tool that is used to predict performance and to understand the impact of change. It refers to a broad collection of methods and applications to mimic the behaviour of a real system. Simulation has also become a powerful tool available to decision-makers especially to those having the responsibility of designing and operating complex processes and systems (Kelton *et al.*, 1998). Simulation is used in nearly every engineering, scientific and technological discipline. In the fifty years since its formal definition, it has been adapted for a wide variety of applications. Today, the techniques are employed in the design of new systems, the analysis of existing systems, training for all types of activities, and as a form of interactive entertainment (Smith, 1998). It makes it possible to study, analyse and evaluate situations that would not be otherwise possible. Many fields now rely on the extensive use of simulation to test new ideas and options.

5.1 Simulation in Military

Military simulations, also known informally as war games, are simulations in which theories of warfare can be tested and refined without the need for actual hostilities. Many professional analysts object to the term war games as this is generally taken as referring to the civilian hobby, thus the preference for the term simulation. Simulations exist in many different forms, with varying degrees of realism. In recent times, the scope of simulations has widened to include not only military but also political and social factors, which are seen as inextricably entwined in a realistic warfare model.

Whilst many governments make use of simulation, both individually and collaboratively, little is known about it outside the professional circles. Yet modelling is often the means by which governments test and refine their military and political policies. Military simulations are seen as a useful way to develop tactical, strategic and doctrinal solutions, but critics argue that the conclusions drawn from such models are inherently flawed, due to the approximate nature of the models used (Taylor, 1983).

The term military simulation can be used to cover a wide spectrum of activities, ranging from full scale field exercises, to abstract computerised models that can proceed with little or no human involvement, such as the RAND-designed Strategy Assessment Centre (RSAC) (Hall et al., 1993) (Figure 5).



Figure 5: Military simulations range from field exercises through computer simulations to analytical models; the realism of live manoeuvres is countered by the economy of abstract simulations
 (Source: Hall *et al.* (1993))

As a general scientific principle, the most reliable data is produced by actual observation and the most reliable theories are based on it. This is also true in military analysis, where analysts look towards live field exercises and trials as providing data that is likely to be realistic (depending on the realism of the exercise) and verifiable (it has been gathered by actual observation). It can be readily discovered, for example, how long it takes to construct a pontoon bridge under given conditions with given manpower, and this data can then be used to provide norms for expected performance under similar conditions in the future, or to refine the bridge-building process. It is true that any form of training can be regarded as a 'simulation' in the strictest sense of the word (inasmuch as it simulates an operational environment); however, many, if not most exercises, are carried out not to test new ideas or models, but to provide the participants with the skills to operate within existing ones (Carpi & Egger, 2003).

Military simulators replicate the performance characteristics of aircrafts, instruments in cockpits, effects of weapons, support from other combat systems, communications with other pilots, and terrain over which the events occur. Similar systems are used to train the captains of large ocean-going ships to dock without destroying both a real ship and a real dock. Entire mock-ups are made of nuclear power control centres to teach operators how to respond to emergency situations and to identify potential hazards before a crisis occurs. Modern medical equipment is so expensive and scarce that simulations have been constructed to allow interns and nurses to practice, develop and certify their skills without having to schedule

training time on the real equipment, competing for its use by real patients (Smith, 1998).

5.2 Simulation in Manufacturing

One of the largest application areas for simulation modelling is that of manufacturing systems, with the first uses dating back to at least the early 1960s (Law & McComas, 1991). As manufacturing systems are getting complex, the process of making effective decisions regarding these systems are also increasingly difficult. Applying guesswork for finding the best possible solution will be impractical to the management as it involves high risks. An effective analysis tool is therefore required to assist the management to experiment changes within the system, and to seek more options for improving performance and reducing system costs.

It has become a common scenario for engineers and planners to focus more effort with processes, equipment and methods with the goal of getting new manufacturing systems online. They are frequently giving less concentration on overall coordination, integration and scheduling issues of the plant. As a consequence, manufacturing systems are implemented poorly and often perform below anticipated levels.

There are many ways in which simulation technologies have benefited manufacturing sectors. Simulation can be used to evaluate the performance of a system, existing or proposed, under various configurations of interest and over long periods of real time operation. The management needs to have control of their system to reduce the chances of failure to meet specifications, to eliminate unforeseen bottlenecks, to prevent under or over-utilisation of resources, and to optimise system performance. In the manufacturing sector, the management often encounter issues such as the requirement of resources at the plant. It requires the management to evaluate the different alternatives that provide the most benefit to the company. The decision may involve capital investment such as buying different types of machines, changing plant configuration, labour requirement planning, and changing worker shift.

5.3 Simulation in Education and Training

Simulation is often used in the training of civilian and military personnel. This usually occurs when it is prohibitively expensive or simply too dangerous to allow trainees to use the real equipment in the real world. In such situations, they will spend time learning valuable lessons in a "safe" virtual environment. Often the convenience is to permit mistakes during training for a safety-critical system. For example, in sim school, teachers practice classroom management and teaching techniques on simulated students, which avoids "learning on the job" that can damage real students. There is a distinction, though, between simulations used for training and instructional simulation.

Training simulations typically come in one of three categories (Smith, 1998):

- a) "live" simulation (where real people use simulated (or "dummy") equipment in the real world);
- b) "virtual" simulation (where real people use simulated equipment in a simulated world, or virtual environment), or
- c) "constructive" simulation (where simulated people use simulated equipment in a simulated environment). Constructive simulation is often referred to as "war gaming" since it bears some resemblance to table-top war games in which players command armies of soldiers and equipment that move around a board.

In standardised tests, "live" simulations are sometimes called "high-fidelity", producing "samples of likely performance", as opposed to "low-fidelity", "pencil-and-paper" simulations producing only "signs of possible performance", but the distinction between high, moderate and low fidelity remains relative, depending on the context of a particular comparison (Havighurst *et al.*, 1990).

Simulations in education are somewhat like training simulations. They focus on specific tasks. The term 'microworld' is used to refer to educational simulations which model some abstract concept rather than simulating a realistic object or environment, or in some cases model a real world environment in a simplistic way so as to help a learner develop an understanding of the key concepts. Normally, a user can create some sort of construction within the microworld that will behave in a way consistent with the concepts being modelled. Seymour Papert was one of the first to advocate the value of microworlds, and the Logo programming environment developed by Papert is one of the most famous microworlds. Another example is the Global Challenge Award online STEM learning web site which uses microworld simulations to teach science concepts related to global warming and the future of energy. Other projects for simulations in education are Open Source Physics and its Easy Java Simulations (EJS) environment (Havighurst *et al.*, 1990).

5.4 Clinical Healthcare Simulators

In the health care industry, the models are used to schedule doctors, staff, equipment, and patients in an effort to improve service times and reduce costs. The first medical simulators were simple models of human patients. Since antiquity, these representations in clay and stone were used to demonstrate clinical features of disease states and their effects on humans. Models have been found from many cultures and continents. These models have been used in some cultures (e.g., Chinese culture) as a "diagnostic" instrument, allowing women to consult male physicians while maintaining social laws of modesty. Models are used today to help students learn the anatomy of the musculoskeletal system and organ systems (Meller, 1997).

Medical simulators are increasingly being developed and deployed to teach therapeutic and diagnostic procedures as well as medical concepts and decision making to personnel in the health professions. Simulators have been developed for training procedures ranging from the basics such as blood draw, to laparoscopic surgery (Ahmed *et al.*, 2010) and trauma care. They are also important to help on

prototyping new devices for biomedical engineering problems. Currently, simulators are applied to research and development of tools for new therapies, treatments and early diagnosis in medicine.

Many medical simulators involve a computer connected to a plastic simulation of the relevant anatomy. Sophisticated simulators of this type employ a life size mannequin that responds to injected drugs and can be programmed to create simulations of life-threatening emergencies. In other simulations, visual components of the procedure are reproduced by computer graphics techniques, while touch-based components are reproduced by haptic feedback devices combined with physical simulation routines computed in response to the user's actions. Medical simulations of this sort will often use 3D CT or MRI scans of patient data to enhance realism. Some medical simulations are developed to be widely distributed (such as web-enabled simulations that can be viewed via standard web browsers) and can be interacted with using standard computer interfaces, such as the keyboard and mouse (Meller, 1997).

5.5 Simulation in Entertainment

The entertainment industry makes wide use of simulation to create games that are enjoyable and exciting to play (Figure 6). These contain many, but usually not all, of the components of simulation described in this article. Arcade games, computer games, board wargames, and role playing games all require the creation of a consistent model of an imaginary world and devices for interacting with that world. These simulations often appear very similar to training simulations, but differ in that their purpose is entertainment rather than practice for real-world events. This fact allows game developers the freedom to modify the laws of physics and other behaviours, rather than accurately capturing their real world equivalents. Advances in these simulations, together with the prevalence of the Internet, are allowing the creation of multi-player on-line games that pit players against multiple opponents around the world. Though the purpose of these simulations is entertainment, the technical challenges faced by their developers are just as daunting as those in the other categories (Smith, 1998).

6. CONCLUSION

A broad collection of simulation methods is used to study and analyse the behaviour and performance of actual or theoretical systems. Simulation studies are performed, not on the real-world system, but on a (usually computer-based) model of the system created for the purpose of studying certain system dynamics and characteristics. The purpose of any model is to enable its users to draw conclusions about the real system by studying and analysing the model. The major reasons for developing a model, as opposed to analysing the real system, include economics, unavailability of a "real" system, and the goal of achieving a deeper understanding of the relationships between the elements of the system.



Figure 6: A tank simulator computer game.

(Source: Smith, 1998)

With simulation, decision-makers can try out new designs, layouts, software programs and systems before committing resources to their acquisition or implementation; test why certain phenomena occur in the operations of the system under consideration; compress and expand time; gain insight about which variables are most important to performance and how these variables interact; identify bottlenecks in material, information, and product flow; better understand how the system really operates (as opposed to how everyone thinks it operates); and compare alternatives and reduce the risks of decisions.

ACKNOWLEDGEMENT

The author is grateful to Mdm Halijah Ahmad, Mdm Zariyah Ariffin and Mr Khalid Mohammad for their support.

REFERENCES

- Ahmed, K., Keeling, A.N., Fakhry, M., Ashrafiyan, H., Aggarwal, R., Naughton, P.A., Darzi, A., Cheshire, N., Athanasiou, T. & Hamady, M. (2010). Role of virtual reality simulation in teaching and assessing technical skills in endovascular intervention. *J. Vasc. Interv. Radiol.*, **21**:55-66.
- Banks, J. (1999). Introduction to Simulation. *Proceeding of the 1990 Winter Simulation Conference*, New Jersey, December 1999, pp. 7-13.
- Carpi, A. & Egger, A.E. (2003). *The Scientific Method*. Available online at: http://www.visionlearning.com/library/module_viewer.php?mid=45 (Last access date: 27th April 2010).
- Davenport, L.H. (1992). Primality testing revisited. *International Conference on Symbolic & Algebraic Computation*. pp. 123-129.

- Evans, D. & Leemis, L. (2000). Input modeling using a computer algebra system. *Proceedings of the 2000 Winter Simulation Conference*. Institute of Electrical and Electronics Engineers, Orlando, Florida, pp. 577-586.
- Fishwick, P. (1995). *What Is Simulation?* Available online at: <http://www.cise.ufl.edu/~fishwick/introsim/node1.html> (Last access date: 29th April 2010).
- Hall, H.E., Shapiro, N. & Shukiar, H.J. (1993). Overview of RSAC System Software: A Briefing. RAND Corporation, Santa Monica, California.
- Havighurst, L.C., Fields, L.E. & Fields, C.L. (1990). *High Versus Low Fidelity Simulations: Does the Type of Format Affect Candidates' Performance or Perceptions?* Fields Consulting Group, McLean, Virginia.
- Hong, L. & Zhenkai, W. (2007). The computer simulation for queuing system. *World Acad. Sci. Eng. Technol.*, **34**: 176-179.
- Kelton, W.D., Sadowski, R.P. & Sadowski, D.A. (1998). *Simulation with ARENA*. The Mc Graw-Hill Companies, Inc., New York.
- Law, A.M. & McComas, M.G. (1991). Secrets of Successful Simulation Studies. *Proceeding of the 1991 Winter Simulation Conference*, Phoenix, Arizona, 8th - 11th December 1991.
- Meller, G. (1997). A typology of simulators for medical education. *J. Digit. Imaging*, **10**: 194-196.
- Moore, K. (2008). *A Brief History of Aircraft Flight Simulation*. England. Available on line at: <http://homepage.ntlworld.com/bleep/index.html> (Last access date: 28th April 2010).
- Render, B. & Stair, R.M. (1992). *Introduction to Management Science*. Prentice Hall, Boston, Massachusetts.
- Smith, R.D. (1998). *Simulation Article, Encyclopedia of Computer Science*. Nature Publishing Group, London.
- St. James Press (2000). *International Directory of Company Histories, Vol. 32*. Available online at: <http://www.fundinguniverse.com/company-histories/The-Boeing-Company-Company-History.html> (Last access date: 3rd May 2010).
- Stat Trek. (2009). *Random Number Generator*. Available online at: <http://stattrek.com/Tables/Random.aspx> (Last access date: 5th May 2010).
- Taylor, J.G. (1983). Modeling and simulation of land combat. In Callahan, L.G. (Ed.), *Proceedings of the Workshop on Modeling and Simulation of Land Combat*, Georgia Institute of Technology, Atlanta, Georgia.
- Wittwer, J.W. (2004). *Monte Carlo Simulation Basics*. Available online at: <http://vertex42.com/ExcelArticles/mc/MonteCarloSimulation.html> (Last access date: 6th May 2010).

CBRN EVENTS IN THE SUBWAY SYSTEM OF ROME: TECHNICAL-MANAGERIAL SOLUTIONS FOR RISK REDUCTION

Andrea Malizia, Riccardo Quaranta & Roberto Mugavero*

Department of Mechanical Engineering, Faculty of Engineering, University of
Rome "Tor Vergata", Italy

*Email: mugavero@ing.uniroma2.it

ABSTRACT

The acronym CBRN stands for Chemical, Biological, Radiological and Nuclear. CBRN risks are those caused by chemical, biological, radiological or nuclear agents that can produce serious harm to persons and things. The accidents connected with this type of substances can be either due to man (industrial accidents, road accidents, human mistakes in manipulation and/or storage of materials, etc.) or natural causes, when the structures where these substances are produced or stored are damaged by natural events (earthquakes, flood, etc.). Sometimes, in cases of terrorism, man voluntarily causes this kind of incidents. In Italy, as well as in the rest of the world, subways are one of the critical infrastructures that are more at risk in case of a CBRN event. In this work, the authors will analyse the case study of the subway system of Rome and propose technical-managerial solutions to improve the response in case of release of CBRN agents. In order to evaluate the quality of the proposals, a risk analysis will be carried out, both before and after the application of the suggestions.

Keywords: Chemical, Biological, Radiological and Nuclear (CBRN); Rome; safety; subway; terrorism.

1. INTRODUCTION

A Chemical, Biological, Radiological and Nuclear (CBRN) release can be very hazardous, especially when happening indoor, in conditions of bad ventilation and in the presence of big crowds, such as in a subway. It is easy to remember the terrorist attack that took place in the subway of Tokyo, Japan, between 8:00 and 9:00 am on March 20th, 1995, which caused the death of 12 people and the intoxication of over 5,000. In that occasion, the chemical agent Sarin was released during the rush hour, when more than 10 million people were on the trains of Tokyo's underground lines. In the area between the government departments and the harbour, chaos and terror immediately grew; there were victims experiencing unconsciousness, vomiting, sore throat and blindness. The rescue was fast, with the three stricken lines being promptly closed, while hundreds of ambulances intervened together with the support of 6 helicopters to rescue the injured. Among the casualties was the vice head of the Kasumigaseki station, who asphyxiated a few instants after removing a wrapper, dripping the agent, from a train. That morning,

Tokyo saw the collapse of a certainty; the myth of the safest city in the world. For the first time in its history, it knew terrorism (Murakami, 2000; Tu, 2000).

In Italy, the current prevention, control and operation system does not include an effective response in case of accidental release of CBRN agents inside the subway system of Rome. Considering the history of the city, institutions, monuments and innumerable events that populate the city and subway every year, it represents a public transport infrastructure in the city of Rome with a very high risk level.

At present, the subway system is highly vulnerable as:

- The operations of first rescue are not always carried out by trained CBRN first responders;
- The zoning is not optimised for CBRN events;
- It is not possible to prevent this type of events and, often, the warning is belated.

For these reasons, it is necessary to propose solutions that can meet higher safety requirements and can bring benefits in terms of:

- Rapidity of response;
- Enhancement of safety for the first responder teams and for the persons injured;
- Better management of the event and decongestion of the traffic in the surroundings of the scene.

In this work, a method to carry out a preliminary assessment of the risks connected to an unconventional event has been developed. This has lead to the achievement of a preliminary risk analysis applied to a hypothetical CBRN attack inside the subway system of Rome, in order to prove the quality of the proposed solutions.

2. CREATION OF A FIRST RESPONDER CBRN UNIT AND DEPLOYMENT OF CBRN TEAMS ON THE SUBWAY SYSTEM

From the analysis of the Italian national response system, it can be seen that the first rescue teams are formed by operators belonging to security forces and, often, they are not trained to face CBRN events. Therefore, these teams can encounter two main problems:

- Risk of contamination for the operators of the team caused by the lack of proper protective equipment that are usually only provided to fire fighter teams;
- Risk of adoption of wrong rescue actions due to the lack of specific skills in CBRN matters.

In consideration of the importance of these problems, it is believed that the formation of special teams trained to deal with CBRN events, with the task of

performing first rescue operations together with security forces, can be a good solution. The CBRN teams should meet at least the following requirements:

- Be made up of at least 4-5 firemen with proper CBRN expertise;
- Be provided with the necessary personal protective equipment, such as:
 - Protective suits (category III type 1a-ET) to enter the red zone, where these teams are asked to work (DOA, 1995);
 - Protective suits (category III type 2) to be used in the warm zone for the decontamination of the operators (DOA, 1995);
 - Filtered masks and re-breathers for the rescue of the victims.
- Wear the protective equipment from the beginning of their action (DOA, 1995);
- Be provided with specific detectors for CBRN agents;
- Be able to carry out first zoning and demarcation of the hot zone, taking into account safety approximation;
- Be ready to intervene in case of non-CBRN events;
- Have at disposal special premises for the decontamination of the operators;
- Be in command in the hot zone before the arrival of the other responders;
- Pay attention to possible second explosive devices;
- Take into account that the aggressors can be among the casualties;
- Warn all the other rescue teams.

It is important that these teams are deployed in a proper manner on the territory in order to optimise the response time.

This was applied to the case study of the subway system of Rome. An appropriate deployment of the CBRN teams along the subway (Figure 1 and Table 1) was defined to guarantee a fast and effective operation.

Teams 1A - 4A and 1B - 2B are assigned with 8 - 10 firemen (alternating in three 8-hour shifts). The central team was assigned with twice the number of firemen (16 - 20) as compared to the other teams in order to command two different squads in case of attacks on both subway lines. The collocation of the teams and the lengths of the subway covered by any of them were chosen in order to allow the arrival on the scene in a short time (approximately 10 - 15 minutes), by moving on the surface roads, wherever the event happens. This feature permits the rapid deployment of forces prepared to deal with CBRN emergencies protecting, and, at the same time, the members of the security forces, that in Italy are not well equipped and trained for this kind of events but are usually the very first responders. Moreover, this solution allows for first aid to be provided to a larger number of victims and minimises the diffusion of the contamination.

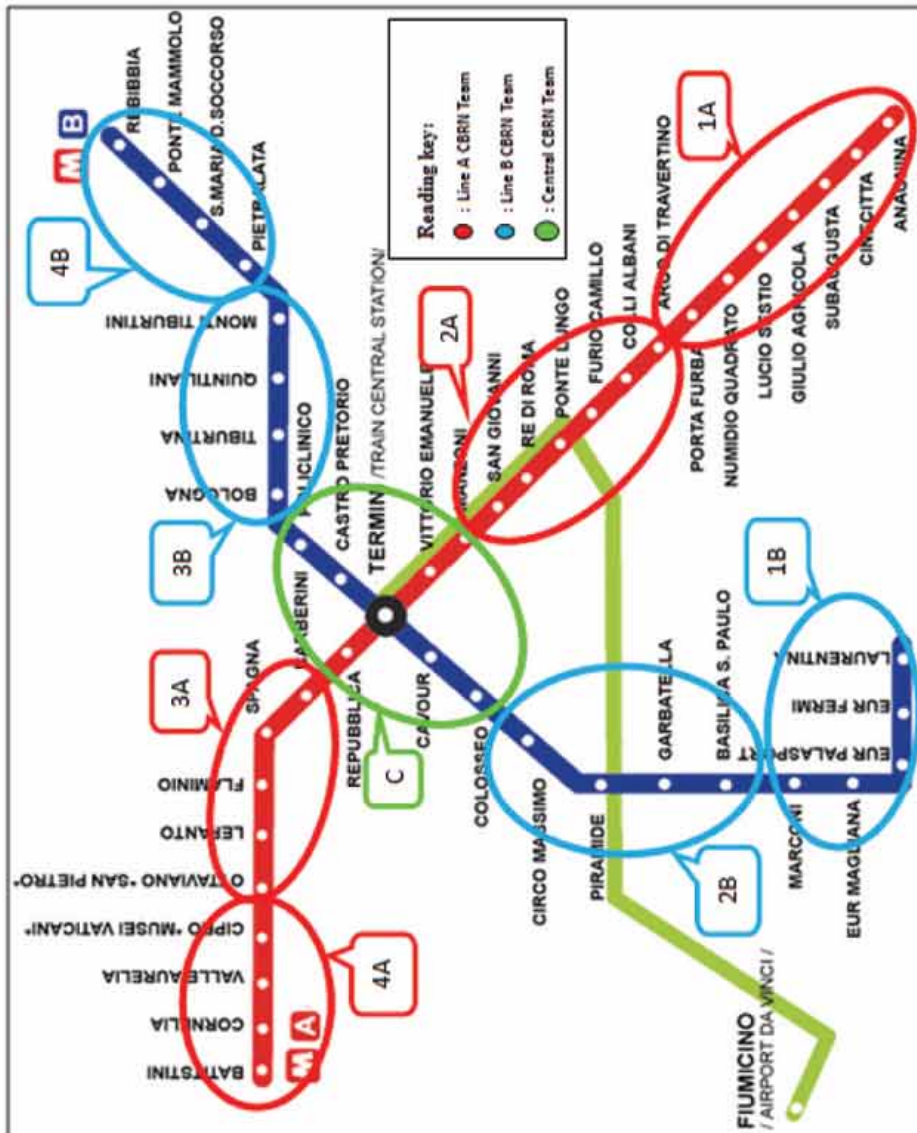


Figure 1: The subway system of Rome and areas covered by the CBRN teams.

Table 1: Deployment of the CBRN teams along the Roman subway system.

CBRN Team	Location	Range of Action
1A	Between the Subaugusta and Cinecittà stations	Line A: Between the Anagnina (terminus) and Arco di Travertino stations
2A	Close to the Ponte Lungo station	Line A: Between the Colli Albani and San Giovanni stations
3A	Between the Spagna and Flaminio stations	Line A: Between the Barberini and Ottaviano stations
4A	Close to the Valle Aurelia stations	Line A: Between the Cipro and Battistini (terminus) station
Central	Close to the Termini station	Line A: Between the Manzoni and Repubblica stations Line B: Between the Colosseo and Policlinico stations
1B	Close to the Eur Magliana station	Line B: Between the Laurentina and Marconi stations
2B	Close to the Colosseo station	Line B: Between the Basilica S. Paolo and Circo Massimo stations
3B	Close to the Tiburtina station	Line B: Between the Bologna and Monti Tiburtini stations
4B	Close to the Ponte Mammolo station	Line B: Between the Pietralata and Rebibbia stations

3. IMPROVEMENT OF EMERGENCY ZONING

Emergency zoning (Figure 2) is the determination of the different areas that characterise a CBRN event (DOD, 1998; Jarrett, 1999):

- Contaminated zone (Hot Zone);
- Possibly contaminated zone (Warm Zone);
- Safe zone (Cold Zone).

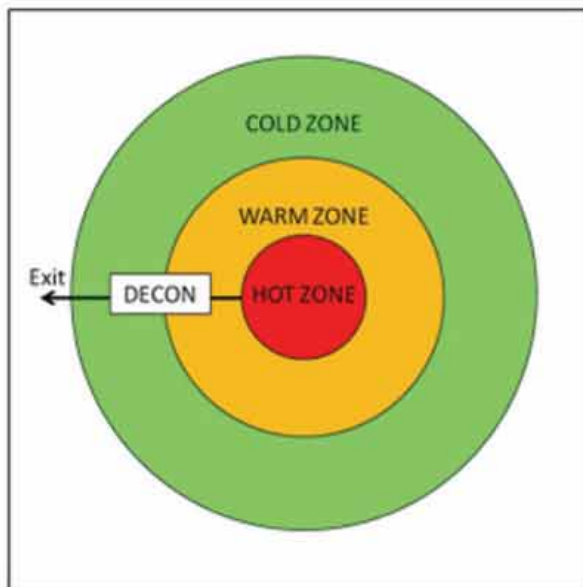


Figure 2: Standard emergency zoning.

After analysing the British response system for unconventional events, it has been decided to add one more zone to the standard emergency zoning. This new "pedestrian only" zone is delimited by a traffic barrier and is useful to prevent vehicles from entering the operative area. Furthermore, it has been considered advantageous to create a rendezvous point (RVP) and a sorting area (DOA, 1991; DOD, 1996). The advantages gained through this new configuration are:

- Traffic barrier:
 - The traffic barrier is placed so as to prevent the access of vehicles to the area of the operations;
 - Measures to avoid congestions of the traffic and guarantee that the arrival of rescue teams on the scene and surroundings, in case of emergency, can be easily undertaken;
 - The decontamination unit can be set up inside the pedestrian area in case of special requirements.
- Rendezvous point (RVP):
 - The RVP is to be located outside Hot Zone and will be under the control of the Police;
 - At the beginning of the rescue, all the emergency services will head to the RVP;
 - Any request that cannot be satisfied immediately by the person in charge of the RVP will be assigned to the sorting area.

- Sorting area:
 - This area (where it is appropriate to wear reflective coats) is located near the RVP and the hot zone. The precise location will be decided by the Head of Police and the Head of Fire Fighters after consultation. However, fire fighters do not take part in the operation in this area as it is under the control of the medical services.
 - The area is used for the arrival and departure of ambulances and other vehicles, and can also be used to recover the personnel involved. It can be maintained throughout the operation.

The new configuration of the emergency zoning is shown in Figure 3.

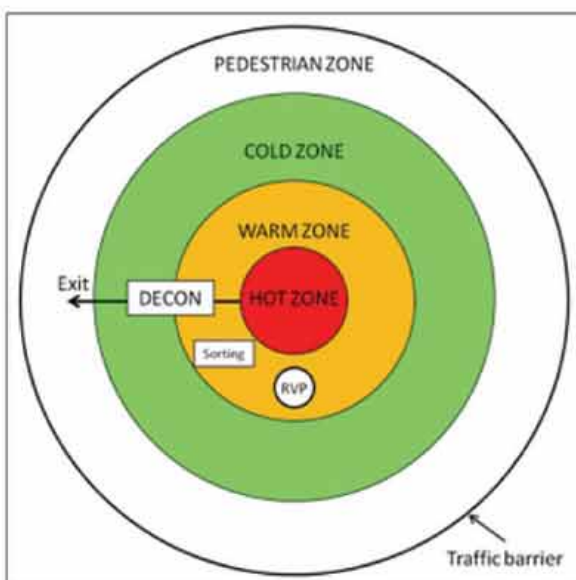


Figure 3: The emergency zoning after the suggested improvements.

4. SYSTEM OF DETECTION AND WARNING OF THE PRESENCE OF CBRN AGENTS

In order to further increase safety in case of an attack in the subway, it has been decided to add a system to detect CBRN agents that is, at present, missing. This detection system should be made up of:

- Real time chemical agents detector;
- Biological agents detector; since the real time detection of biological agents is not possible (CRPC, 2004), this system should collect air samples that are to be analysed remotely every 15 -20 minutes;
- Gamma dosimeter or counter for radiological detection.

All the detectors have to be placed in a “detection apparatus” at the entrance of every subway station, on both sides of the staircase, and will be connected to an automatic warning system. The positioning of the apparatus is shown in Figure 4.



Figure 4: Positioning of the detection system.

The detection system will work using a threshold criterion. If an aggressor is trying to enter the subway with an amount of chemical, biological or radiological substances that is higher than the threshold, the alarm activates automatically. The system is placed on the entrance of the subway in order minimise the dispersion of the agent in case the aggressor tries to spread it anyway. The warning system has three main tasks:

- i. Activation of an acoustic alarm to:
 - Alert the security personnel in the subway;
 - Alert the passengers entering the subway.
- ii. Sending of a warning to the CBRN teams so as to:
 - Activate the CBRN team in charge of that station;
 - Activate all the required rescue procedures.
- iii. In order to prevent the aggressor from entering the subway, a system of doors, with reinforced glass, placed at the end of the staircase that leads to the station (Figures 5 and 6), will automatically close. The activation of the doors will happen only in case of detection of chemical or radiological agents because biological agents cannot be detected in real time.



Figure 5: Position of the emergency doors.



Figure 6: Example of emergency door with reinforced glass.

Moreover, in order to enhance the safety of passengers in case an aggressor manages to bypass the detection system and enters the subway station to release the agent, a manual alarm is to be placed on the platforms. When the button is pushed, this alarm activates functions 1 and 2 of the previous list, while function 3 must not be activated, otherwise it would impede the access of the rescue teams and the evacuation of the people inside the station. The push buttons of the alarm should be placed every 10 to 20 m, at a height of 1.20 - 1.30 m from the floor (Figure 7) so as to make the use of them easy, in particular in case of very crowded platforms

(Figure 8). The buttons can also be placed inside the coaches, in order to facilitate the use of them and improve safety (Figure 9).



Figure 7: Positioning of the manual alarm buttons on the platform.



Figure 8: Easy use of the manual alarm buttons in case of crowded platform.



Figure 9: Possible positioning of the manual alarm buttons inside the train.

5. PRELIMINARY RISK ANALYSIS IN THE EVENT OF A CBRN ATTACK IN THE SUBWAY SYSTEM OF ROME

In this section, the risks associated with the hypothesis of a terrorist CBRN attack in the subway system of Rome before and after the application of the proposed solutions will be analysed. This analysis will be carried out in three phases:

- Identification of risk sources: This phase will help in the identification of the risks connected with the exposure to CBRN agents;
- Preliminary identification of the risks: This phase will have the dual task of identifying the risks both in absence and in presence of the solutions proposed;
- Preliminary assessment of the risks identified: In this phase, a preliminary assessment of the risks involving the “Total Risk”, that is the risk that the attack will be perpetrated, causing an emergency associated with the presence of casualties, injured persons and a contamination that can potentially spread, will be carried out. In this phase, it will be considered, to simplify the calculations, that the risks identified are disconnected, so it is possible to estimate the Total Risk as the mean of the single risks considered.

5.1 Identification of Risk Sources

In order to identify the risk sources, a short but accurate description of the environment is necessary:

- Classification of the considered environment: Public environment – transport infrastructure;
- Structural characteristics: The rail tunnels are from 10 – 15 m to 80 – 90 m deep. This characteristic makes the subway an ideal target for attacks because of the small space available that hinders the escape routes of the victims and makes the dispersion of the agents more effective;
- Number of people that can be on the platform / in the train: This value changes from station to station and it can be up to a few hundred.

The main risk sources that have been identified are shown in Table 2.

Table 2: Identified risk sources.

No.	Risks	Causes
A	Safety	<ul style="list-style-type: none">• Hazardous substances• Malfunction of the detection-warning system• Fire-explosion
B	Health	<ul style="list-style-type: none">• Chemical agents• Biological agents• Radiological agents
C	Safety and health	<ul style="list-style-type: none">• Not optimised organisation of the first responders• Not optimised deployment of the first responders• Not optimised emergency zoning

5.2 Preliminary Identification of the Risks

Table 3 shows the risks connected with an attack in the subway both in absence and in presence of the proposed solutions.

5.3 Preliminary Assessment of the Risks Identified

In order to assess the value of the identified risks, it is necessary to:

- Evaluate the probability of occurrence of any single risk;
- Evaluate the amount of harm.

It will be use:

- 4 probability scales;
- 4 harm scales.

Table 3: Risks connected with an attack in the subway system.

Risks Identified in Absence of Countermeasures	Risks Identified in Presence of Countermeasures
Contamination of the first responders (security forces) from CBRN agents	Contamination of the first responders (CBRN trained teams) from CBRN agents
Diffusion of the contamination outside the area of the event (standard zoning)	Diffusion of the contamination outside the area of the event (improved zoning)
Traffic congestion with the standard zoning	Traffic congestion with the improved zoning
Transport of CBRN agents in the absence of the detection-warning system	Unsuccessful detection of CBRN agents by the proposed system
Failure of the rescue in the absence of the automatic warning system	Malfunction of the automatic warning system
Delay in the rescue due to the deployment of the responder teams	Delay in the rescue due to the proposed deployment of the CBRN teams

Tables 4 and 5 indicate the criteria used for the assessment of:

- Probability occurrence P ;
- Amount of possible harm H .

Once probability and harm are defined, the risk R is automatically calculated using the following equation:

$$R = P \times H \quad (1)$$

The result obtained is given a scale of the risk from 0 (no risk) to 16 (maximum risk). In order to transform this result into a percentage value, it is necessary to perform the following simple ratio:

$$16 : 100 \% = x : y \quad (2)$$

x : estimated risk from Equation 1, extracted from Tables 4 and 5.

Y : percentage of risk calculated case by case.

Table 6 shows the values assigned to the risks identified in Table 3, using the proposed procedure, with the values taken from Tables 4 and 5. Figure 10 illustrates the significant reduction of the risks using the proposed countermeasures.

Table 4: Scale of probability P .

Value	Level	Definitions / Criteria
4	Highly probable	<ul style="list-style-type: none"> • There is a direct correlation between the observed failure and the occurrence of the hypothesised harm; • Harms already occurred due to the same observed failure in the same or similar environments; • The occurrence of the harm due to the failure would not cause surprise.
3	Probable	<ul style="list-style-type: none"> • The observed failure might cause a harm, even if not directly or automatically; • Some harm already occurred due to the failure; • The occurrence of the harm due to the failure would cause moderate surprise.
2	Unlikely	<ul style="list-style-type: none"> • The observed failure might cause a harm only in unfortunate circumstances; • Rare harms already occurred due to the failure; • The occurrence of the harm due to the failure would cause big surprise.
1	Completely Unlikely	<ul style="list-style-type: none"> • The observed failure might cause a harm in concomitance of other unlikely independent events; • No known harm occurred; • The occurrence of the harm due to the failure would cause incredulity.

Table 5: Scale of harm H .

Value	Level	Definitions / Criteria
4	Very serious	<ul style="list-style-type: none"> • Accident or acute exposure with lethal or total disability effects; • Chronic exposure with lethal or total disability effects.
3	Serious	<ul style="list-style-type: none"> • Accident or acute exposure with partial disability effects; • Chronic exposure with irreversible and/or partial disability effects.
2	Medium	<ul style="list-style-type: none"> • Accident or acute exposure with reversible disability effects; • Chronic exposure with reversible effects.
1	Minimum	<ul style="list-style-type: none"> • Accident or acute exposure with quickly reversible disability inability; • Chronic exposure with quickly reversible effects.

Table 6: Results of the risk analysis.

Assessment of the Risks Identified in Absence of Countermeasures	Assessment of the Risks Identified in Presence of Countermeasures
<p>Contamination of the first responders (security forces) from CBRN agents:</p> <ul style="list-style-type: none"> • Probability: <ul style="list-style-type: none"> – Level: Highly probable – Probable – Value: 3.8 • Magnitude: <ul style="list-style-type: none"> – Level: Very serious – Serious – Value: 3.5 <p>Risk = $R1 = 13.3 \cong 83\%$</p>	<p>Contamination of the first responders (CBRN trained teams) from CBRN agents:</p> <ul style="list-style-type: none"> • Probability: <ul style="list-style-type: none"> – Level: Unlikely – Completely unlikely – Value: 1.5 • Magnitude: <ul style="list-style-type: none"> – Level: Very serious – Serious – Value: 3.5 <p>Risk = $R1 = 5.25 \cong 33\%$</p>
<p>Diffusion of the contamination outside the area of the event (standard zoning):</p> <ul style="list-style-type: none"> • Probability: <ul style="list-style-type: none"> – Level: Unlikely – Value: 2.0 • Magnitude: <ul style="list-style-type: none"> – Level: Serious – Medium – Value: 2.5 <p>Risk = $R2 = 5.0 \cong 32\%$</p>	<p>Diffusion of the contamination outside the area of the event (improved zoning):</p> <ul style="list-style-type: none"> • Probability: <ul style="list-style-type: none"> – Level: Completely unlikely – Value: 1.0 • Magnitude: <ul style="list-style-type: none"> – Level: Serious – Medium – Value: 2.0 <p>Risk = $R2 = 2.5 \cong 16\%$</p>
<p>Traffic congestion with the standard zoning:</p> <ul style="list-style-type: none"> • Probability: <ul style="list-style-type: none"> – Level: Unlikely – Value: 2.0 • Magnitude: <ul style="list-style-type: none"> – Level: Medium – Value: 2.0 <p>Risk = $R3 = 4.0 \cong 25\%$</p>	<p>Traffic congestion with the improved zoning:</p> <ul style="list-style-type: none"> • Probability: <ul style="list-style-type: none"> – Level: Unlikely – Completely unlikely – Value: 1.5 • Magnitude: <ul style="list-style-type: none"> – Level: Medium – Value: 2.0 <p>Risk = $R3 = 3.0 \cong 19\%$</p>
<p>Transport of CBRN agents in absence of the detection-warning system:</p> <ul style="list-style-type: none"> • Probability: <ul style="list-style-type: none"> – Level: Highly probable – Value: 4.0 • Magnitude: <ul style="list-style-type: none"> – Level: Very serious – Serious – Value: 3.5 <p>Risk = $R4 = 14.0 \cong 87\%$</p>	<p>Unsuccessful detection of CBRN agents by the proposed system:</p> <ul style="list-style-type: none"> • Probability: <ul style="list-style-type: none"> – Level: Unlikely – Value: 2.0 • Magnitude: <ul style="list-style-type: none"> – Level: Very serious – Serious – Value: 3.5 <p>Risk = $R4 = 7.0 \cong 45\%$</p>

Table 6 (Continued): Results of the risk analysis.

Assessment of the Risks Identified in Absence of Countermeasures	Assessment of the Risks Identified in Presence of Countermeasures
Failure of the rescue in the absence of the automatic warning:	Malfunction of the automatic warning system:
<ul style="list-style-type: none"> • Probability: <ul style="list-style-type: none"> – Level: Highly probable – Probable – Value: 3.5 • Magnitude: <ul style="list-style-type: none"> – Level: Very serious – Serious – Value: 3.5 	<ul style="list-style-type: none"> • Probability: <ul style="list-style-type: none"> – Level: Unlikely – Completely unlikely – Value: 1.5 • Magnitude: <ul style="list-style-type: none"> – Level: Very serious – Serious – Value: 3.5
Risk = $R5 = 12.25\% \equiv 77\%$	Risk = $R5 = 5.25\% \equiv 33\%$
Delay in the rescue due to the deployment of the responder teams:	Delay in the rescue due to the proposed deployment of the CBRN teams:
<ul style="list-style-type: none"> • Probability: <ul style="list-style-type: none"> – Level: Probable – Unlikely – Value: 2.5 • Magnitude: <ul style="list-style-type: none"> – Level: Medium – Value: 2.0 	<ul style="list-style-type: none"> • Probability: <ul style="list-style-type: none"> – Level: Unlikely – Completely unlikely – Value: 1.5 • Magnitude: <ul style="list-style-type: none"> – Level: Medium – Value: 2.0
Risk = $R6 = 5.0\% \equiv 32\%$	Risk = $R6 = 3.0\% \equiv 19\%$

6. CONCLUSIONS

This work has focused on the improvement of the safety of the subway system of Rome in case of a CBRN event. The proposed solutions contributed to:

- Improvement of the first response system: By means of the creation of first responder CBRN teams and the proposal of a proper deployment. This was analysed using the case study of a CBRN attack in the subway system of Rome;
- Improvement of the emergency zoning: Based on the British system, it has been possible to suggest a new approach for the emergency zoning with the following advantages:
 - Reduction in the dispersion of the contamination outside the area of the event;
 - Reduction of the traffic inside the area of the event.
- Creation of an automatic detection and warning system: This system was elaborated for the special case of the subway system of Rome, but with

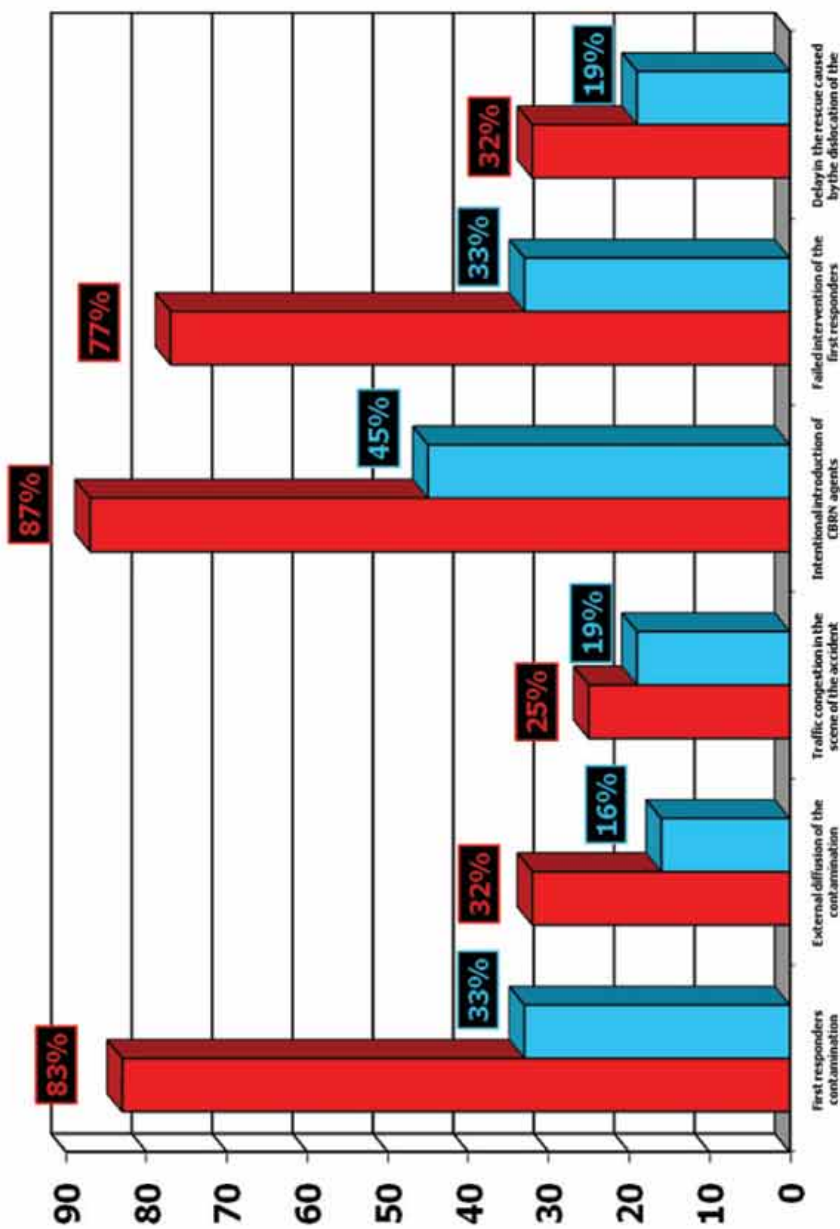


Figure 10: Comparison of the results of the risk analysis before and after the introduction of the solutions proposed.

proper modifications, it might be feasible for other sensitive targets in Italy;

- Study of a method to carry out a preliminary assess of the risks connected to an unconventional event: This method was applied to the case study, showing the effectiveness of the proposed solutions. There has been a reduction of the risks of about 30 %, calculated by the difference between the mean values of the Total Risk before and after the introduction of the solutions.

In conclusion, the aim of improving safety in case of a CBRN attack in a confined environment, such as the subway system of Rome, has been achieved.

REFERENCES

- Counterproliferation Programme Review Committee (CPRC) (2004). *Report on Activities and Programmes for Countering Proliferation and NBC Terrorism*. Counterproliferation Programme Review Committee (CRPC), Washington D.C.
- Department of the Army (DOA) (1991). *First Aid for Soldiers*. Field Manual No. 21-11 (FM 21-11), Department of the Army (DOA), Washington D.C.
- Department of the Army (DOA) (1995). *Treatment of Chemical Agent Casualties and Conventional Military Chemical Injuries*. Field Manual No. 8-285 (FM 8-285), Department of the Army (DOA), Washington D.C.
- Department of the Army (DOA) (1996). *Health Service Support in a Nuclear, Biological, and Chemical Environment*. Field Manual No. 8-10-7 (FM 8-10-7), Department of the Army (DOA), Washington D.C.
- Department of Defense (DOD) (1998). *The Militarily Critical Technologies List, Part II: Weapons of Mass Destruction Technologies*. Office of the Under Secretary of Defense for Acquisition and Technology, Department of Defence (DOD), Washington, D.C.
- Jarrett, D. (Ed.) (1999). *Medical Management of Radiological Casualties Handbook, 1st Edition*. Armed Forces Radiobiology Research Institute, Bethesda, Maryland.
- Murakami, H. (2000). *Underground: The Tokyo Gas Attack and the Japanese Psyche*. Vintage International, New York.
- Tu, A.T. (2000). Overview of sarin terrorist attacks in Japan. *ACS Symp. Series*, 745: 304-317.

MORPHOLOGICAL SPATIAL PATTERN ANALYSIS OF MOUNTAINS EXTRACTED FROM DIGITAL ELEVATION MODELS

Dinesh Sathyamoorthy

Instrumentation and Electronics Technology Division (BTIE), Science & Technology Research Institute for Defence (STRIDE), Ministry of Defence, Malaysia

E-mail: dinsat60@hotmail.com

ABSTRACT

Morphological spatial pattern analysis (MSPA) employs concepts of mathematical morphology to segment input binary objects into a series of categories revealing information about size, shape and connectivity. It emphasises on connectivity between the objects' parts as measured via various values of size parameters s. MSPA has become a popular tool for landscape modelling, but has yet to receive significant attention in other areas of applications. In this paper, MSPA is employed to segment mountains extracted from digital elevation models (DEMs) into seven mutually exclusive categories: core, islet, bridge, loop, edge, perforation and branch. The effect of various values of s on the classification of these categories is studied. It is observed that smaller values of s provide more differentiation among the categories, and hence, better information about the classification of the extracted mountains. However, as pattern measurements are scale-dependent, and since s is a part of the definition of scale of observation, it is advisable that various values of s are employed to determine the appropriate levels of classification for various applications.

Keywords: digital elevation models (DEMs); mountains; morphological spatial pattern analysis (MSPA); size parameter; classification.

1. INTRODUCTION

Mountains are the portions of a terrain that are sufficiently elevated above the surrounding land (greater than 300 to 600m) and have comparatively steep sides. In a mountain, two parts are distinctive:

- i. The summit, the highest point (the peak) or the highest ridges
- ii. The mountainside, the part of a mountain between the summit and the foot (Bates & Jackson, 1987).

The mapping of mountains is generally performed manually through fieldwork and visual interpretation of topographic maps, which is time consuming and labour intensive. In recent times, extraction techniques have evolved from manual through computer assisted to automated methods with digital elevation models (DEMs) as

the input data. In seeking the efficient extraction of mountains from DEMs, various algorithms have been proposed (Graff & Usery, 1993; Miliaresis & Argialas, 1999; Miliaresis, 2000; Dinesh, 2006).

A number of studies have been conducted on the quantitative categorisation and classification of mountains for accurate and repeatable interpretation and analysis in various applications, including mountain ordering (Yamada, 1999), geomorphometric mapping (Miliaresis, 2001, 2006), cluster analysis (Miliaresis & Argialas, 2002; Miliaresis & Iliopoulou, 2004), granulometry (Dinesh & Fadzil, 2007), and landform metrics (Dinesh, 2009). Mountain ordering, geomorphometric mapping and cluster analysis are able to provide concise classifications based on applicable attributes of the extracted mountains (e.g. gradient, local relief, relative massiveness etc.). However, the accuracy of the classifications is dependent on the accuracy of the attributes computed from the DEM. Granulometry characterises mountains based on only size, which is insufficient for effective classification. While statistics provided from landform metrics have been widely accepted (O'Neill *et al.*, 1988; Turner, 1990; Haines-Young & Chopping, 1995; Neel *et al.*, 2004; Buyantuyev & Wu, 2007), their applicability without prior testing with applicable neutral models has been called into question (Turner *et al.*, 2001; Li *et al.*, 2004; Gardner & Urban, 2007). In addition, while literally hundreds of landform metrics have been developed, only a few are useful for mountain characterisation (Dinesh, 2009), which are interdependent and non-intuitive for classification (McGarigal *et al.*, 2009; Vogt, 2009).

Morphological spatial pattern analysis (MSPA) (Vogt *et al.*, 2007a; Soille & Vogt, 2009) employs concepts of mathematical morphology (Matheron, 1975; Serra, 1982; Soille, 2003) to segment input binary objects into a series of categories revealing information about size, shape and connectivity. It emphasises on connectivity between the objects' parts as measured via various values of size parameters s . MSPA has become a popular tool for landscape modelling (Vogt *et al.*, 2007a,b, 2009; Riiters *et al.*, 2007; Ostapowicz *et al.*, 2008; Vogt, 2009), but has yet to receive significant attention in other areas of applications.

In this paper, MSPA is employed to segment mountains extracted from DEMs into seven mutually exclusive categories. The effect of various values of s on the classification of these categories is studied. The seven categories, as defined by Soille & Vogt (2009), are:

- **Core**
 - (1) *Core* pixels are defined as foreground pixels with distance to the background greater than s .
- **Islet**
 - (2) *Islet* pixels are defined as disjoint foreground connected components that are too small to contain core pixels.
- **Connectors: Bridge and loop**

Connector pixels are groups of foreground pixels linking core connected components so that their removal would modify the homotopy of the

object. Connector pixels are subdivided into two categories depending on whether the same core connectors link the same core connected component or not:

- (3) *Bridge* pixels are connector pixels emanating from two or more core connected components.
- (4) *Loop* pixels are connector pixels emanating from the same core connected component.

➤ **Boundaries: Edge and perforation**

Boundary pixels are defined as yet unclassified foreground pixels with distance to the core pixels lower or equal to s . Boundary pixels are subdivided into:

- (5) *Edge* (outer boundary) pixels are boundary pixels forming the outer perimeter of the core connected components.
- (6) *Perforation* (inner boundary) pixels are boundary pixels forming the perimeter of holes within core connected components.

➤ **Branch**

(7) *Branch* pixels are pixels that do not belong to any of the previously defined categories. They emanate either from boundaries or connectors. It should be noted that connector and branch pixels that are adjacent to core pixels could be called junction pixels and classified as such if required by the application.

2. MATHEMATICAL MORPHOLOGY

Mathematical morphology is a branch of image processing that deals with the extraction of image components that are useful for representational and descriptive purposes. Mathematical morphology has a well developed mathematical structure that is based on set theoretic concepts. The effects of the basic morphological operations can be given simple and intuitive interpretations using geometric terms of shape, size and location. The fundamental morphological operators are discussed in Matheron (1975), Serra (1982) and Soille (2003). Morphological operators generally require two inputs; the input image A, which can be in binary or grayscale form, and the kernel B, which is used to determine the precise effect of the operator. Each pixel in A is compared with B by moving B so that its centre hits the pixel. Depending on the type of morphological operator employed, the pixel value is reset to the value or average value of one or more of its neighbours.

Dilation sets the pixel values within the kernel to the maximum value of the pixel neighbourhood. Binary dilation gradually enlarges the boundaries of regions of foreground pixels, resulting in areas of foreground pixels growing in size, and holes within those regions becoming smaller (Duchane & Lewis, 1996). The dilation operation is expressed as:

$$A \oplus B = \{a+b: aeA, beB\} \quad (1)$$

Erosion sets the pixels values within the kernel to the minimum value of the kernel. Binary erosion gradually removes the boundaries of regions of foreground pixels, resulting in areas of foreground pixels shrinking in size, and holes within these areas becoming larger (Duchane & Lewis, 1996). Erosion is the dual operator of dilation:

$$A \ominus B = (A^c \oplus B)^c \quad (2)$$

Morphological reconstruction allows for the isolation of certain features within an image based on the manipulation of a mask image X and a marker image Y . It is founded on the concept of geodesic transformations, where dilations or erosion of a marker image are performed until stability is achieved (represented by a mask image) (Vincent, 1993).

The geodesic dilation δ^G used in the reconstruction process is performed through iteration of elementary geodesic dilations $\delta_{(l)}$ until stability is achieved.

$$\delta^G(Y) = \delta_{(l)}(Y) \circ \delta_{(l)}(Y) \circ \delta_{(l)}(Y) \dots \text{until stability} \quad (3)$$

The elementary dilation process is performed using a standard dilation of size one followed by an intersection.

$$\delta_{(l)}(Y) = Y \oplus B \cap \quad (4)$$

The operation in Equation 4 is used for elementary dilation in binary reconstruction (Vincent, 1993).

A skeleton is a one pixel thick line representation of an object that summarizes the overall shape, size and orientation of the object. Skeletonisation is the process of reducing foreground regions in a binary image to a skeleton, while discarding the remaining foreground pixels. The resultant skeleton is used for the computation of length and direction, or for the detection of special topological structures such as end points and triple points (Pitas, 1993).

In this paper, skeletonisation is implemented using the morphological thinning algorithm proposed in Jang & Chin (1990). Skeletonisation by morphological thinning is defined as the successive removal of outer layers of pixels from an object while retaining any pixels whose removal would alter the connectivity or shorten the legs of the skeleton. The process is converged or completed when no further pixels can be removed without altering the connectivity or shortening the skeletal legs.

3. IMPLEMENTATION OF MPSA

➤ Core

Core pixels are identified by eroding the mountain pixels with a disk kernel of size s . This removes mountain pixels that have distance of less than s pixels from the background. The difference between the core pixels and the original foreground pixels defines the pixels that are candidates for the remaining classes, known as non-core pixels.

➤ **Islet**

Morphological reconstruction is implemented using the core pixels as the marker and the original mountain pixels as the mask. This step flags all core and mountain pixels that are connected to the core pixels. Islet pixels are identified by computing the difference between the original foreground pixels and the reconstructed pixels.

➤ **Connector**

The skeletons of the core connected components are computed. Conditional dilation is performed on the skeletons for s iterations. For each iteration of conditional dilation, the skeletons are dilated with a square kernel of size 3, and the dilated pixels that do not correspond to non-core pixels are deleted. The resulting pixels form the connector pixels:

- Connector pixels that are connected to two or more core connected components are identified as bridge pixels.
- The remaining connector pixels are identified as loop pixels.

➤ **Boundary**

Only the remaining mountain pixels are considered for boundary classification. The complement of the core pixels is eroded with a disk kernel of size s . This removes non-core pixels that are less or equal than s pixels from the core pixels. The boundary pixels are identified by computing the difference between the non-core pixels and the eroded pixels.

- The holes in the core connected components are filled. The filled core connected components are eroded with a disk kernel of size s . The perforation pixels are identified by performing an intersection between the filled core connected components and the boundary pixels.
- The remaining boundary pixels are identified as edge pixels.

➤ **Branch**

The mountain pixels that have not been classified to the previous categories are identified as branch pixels.

4. CASE STUDY

The DEM in Figure 1 shows the area of Great Basin, Nevada, USA. The area is bounded by latitude $38^{\circ} 15'$ to 42° N and longitude $118^{\circ} 30'$ to $115^{\circ} 30'$ W. The DEM was rectified and resampled to 925 m in both x and y directions. The DEM is a Global Digital Elevation Model (GTOPO30) and was downloaded from the USGS GTOPO30 website (GTOPO30, 1996). GTOPO30 DEMs are available at a global scale, providing a digital representation of the Earth's surface at a 30 arc-seconds sampling interval. The land data used to derive GTOPO30 DEMs are obtained from

digital terrain elevation data (DTED), 1-degree DEMs for USA and the digital chart of the world (DCW). The accuracy of GTOPO30 DEMs varies by location according to the source data. The DTED and the 1-degree dataset have a vertical accuracy of ± 30 m while the absolute accuracy of the DCW vector dataset is $\pm 2,000$ m horizontal error and ± 650 m vertical error (Miliaresis & Argialas, 2002). Tensional forces on the terrain's crust and thins by normal faulting cause the formation an array of tipped mountain blocks that are separated from broad plain basins, producing a basin-and-range physiography (Howell, 1995; Summerfield, 1996, 2000; Miliaresis & Argialas, 1999; Miliaresis, 2008).

The mountains of the DEM of Great Basin (Figure 2(a)) are extracted using the mathematical morphological based algorithm proposed in Dinesh (2006). First, ultimate erosion is performed on the DEM to extract the peaks of the DEM. Conditional dilation is performed on the extracted peaks to obtain the mountains of the DEM. A total of 14 distinct individual mountains objects are extracted from the DEM (Figure 2(b)).

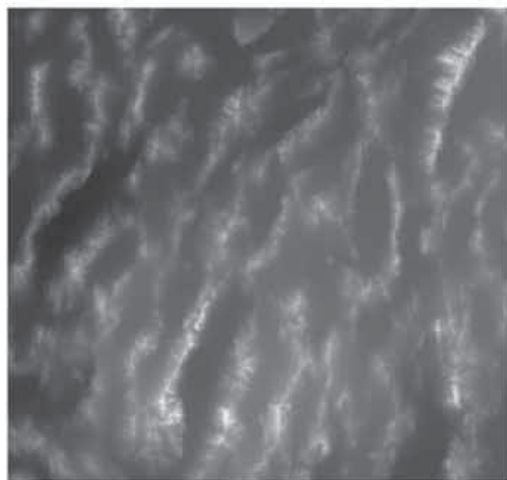


Figure 1: The GTOPO30 DEM of Great Basin. The elevation values of the terrain (minimum 1005 meters and maximum 3651 meters) are rescaled to the interval of 0 to 255 (the brightest pixel has the highest elevation). The scale is approximately 1:3,900,000.

MSPA is used to segment the extracted mountains into the seven categories using size parameters s of 1 to 40 (Figure 3). Figure 4 shows the proportions of each category for increasing values of s . In general, the value of s drives the proportions of the core and non-core categories. Initially, at $s = 0$, all the mountain pixels are assigned to the core category. When s is larger than the size of the individual mountain objects (at $s = 37$), all the mountain pixels are assigned to the islet category. Simultaneous existence of core and non-core categories occurs when the value of s varies between these two boundary values. With increasing values of s , the core proportion decreases, while the islet proportion either increases or remains stable.

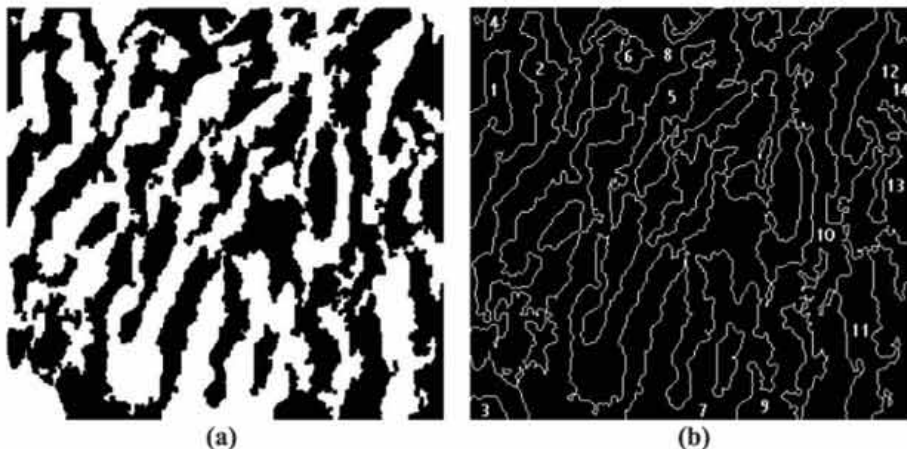
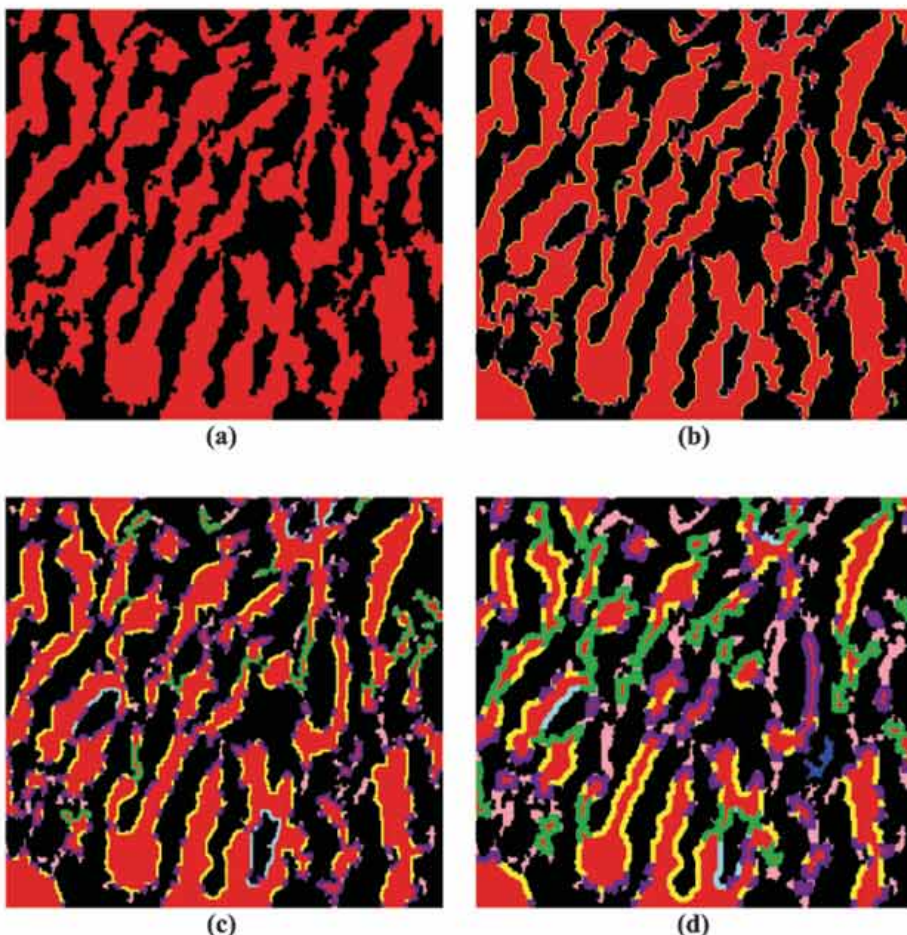


Figure 2: Extraction of mountains from DEM. (a) The extracted mountains (The pixels in white); (b) A total of 14 individual mountains objects are identified using connected component labelling (Pitas, 1993).



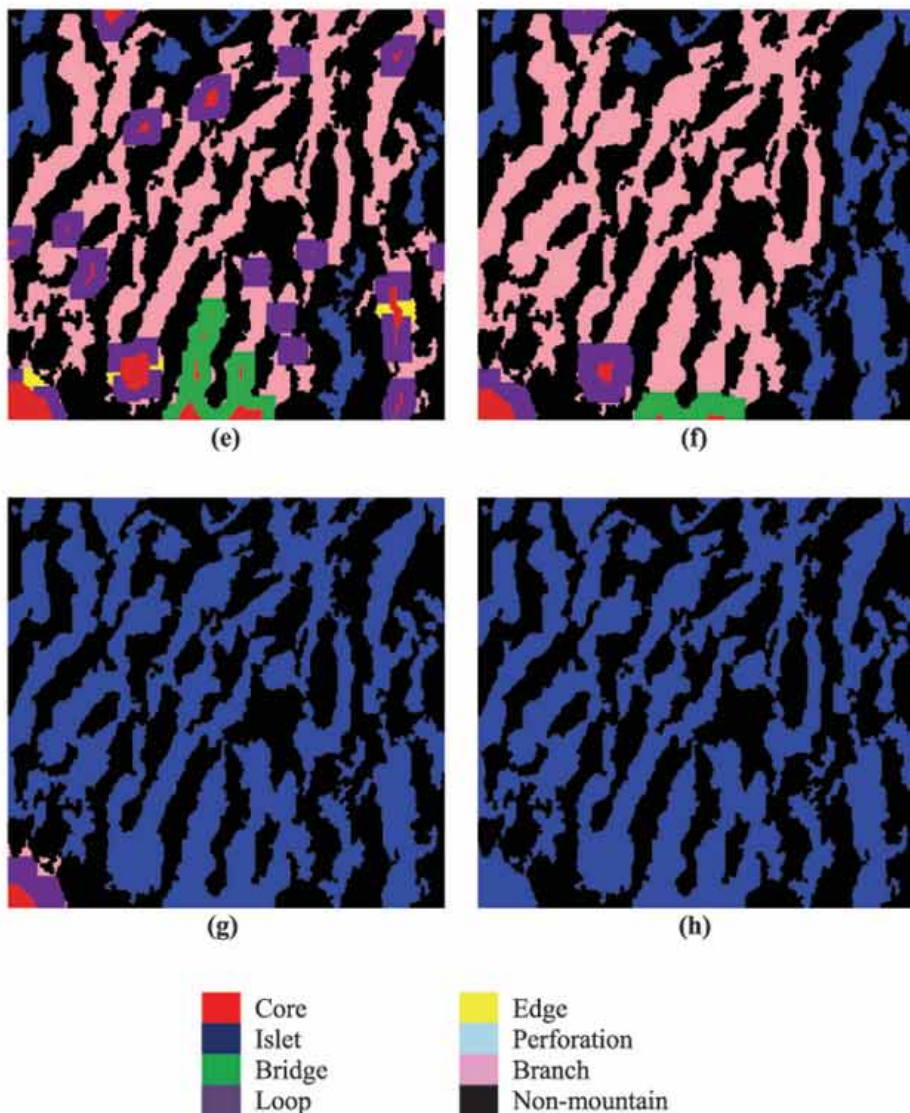


Figure 3: Morphological spatial patterns of the extracted mountains computed using size parameters s of: (a) 0; (b) 1; (c) 3; (d) 5; (e) 10; (f) 15; (g) 20; (h) 37.

The change in proportion of the remaining categories with increasing values of s depends on the number and distribution of the remaining core connected components. Starting at $s = 0$, as s is increased, the number of distinct individual core connected components increases, while the width of bridges, loops, edges and perforations increases. This results in increases in proportions of the bridge, loop, edge and perforation categories. However, as s is further increased, the number and area of core connected components reduce, resulting in reduction in the proportions of the four categories.

With increasing s , smaller portions of the individual mountain objects are assigned to the core category, with the remaining parts of the mountain objects being assigned to branch category. This results in a significant increase in proportions of the branch category. As s is further increased, these mountain objects are increasingly assigned to the islet category, resulting in reductions in the proportions of the branch category.

It is observed in Figure 3 that smaller values of s provide more differentiation among the categories, and hence, better information about the classification of the extracted mountains. However, as pattern measurements are scale-dependent, and since s is a part of the definition of scale of observation, it is advisable that various values of s are employed to determine the appropriate levels of classification for various applications.

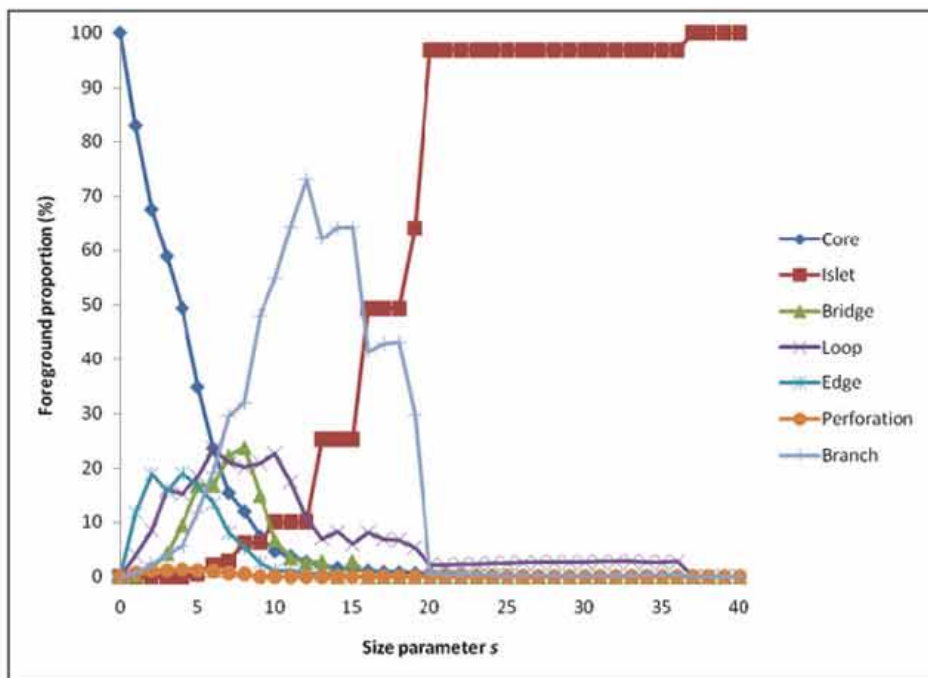


Figure 4: Proportions of each category of the extracted mountains for increasing size parameter s .

5. CONCLUSION

In this paper, the effect of various values of size parameters s on the segmentation of mountains extracted from DEMs into seven mutually exclusive categories (core, islet, bridge, loop, edge, perforation and branch) via MSPA was studied. The value of s controls the width of the bridge, loop, edge and perforation categories, the maximum size of islet categories, and the minimum size of core categories. An increase in s results in less core area, and more non-core area. Smaller values of s

provide more differentiation among the categories, and hence, better information about the classification of the extracted mountains. However, various values of s should be experimented to determine the appropriate levels of classification for various applications.

Scale variations can constrain the detail with which information can be observed, represented and analyzed. Changing the scale without first understanding the effects of such an action can result in the representation of patterns or processes that are different from those intended (Robinson *et al.*, 1984; Lam & Quattrochi, 1992; Goodchild & Quattrochi, 1997; Lam *et al.*, 2005; Summerfield, 2005; Wu *et al.*, 2008). Hence, feature detection and characterization often need to be performed at different scales measurement. Wood (1996a, b) and Wu *et al.* (2008) demonstrated that analyses of a location at multiple scales allow for a greater amount of information to be extracted from a DEM about the spatial characteristics of a feature. Work is currently being conducted to study the effect of MSPA classification on mountains extracted from multiscale DEMs.

REFERENCES

- Bates, R.L. & Jackson, J.A. (Eds.) (1987). *Glossary of Geology*. American Geological Institute, Alexandria, Virginia.
- Buyantuyev, A. & Wu, J. (2007). Effects of thematic resolution on landscape pattern analysis. *Landscape Ecol.*, **22**: 7-13.
- Dinesh, S. (2006). Extraction of mountains from digital elevation models using mathematical morphology. *GIS Malaysia* **1**: 16-19.
- Dinesh, S. (2009). Analysis of landform metrics of mountains extracted from multiscale digital elevation models. *Australian J. Basic Appl. Sci.*, **3**: 3997-4010.
- Dinesh, S. & Ahmad Fadzil, M.H. (2007). Characterization of the size distribution of mountains extracted from multiscale digital elevation models. *J. Appl. Sci.*, **7**: 1410-1415.
- Duchene, P. & Lewis, D. (1996). *Visilog 5 Documentation*. Noesis Vision, Quebec.
- Gardner, R.H. & Urban, D.L. (2007). Neutral models for testing landscape hypotheses. *Landscape Ecol.*, **22**: 15-29.
- Goodchild, M.F. & Quattrochi, D.A. (1997). Scale, multiscaling, remote sensing and GIS. In Quattrochi, D.A. and Goodchild, M.F. (Eds.), *Scale in Remote Sensing and GIS*. Lewis Publishers, Boca Raton, Florida, pp. 1-11.
- Graff, L.H. & Usery., E.L. (1993). Automated classification of generic terrain features in digital elevation models. *Photogramm. Eng. Rem. S.*, **59**: 1409-1417.
- GTOPO30 (1996). *GTOPO30: Global 30 Arc Second Elevation Data Set*. Available online at: <http://edcwww.cr.usgs.gov/landdaac/gtopo30/gtopo30.html> (Last access date: 1st June 2009)

- Haines-Young, R. & Chopping, M. (1996). Quantifying landscape structure: a review of landscape indices and their application to forested landscapes. *Prog. Phys. Geog.*, **20**: 418-445.
- Howell, D. (1995). *Principles of Terrain Analysis: New Applications for Global Tectonics*. Chapman and Hall, London.
- Jang, B.K. & Chin, R.T. (1990). Analysis of thinning algorithms using mathematical morphology. *IEEE T. Pattern Anal.*, **12**: 541-550.
- Lam, N. & Quattrochi, D. (1992). On the issues of scale, resolution, and fractal analysis in the mapping science. *Prof. Geogr.* **44**: 88-98.
- Lam, N., Catts, D., Quattrochi, D., Brown, D. & McMaster, R. (2005). Scale. In McMaster, R.B., and Usery, E.L. (Eds.), *A Research Agenda for Geographic Information Science*. CRC Press, New York, pp. 93-128.
- Li, X., He, H.S., Wang, X., Bu, R. & Chang, Y. (2004). Evaluating the effectiveness of neutral landscape models to represent a real landscape. *Landscape Urban Plan.*, **69**: 137-148.
- Matheron, G. (1975). *Random Sets and Integral Geometry*. Wiley, New York.
- McGarigal, K., Serbin, T. & Cushman, S.A. (2009). Surface metrics: An alternative to patch metrics for the quantification of landscape structure. *Landscape Ecol.*, **24**: 433-500.
- Milaresis, G. (2000). The DEM to mountain transformation of Zagros Ranges. *5th International Conference on GeoComputation*, 23rd-25th August 2000, University of Greenwich.
- Milaresis, G. (2001). Geomorphometric mapping of Zagros Ranges at regional scale. *Comput. Geosci.*, **27**: 775-786.
- Milaresis G. (2006). Geomorphometric mapping of Asia Minor from Globe DEM. *Geogr. Ann.*, **88A**: 209-221.
- Milaresis G. (2008). Quantification of terrain processes. *Lect. Notes Geoinform. Cartogr.* **XIV**: 13-28.
- Milaresis, G. & Argialas, D.P. (1999). Segmentation of physiographic features from Global Digital Elevation Model/GTOPO30. *Comput. Geosci.*, **25**: 715-728.
- Milaresis, G. & Argialas, D.P. 2002. Quantitative representation of mountain objects extracted from the Global Digital Elevation Model (GTOPO30). *Int. J. Remote Sens.*, **23**: 949-964.
- Milaresis, G. & Iliopoulou, P. (2004). Clustering of Zagros Ranges from the Globe DEM representation. *Int. J. Appl. Earth Observation Geoinform.*, **5**: 17-28.
- Neel, M. C., McGarigal, K. & Cushman, S.A. 2004. Behavior of class-level landscape metrics across gradients of class aggregation and area. *Landscape Ecol.*, **19**: 435-455.
- Ostapowicz, K., Vogt, P., Riitters, K.H., Kozak, J. & Estreguil, C. 2008. Impact of scale on morphological spatial pattern of forest. *Landscape Ecol.*, **23**: 1107-1117.
- Pitas, I. (1993). *Digital Image Processing Algorithms*. Prentice Hall, London.

- Riitters, K.H., Vogt, P., Soille, P., Kozak, J. & Estreguil, C. (2007). Neutral model analysis of landscape patterns from mathematical morphology. *Landscape Ecol.*, **22**: 1033-1043.
- Robinson, A.H., Sale, R.D., Morrison, J.L. & Muehrcke, P.C. (1984). *Elements of Cartography*. John Wiley & Sons, New York.
- Serra, J. (1982). *Image Analysis and Mathematical Morphology*. Academic Press, London.
- Soille, P. (2003). *Morphological Image Analysis: Principles and Applications*. Springer Verlag, Berlin.
- Soille, P. & Vogt, P. (2009). Morphological segmentation of binary patterns. *Pattern Recogn. Lett.*, **30**: 456-459.
- Summerfield, M. (1996). *Global Geomorphology*. Longman, Essex.
- Summerfield, M. (Ed.) (2000). *Geomorphology and Global Tectonics*. John Wiley & Sons, New York.
- Summerfield, M.A. (2005). A tale of two scales, or two geomorphologies. *Trans. Inst. Bri. Geog.*, **30**: 402-415.
- Turner, M.G., 1990. Landscape changes in nine rural counties in Georgia. *Photogramm. Eng. Rem. S.* **56(3)**: 379-386.
- Turner, M.G., Gardner, R.H. & O'Neill, R.V. 2001. *Landscape Ecology in Theory and Practice: Pattern and Process*. Springer-Verlag, New York.
- Vincent, L. (1993). Morphological reconstruction in image analysis: applications and efficient algorithms. *IEEE T. Image Process.*, **2**: 176-201.
- Vogt, P. (2009). *Morphological Spatial Pattern Analysis*. Institute for Environment and Sustainability, Joint Research Centre, European Commission, Ispra, Italy.
- Vogt, P., Riitters, K.H., Estreguil, C., Kozak, J., Wade, T.G. & Wickham, J.D. 2007a. Mapping spatial patterns with morphological image processing. *Landscape Ecol.*, **22**: 171-177.
- Vogt, P., Riitters, K.H., Iwanowski, M., Estreguil, C., Kozak, J. & Soille, P. 2007b. Mapping landscape corridors. *Ecol. Indic.*, **7**: 481-488.
- Vogt, P., Ferrari, J.R., Lookingbill, T.R., Gardner, R.H., Riitters, K.H. & Ostapowicz, K. (2009). Mapping functional connectivity. *Ecol. Indic.*, **9**: 64-71.
- Wood, J. (1996a). Scale-based characterization of digital elevation models. In Parker, D. (Ed.) *Innovation in GIS 3*. Taylor & Francis, London, 163-175.
- Wood, J. (1996b). *The Geomorphological Characterization of Digital Elevation Models*. PhD Thesis, Department of Geography, University of Leicester, Leicester.
- Wu, S., Li, J. & Huang, G.H. (2008). A study on DEM-derived primary topographic attributes for hydrologic applications: Sensitivity to elevation data resolution. *Appl. Geog.*, **28**: 210-223.
- Yamada, S. (1999). Mountain ordering: A method for classifying mountains based on their morphometry. *Earth Surf. Proc. Land.*, **24**: 653-660.

PATHOGENIC BACTERIA DETECTION IN DENTAL UNIT WATER LINES OF MALAYSIAN ARMED FORCES (MAF) DENTAL CENTRES

Ahmad Razi Mohamed Yunus¹, Haryanti Toosa¹, Zukri Ahmad¹, Mazlan Eni¹, Norisah Othman¹, Liana Ma Abdullah² & Zalini Yunus^{1*}

¹Protection & Biophysical Technology Division, Science & Technology Research Institute for Defence (STRIDE), Ministry of Defence, Malaysia

²Dental Specialist Polyclinic, Tunku Mizan Armed Forces Hospital, Ministry of Defence, Malaysia

*Email: zalini.yunus@stride.gov.my

ABSTRACT

Various microorganisms, including bacteria, fungi and protozoans, have been shown to colonise and replicate in dental unit water lines (DUWLs), resulting in the formation of biofilms. The quality of dental unit water is of considerable importance since patients and dental staffs are regularly exposed to water and aerosols generated from DUWLs. A total of 95 dental unit water samples from 11 Malaysian Armed Forces (MAF) Dental Centres were collected in the period of 7 months, from August 2008 to February 2009. The results obtained from this study indicate that 9.47 % of the samples were contaminated with *Pseudomonas aeruginosa*. The presence of *Pseudomonas aeruginosa* was confirmed using the polymerase chain reaction (PCR) technique. DNA sequencing determined that they were closely related to *Pseudomonas aeruginosa* strain R285, while a few were related to *Pseudomonas aeruginosa* PA7.

Keywords: dental unit water lines (DUWLs); Malaysian Armed Forces (MAF) Dental Centres; *Legionella pneumophila*; *Pseudomonas aeruginosa*; polymerase chain reaction (PCR).

1. INTRODUCTION

Dental unit water line (DUWL) systems are used to irrigate oral cavities during dental treatment. DUWLs are the tubes that connect the high-speed hand piece, three way syringe and ultrasonic scaler to the water supply, which is either from public water supply or independent water reservoir. The water delivered from these devices is not sterile and has been shown to contain high numbers of bacteria, including opportunistic pathogens, in general dental practice (Schel *et al.*, 2006). The quality of dental unit water is of considerable importance in practicing good dental treatment and procedures since patients and dental staffs are regularly exposed to water and aerosols generated from DUWLs.

Various microorganisms, including bacteria, fungi and protozoans, have been shown to colonise and replicate in DUWLs, resulting in the formation of biofilms,

which play an important role in microbial contamination of water systems. Pathogenic bacteria *Pseudomonas aeruginosa* and *Legionella pneumophilla* have been reported to be common colonisers of biofilms in DUWLs (Barbeau *et al.*, 1996; Atlas *et al.*, 1995). *Pseudomonas aeruginosa* can thrive in low nutrient environments, such as distilled water (Pankhurst & Coulter, 2007), and has been reported to give rise to infections in immunocompromised patients, such as those on ventilators, burn patients and patients suffering from cystic fibrosis (Martin, 1987). *Legionella pneumophilla* can be present either as an atypical pneumonia or as milder flu-like illness, known as Pontiac fever. Transmission of legionella infection occurs via inhalation of contaminated aerosol droplets or, rarely, aspiration of contaminated water by susceptible individuals. The vast majority of cases of Legionnaires' disease are caused by *Legionella pneumophilla* serogroup 1 (Field *et al.*, 2002).

The objective of this study is to determine the occurrence of pathogenic bacteria *Legionella pneumophilla* and *Pseudomonas aeruginosa* in DUWLs in Malaysian Armed Forces (MAF) Dental Centres. The findings of this study are used to provide suggestions and recommendations for improving the quality of water from dental units in MAF Dental Centres.

2. MATERIALS AND METHODS

A total of 95 dental unit water samples from 11 MAF Dental Centres (Figure 1) were collected in the period of 7 months, from August 2008 to February 2009. The water from the high speed hand piece before flushing (HPB), ultrasonic scaler (SC), water syringe (WS), cup filler (CF) and water reservoir distilled water (WRD) (Figure 2) were flushed for 15 seconds before collection. The water samples were collected aseptically in sampling bags treated with sodium thiosulphate (Whirl-Pak).



Figure 1: Example of a dental unit chair from MAF Dental Centres.

Each water sample was analysed using microbiological analysis, comprising of tests for detection of *Legionella pneumophilla* (modified from BS 6068-4.12:1998 and ISO 11731:1998 Water Quality-Part 4) and *Pseudomonas aeruginosa* using the membrane filter method (Milipore). The presence of positive samples from microbiological analysis was confirmed using polymerase chain reaction (PCR) analysis.

Genomic DNAs from the positive samples were extracted using an AquaPure Genomic DNA Kit (Bio-Rad). The primers (ITS1 regions) 16F945 5'-GGG CCC GCA CAA GCG GTG G-3' and 23R458 5'-CTT TCC CTC ACG GTA C-3' were used. In each reaction, 49 µl of PCR master mix was added to the target DNA to achieve a final volume of 50 µl. After heating the samples at 94 °C for 5 minutes, the target DNA was amplified in 30 subsequent cycles under the following conditions: 94 °C for 1 minute, 55 °C for 1 minute, 72 °C for 2 minutes, and after the 30th cycle, it was held at 72 °C for 10 minutes to allow the extension polymerisation to finish. The PCR reactions were performed in the Bio-Rad iCycler. The amplified PCR of ITS1 regions were purified using a QIAquick gel extraction kit (Qiagen) and sent to First Base Laboratories Sdn. Bhd. for sequencing.

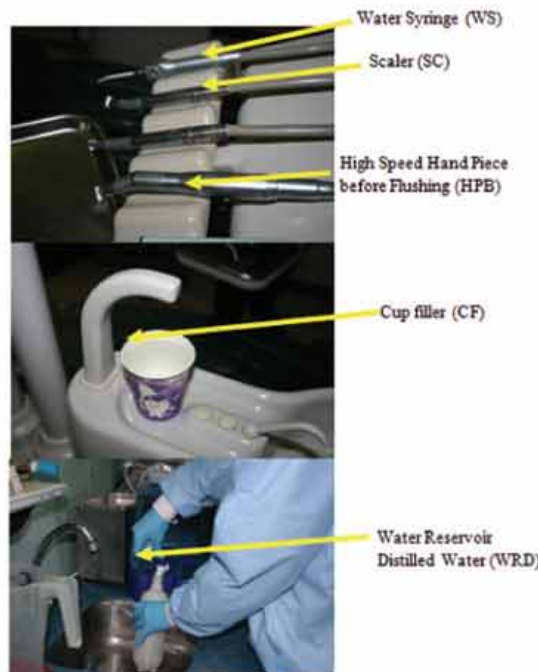


Figure 2: Sources of water sampling.

3. RESULTS AND DISCUSSIONS

It was observed that 6 of the 11 MAF Dental Centres involved in this study were free from the contamination of *Pseudomonas aeruginosa* and *Legionella pneumophilla*. On the other hand, 4 of the 11 dental centres were contaminated with

Pseudomonas aeruginosa. There was no contamination of *Legionella pneumophila* in all the samples in this study. The results obtained indicate that 9.47 % of the samples were contaminated with *Pseudomonas aeruginosa*. Out of the positive *Pseudomonas aeruginosa* samples, the samples from the SC showed the highest presence (66 %). This is followed by the HPB (22 %) and the WS (11 %). The reason for this finding may be due to different water flow rates and the SC being more frequently used than the HPB and WS. Via the PCR technique, it was confirmed that all the positive colonies obtained from the microbiological analysis were *Pseudomonas aeruginosa*. DNA sequencing determined that they were closely related to *Pseudomonas aeruginosa* strain R285, and a few were related to *Pseudomonas aeruginosa* PA7.

It should be noted that 81 % of the dental unit chairs had already been used on the day that the samples were collected. The DUWL contamination may originate from the saliva of the patient and colonisation of biofilm in the DUWL tubing. Water lines create optimal conditions for biofilm formation due to ideal surface chemistries, laminar flow and surface area. The presence of biofilm in DUWLs is a universal problem, and pathogens from patients and dental centres environment can be cultivated from biofilm removed from DUWLs. The water lines of dental units remain a potential weakness in the control of infection in dental practice, as they can easily become contaminated with both patient-derived and municipal impurities (Franco *et al.*, 2005).

The dental unit chairs in the MAF Dental Centres were supplied with either independent bottle reservoirs, or, directly or indirectly, from a municipal mains water supply (data not provided). A good quality water supply is also essential for dental unit chairs as heterotrophic bacteria found in water supplies can convert organic material dissolved in the water into biomass locally. The poorer the quality of the water supplied to dental unit chair, the more readily biofilm will form on its surfaces. In this regard, the dental unit chair connected to the main water supply should be processed to remove particulate matter, chemical residues and soluble organic matter. Some of dental unit chair models contain an air gap system that physically separates the water within the DUWL from the water supply, thus preventing backflow of potentially contaminated DUWLs into the water supply network (Coleman *et al.*, 2007).

4. CONCLUSION

The findings of this study have showed that improved, evidence-based practical methods for controlling the microbial contamination of DUWLs are urgently needed. This is particularly important in view of the increasing number of medically compromised and immunocompromised patients receiving regular dental treatment.

There are still areas that require further work in the future, in terms of controlling the microbial loading of DUWLs, such as studies on biofilm in DUWL tubing, effectiveness of disinfection that is applied in MAF Dental Centres, and the protocols and procedures practiced in dental treatment, in particular in MAF Dental Centres. These further studies can provide comprehensive data and information which can be used to assist MAF Dental Centres in improving dental treatment

quality and safety of the dental procedures. The key to success in reducing microbial loads in DUWLs may hinge upon a more complete understanding of the biofilms and how to control this multispecies, dynamic surface-associated community.

ACKNOWLEDGEMENTS

The authors are grateful to Dr Norazah Ahmad, Head of the Bacteriology Unit of the Institute of Medical Research (IMR), Malaysia, and her supporting staff for providing laboratory training to detect *Legionella pneumophila* and *Pseudomonas aeruginosa*. We would also like to thank the officers and staff of the MAF Dental Centres for their assistance in collection of samples. This work was supported by grants from the Science & Technology Research Institute for Defence (STRIDE), Ministry of Defence, Malaysia.

REFERENCES

- Atlas, R.M., Williams, J.F. & Huntington, M.K. (1995). *Legionella* contamination of dental unit waters. *App. & Env. Microbiol.*, **61**: 1208-1213.
- Barbeau, J., Tanguay, R., Faucher, E., Avezard, C., Trudel, L., Cote, L. & Prevost, A.P. (1996). Multiparametric analysis of waterline contamination in dental units. *Appl. Env. Microbiol.*, **62**:3954-9.
- Coleman, D.C., O'Donnell, M.J., Shore, A.C., Swan, J. & Russel, R.J. (2007). The role of manufacturers in reducing biofilms in dental chair waterlines. *J. Dent.*, **35**:701-711
- Fields, B.S., Benson, R.F. & Besser, R.E. (2002). Legionella and Legionnaires' disease. *Clin. Microbiol. Rev.*, **15**:506-526.
- Franco, F.F.S., Spratt, D., Leao, J.C. & Porter, S.R. (2005). Biofilm formation and control in dental unit waterlines. *Biofilm*, **2**:9-17.
- Martin, M.V. (1987). The significance of the bacterial contamination of dental unit water systems. *Br. Dent. J.*, **163**:152-153.
- Pankhurst, C.L. & Coulter, W.A. (2007). Do contaminated dental unit waterlines pose a risk of infection? *J. Dentistry*, **35**:712-720.
- Schel, A.J., Marsh, P.D., Bradshaw, D.J., Finney, M., Fulford, M.R., Frandsen, E., Østergaard, E., Ten Cate, J.M., Moorer, W.R., Mavridou, A., Kamma, J.J., Mandilara, G., Stösser, L., Kneist, S., Araujo, R., Contreras, N., Goroncy-Bermes, P., O'Mullane, D., Burke, F., O'Reilly, P., Hourigan, G., O'Sullivan, M., Holman, R. & Walker, J.T. (2006). Comparison of the efficacies of disinfectants to control microbial contamination in dental unit water systems in general dental practices across the European Union. *App. Env. Microbiol.*, **72**:1380-1387.

STATUS PEMAKANAN DI KALANGAN WARGA STRIDE

Razalee Sedek^{1*}, Mohd Badrolnizam Jamhari², Noorhasifah Ab Aziz², Abd Jalani Hj. Aini², Seti Salmah Khalid² & Nadira Mahadi²

¹Pusat Pengajian Sains dan Teknologi Makanan, Fakulti Sains dan Teknologi,
Universiti Kebangsaan Malaysia (UKM), Malaysia

²Bahagian Teknologi Perlindungan & Biofizikal (BTPB), Institut Penyelidikan
Sains & Teknologi Pertahanan (STRIDE), Kementerian Pertahanan, Malaysia

*E-mel:razalee@ukm.my

ABSTRAK

Kesihatan populasi adalah dipengaruhi oleh status pemakanan. Objektif kajian ini adalah untuk menilai prevalens berat badan berlebihan dan obes dalam kalangan warga STRIDE, dan menentukan perhubungannya dengan beberapa faktor sosio-demografi. Peratus lemak tubuh dan obesiti abdominal juga dikaji dalam kalangan subjek kajian ini. Kajian hirisan melintang ini melibatkan 215 pegawai dan kakitangan sokongan warga Institut Penyelidikan Sains dan Teknologi Pertahanan (STRIDE) berumur antara 18 hingga 55 tahun. Pengukuran antropometri termasuk ketinggian, berat badan, ukur lilit pinggang dan pinggul. Komposisi tubuh diukur menggunakan kaedah analisis bioelectrical impedance. Min tinggi, berat, indeks jisim tubuh (IJT), peratus lemak tubuh dan ukur lilit pinggang ialah 1.67 ± 0.59 cm, 69.8 ± 12.1 kg, 25.1 ± 0.1 kg/m² (julat 14.8 - 49.8 kg/m²), 26.0 ± 6.7 dan 87.2 ± 9.7 cm masing-masing. Berdasarkan kategori IJT (WHO, 1998), sejumlah 3.7% subjek adalah kurang berat badan, 49.8% normal, 36.3% pra-obes dan 10.2% obes. Keputusan menunjukkan bahawa prevalens berat badan berlebihan dan obesiti adalah lebih tinggi di kalangan subjek lelaki, pegawai, berkahwin, kumpulan umur dan gaji yang lebih tinggi serta tempoh perkhidmatan yang lebih panjang. Terdapat perkaitan signifikan antara status IJT dengan status perkahwinan ($p < 0.001$), umur ($p < 0.05$) dan tempoh perkhidmatan ($p < 0.05$). Secara keseluruhan, sejumlah 39% subjek mempunyai ukur lilit pinggang yang berisiko tinggi terhadap penyakit kardiovacular dan diabetes manakala 80% daripada subjek dikategorikan mempunyai peratus lemak pada tahap yang tinggi dengan min $29.9 \pm 8.7\%$. Hasil kajian juga mendapati bahawa koefisien korelasi antara IJT dan peratus lemak tubuh dalam kalangan subjek kajian ini ialah 0.74 bagi lelaki, manakala 0.81 bagi perempuan ($p < 0.001$). Kesimpulannya ialah hampir separuh daripada subjek kajian berada dalam kategori berat badan berlebihan atau obes, dan lebih satu pertiga berisiko tinggi terhadap penyakit kardiovacular dan diabetes. Sehubungan dengan itu, usaha mengurangkan berat badan berlebihan dan obesiti dengan menekankan pengambilan makanan yang baik dan peningkatan aktiviti fizikal akan memastikan status kesihatan yang optima di kalangan pegawai dan kakitangan sokongan STRIDE.

Kata Kunci: Komposisi tubuh; indeks jisim tubuh; obesiti; Kementerian Pertahanan.

1. PENGENALAN

Obesiti adalah masalah kesihatan awam yang utama yang dikaitkan dengan peningkatan morbiditi dan mortaliti. Organisasi antarabangsa seperti *World Health Organization* (WHO) dan *International Obesity Task Force* (IOTF) mengiktiraf obesiti sebagai wabak di serata dunia (James *et al.*, 2001). Ini adalah penyebab kedua bagi kematian yang boleh dicegah selepas tembakau (WHO, 2002). Pada peringkat populasi, prevalens obesiti yang tinggi disebabkan oleh interaksi kompleks antara perubahan gaya hidup populasi, termasuk penggunaan tenaga dan lemak yang tinggi dan gaya hidup yang semakin sedentari. Obesiti bukan satu masalah di negara maju tetapi adalah masalah global. Perubahan dalam diet dan aktiviti fizikal adalah konsisten dengan perubahan ini (Popkin & Doak, 1998). Pada tahun 2002, hampir 1.6 billion dewasa di dunia mempunyai berat badan berlebihan, dengan 400 juta dewasa dalam kategori obes (WHO, 2006). Malaysia tidak terkecuali daripada masalah ini.

Selari perkembangan pesat Malaysia ke arah status negara membangun, tahap kesihatan populasinya berkemungkinan akan berterusan menurun (Ismail *et al.*, 2002). Beberapa kajian terdahulu telah melaporkan bahawa obes berleluasa dalam semua kumpulan umur (Ismail *et al.*, 1995). Kajian Ismail menunjukkan bahawa dalam kalangan dewasa, sejumlah 21% didapati mempunyai berat badan berlebihan dan 6.2% adalah obes dengan menggunakan kriteria ditetapkan oleh WHO (2000). Kajian yang telah dijalankan oleh *The National Health Morbidity Survey 1996* menunjukkan bahawa prevalens berat badan berlebihan dalam kalangan dewasa secara keseluruhannya ialah 20.7% (IJT antara 25.0 dan 29.9 kg/m²) manakala 5.8% mempunyai IJT lebih daripada 30 kg/m² (Lim *et al.*, 2000). *Malaysian Adult Nutrition Survey* (MANS, 2003) dalam kajiannya mendapati bahawa 12.15% dewasa Malaysia adalah obes dan 29.7% lagi mempunyai berat badan berlebihan (Azmi *et al.*, 2009). Pada masa yang sama, 9.02% didapati kekurangan tenaga kronik (*chronic energy deficiency*) dan 49.27% mempunyai berat badan normal. Kajian yang telah dijalankan pada tahun 2006 oleh *Third National Health and Morbidity Survey* (NHMS III) menunjukkan bahawa prevalens berat badan berlebihan dan obesiti dalam kalangan populasi Malaysia yang berumur lebih 18 tahun adalah 29.1% dan 14.01% masing-masing. Prevalens berat badan berlebihan adalah lebih tinggi dalam kajian NHMS III (29.7%) dibandingkan dengan NHMS II (16.6%), tetapi tidak banyak berbeza dengan kajian MANS 2003 (27.4%). Kadar obesiti juga telah meningkat dengan pantas daripada 4.4% pada 1996 (NHMS II) kepada 12.7% pada 2003 (MANS) dan 14.01% pada 2006 (NHMS III) (KKM, 2008).

Berat badan dan tinggi secara kombinasinya boleh digunakan sebagai pengukuran yang ringkas dan dipercayai untuk menilai status pemakanan dan kesihatan secara keseluruhan, dan juga dalam penyaringan untuk berat badan berlebihan (Ismail *et al.*, 1995). Kaedah yang biasa digunakan untuk mengukur status pemakanan dewasa adalah IJT yang dikira sebagai berat badan (kg) dibahagi dengan tinggi (m) ganda

dua. Pengukuran komposisi tubuh merupakan suatu aspek penting dalam penilaian status pemakanan (Deurenberg *et al.*, 2000). Selain daripada tahap lemak tubuh, taburan tisu adipos turut mempengaruhi risiko bagi berat badan berlebihan. Lemak tubuh di bahagian atas (*abdominal adipose tissue*) menyebabkan risiko morbiditi yang lebih tinggi berbanding tisu adipos yang disimpan di bahagian *subcutaneous* punggung dan paha (NHLBI, 1998). Obesiti *abdominal* adalah satu petunjuk utama bagi adipositi lemak sentral untuk dewasa. Ianya mempunyai kaitan yang kuat dengan risiko pelbagai penyakit kronik seperti penyakit kardiovascular (CVD), diabetes dan barah payu dara (Huang *et al.*, 1999; Balkau *et al.*, 2007). Obesiti *abdominal* berlaku apabila simpanan lemak tubuh utama (tisu adipos) terjadi di sekeliling abdomen (*intra-abdominal* atau *visceral fat*) dan kawasan badan bahagian atas (Bouchard *et al.*, 1990). Dalam kajian populasi yang besar, pengukuran ukur lilit pinggang adalah kaedah yang sering digunakan kerana ia adalah sesuai dan murah (Han *et al.*, 2006).

Keprihatinan warga STRIDE terhadap berat dan tahap lemak tubuh mereka adalah perlu kerana ianya memberi kesan kepada prestasi fizikal dan kesihatan mereka. Menyedari kepentingan memelihara berat badan dan komposisi tubuh, satu kajian telah dijalankan ke atas pegawai dan kakitangan sokongan STRIDE. Objektif kajian ini adalah untuk menilai status pemakanan terkini melalui penilaian ciri-ciri fizikal dan komposisi tubuh serta menentukan perkaitan antara faktor-faktor sosio-demografi terpilih dengan status berat badan dalam kalangan warga STRIDE.

2. METODOLOGI

2.1 Lokasi Kajian, Rekabentuk Kajian dan Subjek

Satu kajian hirisan melintang telah dijalankan terhadap pegawai dan kakitangan sokongan STRIDE. Mereka dijemput untuk menjalani pengukuran melalui surat yang diedarkan kepada setiap bahagian melalui Pengarah Bahagian masing-masing. Kajian ini dijalankan ke atas 215 pegawai serta kakitangan sokongan STRIDE berumur antara 18 hingga 55 tahun yang bertempat di Kajang, Batu Arang dan Lumut. Subjek perempuan yang menyertai kajian ini hendaklah tidak hamil pada masa kajian dijalankan. Kajian dijalankan secara berperingkat mengikut bahagian di STRIDE. Kajian telah dijalankan di Kompleks Induk STRIDE pada 20-21 dan 26-27 Februari 2008, Bahagian Maritim, Lumut, pada 13-14 Mei 2008, Bahagian Persenjataan, Batu Arang, pada 25 November 2008, dan Ibu Pejabat Kajang Utama pula pada 26 November 2008.

2.2 Pengumpulan Data

Subjek perlu melengkapkan satu set borang soal selidik yang mengandungi soalan-soalan berkenaan maklumat sosio-demografi. Soalan-soalan merangkumi latar belakang subjek seperti umur, bangsa, cawangan/bahagian, pangkat, status perkahwinan, tahap pendidikan, jumlah pendapatan, tempoh perkhidmatan dan tahap kesihatan.

2.3 Pengukuran Antropometri dan Komposisi Tubuh

Parameter-parameter yang diukur termasuk ketinggian, berat badan, ukur lilit pinggang, ukur lilit pinggul dan komposisi tubuh. Semua pengukuran dijalankan pada waktu pagi antara pukul 8.00 hingga 9.30 pagi bertempat di Makmal Pemakanan bagi subjek di Kompleks Induk manakala bagi subjek di Bahagian lain, pengukuran dijalankan di bilik persembahan bahagian masing-masing (Rajah 1). Perkara-perkara yang perlu dipatuhi oleh subjek sebelum pengukuran telah pun dimaklumkan melalui surat yang diedarkan. Bagi memastikan status hidrasi yang normal untuk pengujian dan mendapatkan keputusan yang tepat, subjek dikehendaki mengelakkan latihan intensif 12 jam sebelum ujian, elakkan makan atau minum khususnya produk kaffein 4 jam sebelum ujian serta mengosongkan pundi kencing 30 minit sebelum ujian.

Sebelum pengukuran komposisi tubuh dijalankan, ketinggian subjek diukur terlebih dahulu dengan menggunakan SECA bodymeter 208 (SECA, Germany) yang tepat kepada 0.1 cm. Berat badan diukur terus menggunakan fungsi penimbang Tanita TBF-300A Body Fat Analyser (Tanita Corp., Japan) yang tepat kepada 0.1 kg serentak dengan pengukuran komposisi tubuh, di mana IJT dikira sebagai berat (kg) dibahagikan dengan tinggi (m) ganda dua. Subjek tidak boleh membawa atau memakai barang kemas dan lain-lain yang boleh bertindak sebagai konduktor elektrik. Pengukuran ukur lilit pinggang dan pinggul diukur dengan pita lentur berskala 0.1 cm terhampir. Ukuran pinggang dibuat pada paras pertengahan di antara tulang rusuk terakhir dan *iliac crest* tanpa menakukkan kulit. Subjek bernafas seperti biasa dan ukuran diambil pada akhir hembusan nafas. Ukur lilit pinggul dibuat di bahagian lilitan terbesar di pinggul tanpa menakukkan kulit. Nisbah pinggang dan pinggul dikira dengan membahagikan ukur lilit pinggang dengan ukur lilit pinggul.

Subjek dikelaskan kepada kategori berat berpandukan kepada WHO (1998): IJT < 18.5 kg/m^2 (kurang berat badan), IJT $18.5 - 24.9 \text{ kg/m}^2$ (normal), IJT $25.0 - 29.9 \text{ kg/m}^2$ (berat badan berlebihan), dan IJT $\geq 30 \text{ kg/m}^2$ (obes). Pengelasan mengikut kategori lemak tubuh pula berpandukan kriteria BIA, TBF-300A. Pengelasan tahap lemak tubuh mengikut jantina dan kumpulan umur seperti ditunjukkan dalam Jadual 1.

Bagi populasi Asia, ukur lilit pinggang yang lebih atau bersamaan dengan 90 cm bagi subjek lelaki adalah petunjuk kepada risiko yang tinggi terhadap penyakit kardiovascular dan diabetes. Bagi subjek perempuan pula, risiko yang tinggi terjadi apabila ukur lilit pinggang lebih atau bersamaan dengan 80 cm (Baker IDI, 2000).



Rajah 1: Kajian pengukuran antropometri dan komposisi tubuh. (a) Pengukuran tinggi; (b) komposisi tubuh; (c) dan (d) penerangan status pemakanan kepada subjek kajian oleh pegawai penyelidik.

Jadual 1: Tahap peratus lemak tubuh mengikut kumpulan jantina dan umur.

Jantina	Umur	Tahap peratus lemak tubuh		
		Rendah (%)	Normal (julat yang boleh diterima) (%)	Tinggi (%)
Lelaki	< 30 tahun	< 14	14 - 20	> 20
	≥ 30 tahun	< 17	17 - 23	> 23
Wanita	< 30 tahun	< 17	17 - 24	> 24
	≥ 30 tahun	< 20	20 - 27	> 27

3. ANALISIS DATA

Data dianalisis menggunakan *Statistical Package of Social Sciences (SPSS) 13.0 (SPSS Inc., Chicago, Illinois)*. Statistik deskriptif seperti frekuensi, min, sisisian piawai dan peratus digunakan untuk menerangkan ciri-ciri sosio-demografi dan ciri-ciri fizikal. Ujian *khi kuasa* dua digunakan untuk menentukan perkaitan antara

pemboleh ubah *categorical*. Ujian t-tidak berpasangan dan ANOVA satu-hala digunakan untuk membandingkan perbezaan min antara kumpulan masing-masing. Analisis korelasi digunakan untuk menentukan perhubungan antara pemboleh ubah kuantitatif. Paras kebarangkalian statistik pada $p < 0.05$ dikira sebagai signifikan.

4. KEPUTUSAN DAN PERBINCANGAN

4.1 Ciri-ciri Sosio-Demografi

Taburan subjek mengikut ciri-ciri sosio-demografi ditunjukkan dalam Jadual 2. Daripada 215 subjek kajian, majoriti subjek adalah daripada kumpulan umur 25 hingga 29 tahun (23.3%) diikuti kumpulan umur 50 hingga 55 tahun (22.3%) dan kumpulan umur 30 hingga 34 tahun (16.7%). Hanya sejumlah kecil subjek iaitu 3.7% yang berumur dibawah 25 tahun. Dari segi jantina, subjek lelaki (57.7%) adalah lebih ramai berbanding perempuan (42.3%). Sejumlah besar subjek kajian adalah berbangsa melayu (94.4%) diikuti dengan 2.3% masing-masing berbangsa Cina dan India, manakala lain-lain bangsa hanya meliputi 1%. Subjek yang berkahwin mencatat sejumlah besar iaitu 80.1%. Sebahagian besar subjek mempunyai kelayakan SPM/MCE (36.7%), diikuti oleh STPM/Diploma (22.3%) dan Ijazah Sarjana Muda (20.5%). Kelayakan SRP/PMR pula hanya meliputi sejumlah kecil subjek sahaja, iaitu 7% diikuti dengan Sijil (7.0%), Ijazah Sarjana (6%) dan Ijazah Doktor Falsafah (0.5%). Majoriti subjek yang terlibat dalam kajian ini terdiri daripada kakitangan sokongan, iaitu 72.6% berbanding 27.4% yang terdiri daripada pegawai. Dari segi pendapatan isi rumah, subjek dengan pendapatan melebihi RM 4000 sebulan mewakili satu pertiga atau 33% daripada jumlah keseluruhan subjek, hampir separuh subjek berpendapatan antara RM 1,000 hingga RM 3,000 manakala sejumlah kecil sahaja (1.5%) yang berpendapatan kurang daripada RM 1,000. Sebahagian besar subjek yang terlibat dalam kajian ini mempunyai tempoh perkhidmatan antara 1 hingga 5 tahun (32.7%) dan 21 hingga 30 tahun (28.0%) manakala kumpulan tempoh perkhidmatan yang lain hanya terdiri daripada 2.8% hingga 12.8% subjek sahaja.

4.2 Ciri-ciri fizikal dan Komposisi Tubuh

Ciri-ciri fizikal dan komposisi tubuh subjek ditunjukkan dalam Jadual 3. Min umur, berat badan, tinggi, IJT, peratus lemak tubuh, berat lemak, jisim tubuh tanpa lemak (JTTL), jumlah air tubuh, ukur lilit pinggang, ukur lilit pinggul serta nisbah pinggang dan pinggul bagi pegawai dan kakitangan sokongan secara keseluruhan adalah 38.5 ± 10.1 tahun, 66.1 ± 12.8 kg, 1.6 ± 0.1 m, 25.1 ± 0.1 kg/m², 30.0 ± 8.7 %, 20.3 ± 8.4 kg, 45.8 ± 8.6 kg, 33.6 ± 6.3 %, 83.6 ± 10.7 cm, 96.6 ± 8.9 cm dan 0.86 ± 0.89 masing-masing. Keputusan menunjukkan bahawa subjek lelaki mempunyai min umur, tinggi, berat, JTTL, jumlah air tubuh, ukur lilit pinggang dan nisbah pinggang dan pinggul yang lebih tinggi berbanding subjek wanita dan perbezaan min bagi kesemua ciri-ciri tersebut adalah signifikan ($p < 0.001$) kecuali umur. Subjek perempuan pula mempunyai IJT, peratus lemak dan berat lemak yang lebih tinggi berbanding subjek lelaki yang berbeza secara signifikan ($p < 0.001$) kecuali IJT. Secara puratanya, subjek lelaki dan perempuan menunjukkan IJT dalam

kategori berat badan berlebihan iaitu 25.1 kg/m^2 dan 25.2 kg/m^2 masing-masing. Walau bagaimanapun min ukur lilit pinggang bagi kedua-dua kumpulan subjek tidak menunjukkan risiko yang tinggi terhadap penyakit kardiovascular dan diabetis. Perbandingan dengan kajian ke atas kakitangan kerajaan di Bangunan Persekutuan Pulau Pinang (BPPP) mendapat min IJT subjek adalah 25.74 kg/m^2 (Aina Mardiah & Hazizi, 2010) manakala kajian ke atas kakitangan melayu kerajaan di Kangar, Perlis oleh Zahratul & Hazizi (2010) mendapat min IJT subjek adalah 26.59 kg/m^2 . Selain daripada itu, kajian terhadap guru pula mendapat min IJT mereka adalah 26.10 kg/m^2 (Nor Izzati & Rokiah, 2010). Walaupun min IJT subjek kajian ini termasuk dalam kategori berat badan berlebihan iaitu $25.1 \pm 0.1 \text{ kg/m}^2$ tetapi min IJT mereka masih lebih rendah berbanding kajian tersebut di atas.

4.3 Prevalens Berat Badan Berlebihan dan Obesiti

Rajah 2 menunjukkan daripada 215 subjek keseluruhan, separuh daripada subjek didapati mempunyai berat badan normal ($IJT 18.5\text{-}25 \text{ kg/m}^2$) manakala hanya sejumlah kecil sahaja iaitu 3.7% subjek adalah kurang berat badan ($IJT < 18.5 \text{ kg/m}^2$). Prevalens berat badan berlebihan ($IJT \geq 25 \text{ kg/m}^2$) dalam kalangan subjek kajian ini ialah sejumlah 46.5%. Daripada jumlah ini, sebanyak 36.3% ialah pra-obes ($IJT 25\text{-}29.9 \text{ kg/m}^2$) manakala 10.2% adalah obes ($IJT \geq 30 \text{ kg/m}^2$). Kajian MANS (2003) menunjukkan 29.1% dan 14.01% populasi Malaysia adalah berat badan berlebihan dan obes masing-masing. Prevalens berat badan berlebihan bagi subjek kajian ini adalah lebih tinggi manakala prevalens obesiti adalah lebih rendah berbanding kajian MANS (2003). Perbandingan dengan kajian terhadap kakitangan melayu kerajaan di BPPP menunjukkan prevalens berat badan berlebihan yang lebih rendah iaitu 29.6 % dan obes yang lebih tinggi (20.3%) (Aina Mardiah & Hazizi, 2010). Kajian terhadap 225 kakitangan kerajaan di Kangar, Perlis pula menunjukkan prevalens berat badan berlebihan dan obes yang lebih tinggi berbanding subjek kajian ini iaitu 40.4% dan 20.4% masing-masing (Zahratul & Hazizi, 2010). Nor Izzati & Rokiah (2010) dalam kajiannya terhadap 193 guru sekolah di Marang, Terengganu, mendapat kebanyakan subjek (40.4%) adalah dalam kategori berat badan berlebihan ($IJT \geq 25 \text{ kg/m}^2$). Prevalens berat badan berlebihan dalam kalangan guru ini adalah lebih rendah berbanding subjek kajian ini iaitu 46.5%. Perbandingan kajian Razalee (2008) terhadap anggota tentera lelaki Tentera Laut Diraja Malaysia (TLDM) dengan kajian ini mendapat bahawa prevalens berat badan berlebihan dan obes dalam kalangan mereka adalah lebih rendah iaitu 29.3% dan 7.2% masing-masing. Ini adalah kerana anggota tentera adalah lebih aktif secara fizikal berbanding populasi awam.

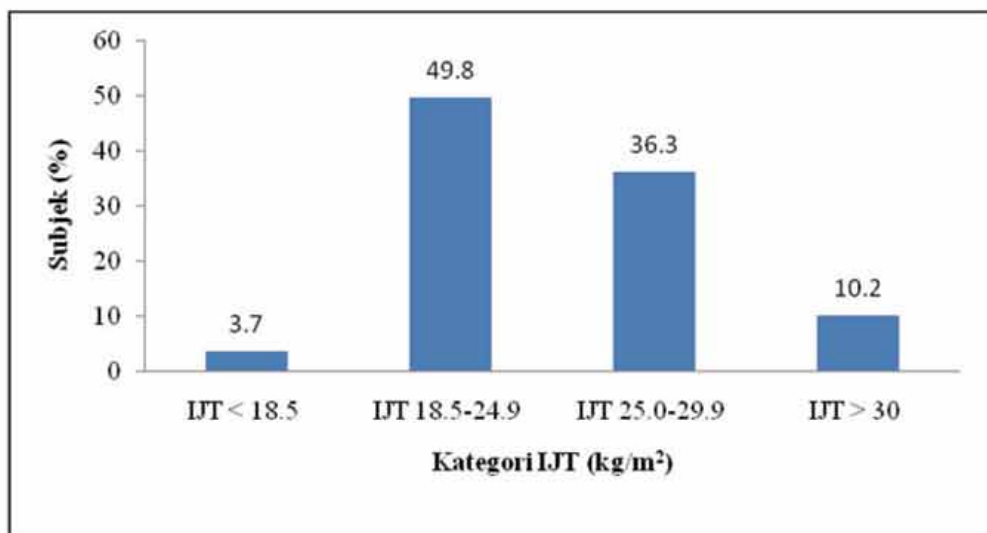
Jadual 2: Taburan subjek mengikut ciri-ciri sosio-demografi.

Ciri-Ciri	Bil. sampel (n) ($\Sigma n = 215$)	Peratus (%)
Umur (tahun)		
18-24	8	3.7
25-29	50	23.3
30-34	36	16.7
35-39	24	11.2
40-44	19	8.8
45-49	30	14
50-55	48	22.3
Bangsa		
Melayu	203	94.4
Cina	5	2.3
India	5	2.3
Lain-lain	2	1
Jantina		
Lelaki	124	57.7
Perempuan	91	42.3
Status perkahwinan		
Bujang	32	14.9
Kahwin	178	82.8
Bercerai	4	1.8
Balu	1	0.5
Tahap pendidikan		
SRP/PMR	15	7.0
SPM/MCE	79	36.7
Sijil	15	7.0
STPM/diploma	48	22.3
Ijazah Sarjana Muda	44	20.5
Ijazah Sarjana	13	6.0
Ijazah Doktor	1	0.5
Falsafah		
Pangkat	59	27.4
Pegawai	156	72.6
Sokongan		
Pendapatan isirumah		
< RM 1000	3	1.5
RM 1001-RM 2000	50	25.4
RM 2001-RM 3000	51	25.9
RM 3001-RM 4000	28	14.2
RM 4000 dan ke atas	65	33
Tempoh perkhidmatan		
< 1 tahun	7	3.3
1 hingga 5 tahun	69	32.7
6 hingga 10 tahun	24	11.4
11 hingga 15 tahun	27	12.8
16 hingga 20 tahun	6	2.8
21 hingga 30 tahun	59	28.0
31 hingga 40 tahun	19	9.0

Jadual 3: Min ciri-ciri antropometri dan komposisi tubuh subjek.

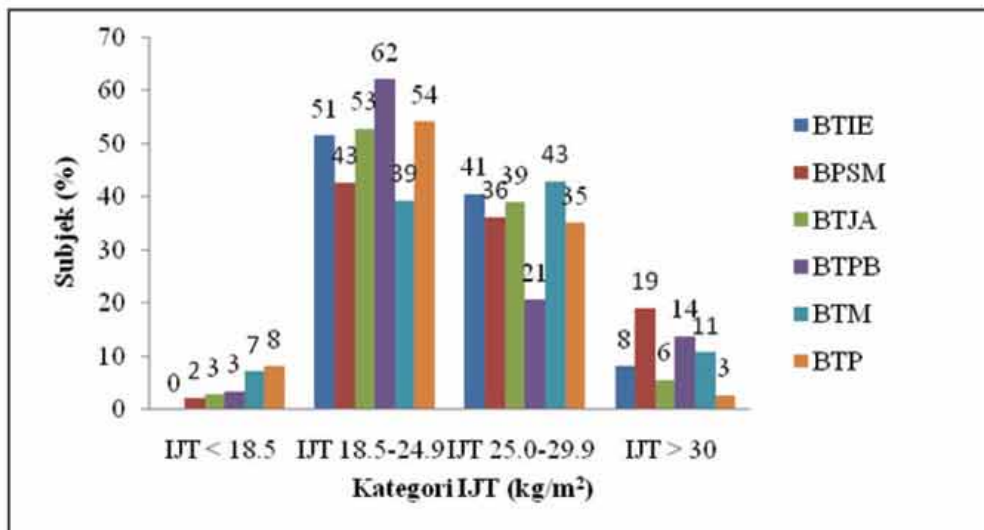
Ciri-ciri fizikal	Min ± SP		
	Lelaki	Perempuan	Total
Umur (tahun)	39.5 ± 10.1 (22-55)	37.2 ± 9.9 (22-53)	38.5 ± 10.1 (22-56)
Tinggi (m)	1.67 ± 0.59 (1.54-1.81)	1.56 ± 0.05* (1.44-1.68)	1.6 ± 0.1 (1.44-1.81)
Berat (kg)	69.8 ± 12.1 (40-111.5)	61.2 ± 12.3* (35.5-110.6)	66.1 ± 12.8 (35.4-111.5)
IJT (kg/m²)	25.1 ± 4.1 (14.9-38.5)	25.2 ± 5.2 (14.8-49.8)	25.1 ± 0.1 (14.8-49.8)
Peratus Lemak (%)	26.0 ± 6.7 (5.8-42)	35.4 ± 8.2* (14.5-53.4)	29.9 ± 8.7 (5.8-53.4)
Berat Lemak (kg)	18.7 ± 7.4 (3.4-40.9)	22.6 ± 9.3* (5.2-56.4)	20.3 ± 8.4 (3.4-56.4)
JTTL (kg)	51.1 ± 6.9 (36.6-86.8)	38.6 ± 4.3* (29.9-54.2)	45.8 ± 8.6 (29.9-86.8)
Jumlah air tubuh (%)	37.5 ± 5.1 (26.8-63.5)	28.2 ± 3.1* (21.9-39.7)	33.6 ± 6.3 (21.9-63.5)
Ukur lilit pinggang (cm)	87.2 ± 9.7 (64-116)	78.6 ± 10.0* (60-113)	83.6 ± 10.7 (60-116)
Ukur lilit pinggul (cm)	94.0 ± 7.5 (73-120)	100.1 ± 9.5* (78-138)	96.6 ± 8.9 (73-138)
Pinggang:Pinggul	0.92 ± 0.06 (0.77-1.12)	0.78 ± 0.06* (0.68-0.92)	0.86 ± 0.89 (0.68-1.12)

* Perbezaan adalah signifikan pada $p < 0.001$



Rajah 2: Status IJT subjek secara keseluruhan.

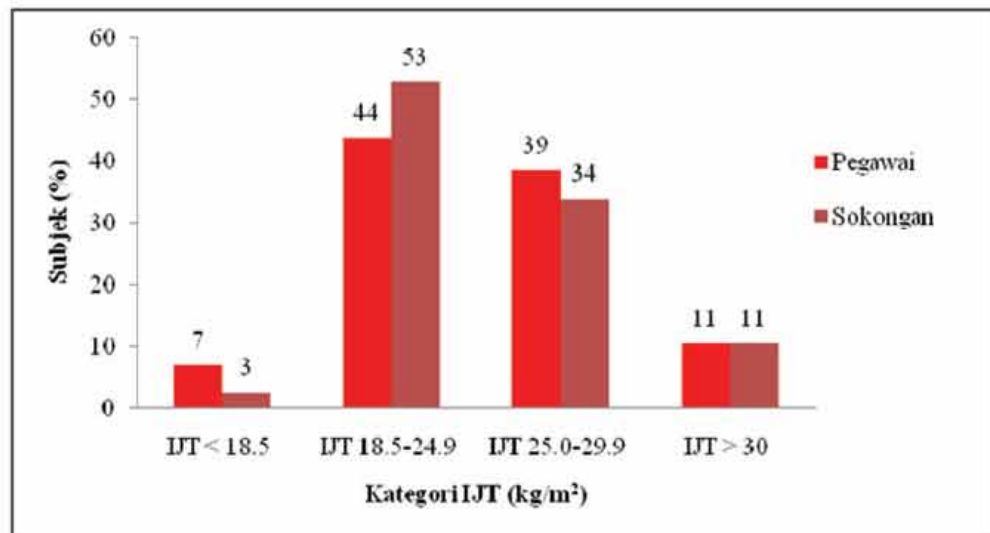
Penelitian mengikut bahagian di STRIDE (Rajah 3) mendapati bahawa subjek di Bahagian Pengurusan dan Sumber Manusia (BPSM) menunjukkan prevalens berat badan berlebihan atau obes ($\text{IJT} \geq 25 \text{ kg}/\text{m}^2$) yang paling tinggi (55%) diikuti dengan Bahagian Teknologi Maritim (BTM) (51%), Bahagian Teknologi Instrumentasi dan Elektrik (BTIE) (49%), Bahagian Teknologi dan Jentera Angkasa (BTJA) (45%), Bahagian Teknologi Persenjataan (BTP) (38%), dan Bahagian Teknologi Perlindungan dan Biofizikal (BTPB) (35%). Peratusan subjek dikategorikan dalam kumpulan obes ($\text{IJT} \geq 30 \text{ kg}/\text{m}^2$) bagi BPSM mencapai sehingga 19% diikuti dengan BTPB (14%) dan BTM (11%). BTP mempunyai prevalens obes yang paling rendah iaitu hanya 3%. Walaupun BTPB mempunyai peratusan obes kedua tertinggi, tetapi prevalens berat badan berlebihan dengan IJT 18.5-25 kg/m^2 dalam kalangan mereka adalah paling rendah iaitu hanya 21%. Di samping itu, BTPB didapati juga menunjukkan peratusan berat badan normal paling tinggi iaitu 62% manakala BTM menunjukkan peratusan berat badan normal yang paling rendah iaitu 39%. Tiada seorang pun subjek di dalam BTIE yang tergolong dalam kategori kurang berat badan manakala BTM pula menunjukkan peratusan kurang berat badan yang paling tinggi iaitu 8%. Tidak terdapat perkaitan yang signifikan antara status IJT dan bahagian di mana subjek bertugas ($p > 0.05$).



Rajah 3: Status IJT subjek mengikut bahagian di STRIDE.

4.4 Prevalens Berat Badan Berlebihan dan Obesiti Mengikut Ciri-ciri Sosio-demografi

Oleh kerana pegawai dan kakitangan sokongan STRIDE memperkenalkan kepelbagaiannya dalam ciri-ciri sosio-demografi, maka pengelasan IJT subjek mengikut ciri-ciri sosio-demografi penting untuk dikenal pasti. Status berat badan subjek mengikut pangkat (Rajah 4) menunjukkan bahawa prevalens berat badan berlebihan atau obes ($IJT \geq 25$) adalah lebih tinggi dalam kalangan pegawai (50%) berbanding kakitangan sokongan (45%). Walau bagaimanapun, sekiranya diteliti dalam kategori obes sahaja, prevalens pegawai dan kakitangan sokongan adalah sama iaitu 11% masing-masing. Separuh daripada kakitangan sokongan dikategorikan sebagai berat badan normal (53%) berbanding pegawai (44%). Manakala peratusan pegawai yang menunjukkan kurang berat badan pula adalah lebih tinggi (7%) berbanding kakitangan sokongan (3%).

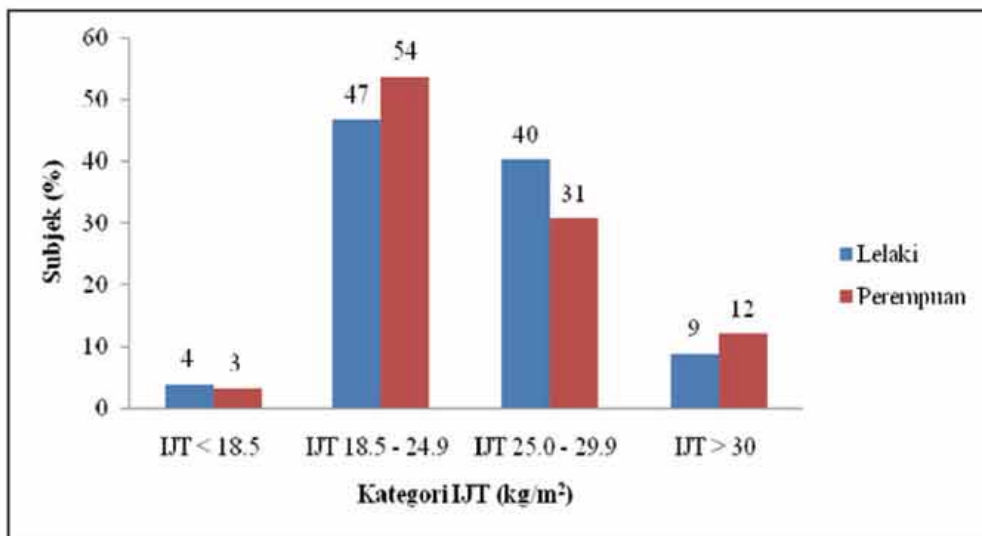


Rajah 4: Status IJT subjek mengikut pangkat.

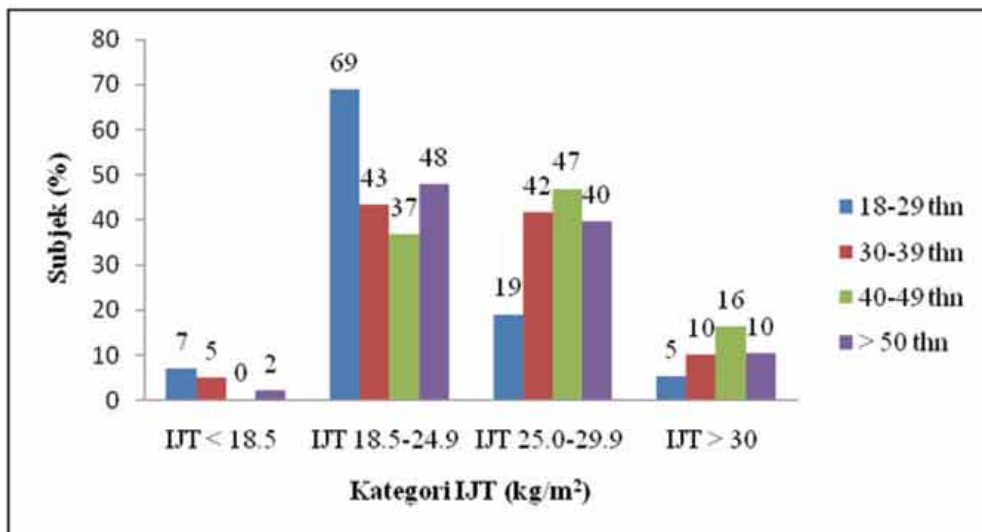
Dari segi jantina, subjek lelaki menunjukkan peratusan berat badan berlebihan yang lebih tinggi (40%) berbanding subjek perempuan (31%) manakala keputusan yang sebaliknya dalam kategori obes di mana prevalens adalah lebih tinggi dalam kalangan subjek perempuan (12%) berbanding subjek lelaki (9%) (Rajah 5). Walau bagaimanapun, secara keseluruhannya peratusan subjek lelaki yang dikategorikan sebagai berat badan berlebihan atau obes (49%) adalah lebih tinggi berbanding subjek perempuan (43%). Dalam kategori berat badan normal (54%) pula, peratusan subjek perempuan di dapatkan lebih tinggi berbanding subjek lelaki (47%) manakala peratusan yang hampir sama bagi kategori kurang berat badan bagi kedua-dua kumpulan tersebut. Keputusan kajian ini adalah konsisten dengan kajian MANS (2003) yang juga mendapat bahawa perempuan (14.66%) mempunyai prevalens obesiti yang lebih tinggi berbanding lelaki (9.72%) manakala prevalens berat badan berlebihan yang lebih tinggi dalam kalangan lelaki (28.55%) berbanding perempuan (24.80%) (Azmi et al. 2009). Keputusan yang serupa juga diperolehi dalam kajian NHMS III yang turut mendapat subjek perempuan menunjukkan prevalens obesiti (17%) yang lebih tinggi berbanding lelaki (10%) (KKM, 2008).

Status IJT subjek mengikut kumpulan umur dapat diperhatikan dalam Rajah 6. Keputusan menunjukkan bahawa prevalens berat badan berlebihan dan obes adalah lebih rendah dalam kalangan kumpulan yang lebih muda berbanding kumpulan yang lebih berumur. Satu trend yang menarik dapat diperhatikan ialah prevalens berat badan berlebihan dan obes kelihatan meningkat dari kumpulan umur yang lebih muda iaitu 18 hingga 29 tahun sehingga kumpulan umur 40 hingga 49 tahun. Walau bagaimanapun ianya menurun sedikit bagi kumpulan umur lebih 50 tahun. Seperti mana yang dijangka, kumpulan umur yang lebih muda (18 hingga 24 tahun) menunjukkan prevalen kurang berat badan (7%) dan berat badan normal yang jauh lebih tinggi (69%) berbanding kumpulan umur yang lain. Tiada seorang pun subjek

dalam kumpulan umur 40 hingga 49 tahun yang tergolong dalam kategori kurang berat badan. Keputusan ini adalah konsisten dengan kajian MANS (2003) yang mendapati prevalensi berat badan berlebihan dan obesiti meningkat dengan umur (Azmi *et al.*, 2009). Ini mungkin disebabkan oleh gaya hidup sedentari dengan peningkatan umur diikuti dengan perubahan dalam komposisi tubuh. Terdapat perkaitan yang signifikan antara status IJT dan kumpulan umur dalam kalangan subjek ($p < 0.05$).



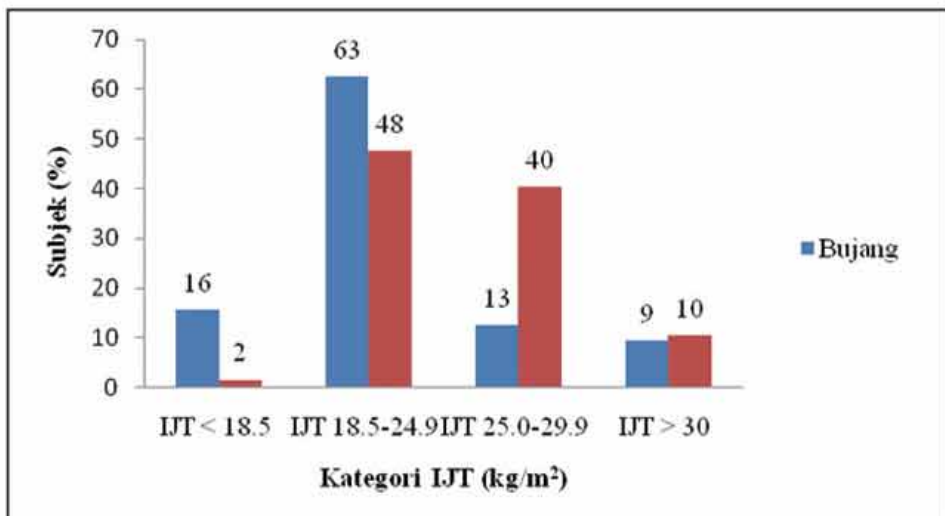
Rajah 5: Status IJT subjek mengikut jantina.



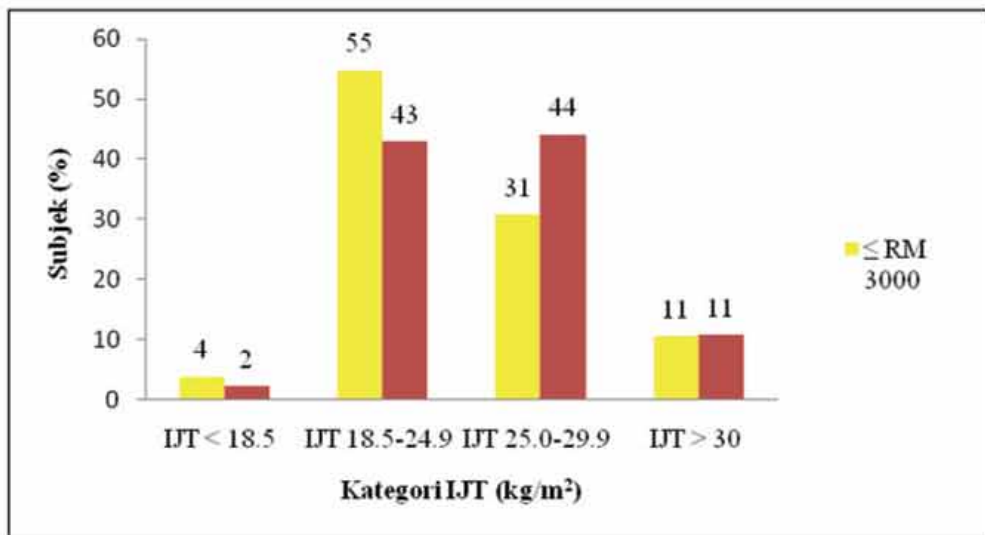
Rajah 6: Status IJT subjek mengikut kumpulan umur.

Pengkelasan IJT mengikut status perkahwinan menunjukkan subjek yang berkahwin mempunyai peratusan berat badan berlebihan atau obes yang jauh lebih tinggi (50%) berbanding dengan subjek bujang (22%) (Rajah 7). Subjek bujang menunjukkan prevalens berat badan normal (63%) dan kurang berat badan (16%) yang jauh lebih tinggi berbanding subjek yang berkahwin. Keputusan seperti ini sememangnya dijangka kerana hampir kesemua subjek bujang adalah dari kumpulan umur yang lebih muda. Di samping itu, penekanan yang kurang kepada rupa bentuk fizikal oleh pasangan apabila berkahwin, gaya hidup sedentari, pengambilan makanan yang kerap dan kesukaran untuk mengurangkan berat badan yang diperolehi semasa mengandung bagi perempuan adalah antara penyumbang kepada berat badan berlebihan. Terdapat perkaitan yang signifikan antara status IJT dan status perkahwinan dalam kalangan subjek ($p < 0.001$).

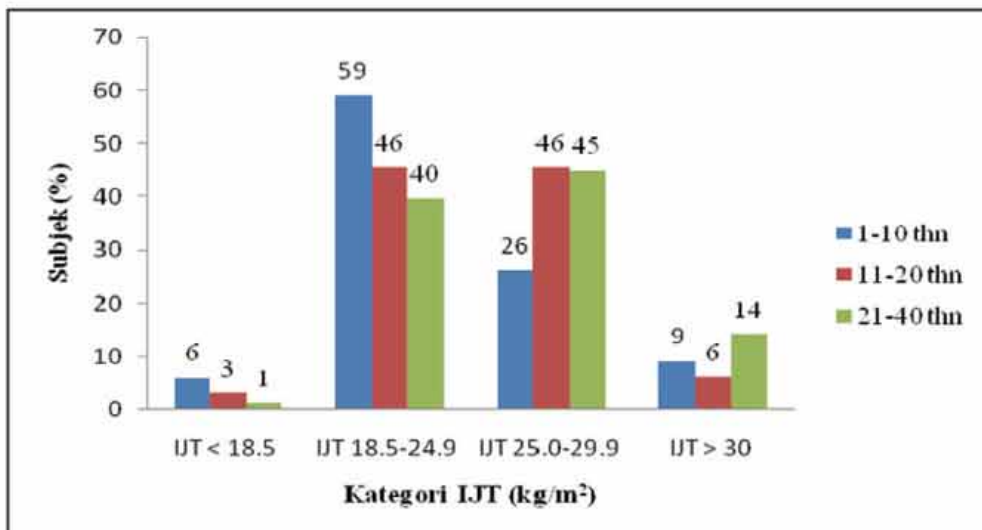
Apabila pendapatan subjek dibahagikan kepada dua kumpulan iaitu kurang RM 3,000 dan lebih RM 3,000 (Rajah 8), kumpulan subjek dengan gaji yang lebih tinggi didapati menunjukkan prevalens berat badan berlebihan atau obes yang lebih tinggi (55%) berbanding kumpulan subjek yang berpendapatan lebih rendah (42%). Selari dengan keputusan itu, subjek yang berpendapatan kurang daripada RM 3,000 pula menunjukkan prevalens berat badan normal yang lebih tinggi iaitu 55% berbanding 43%. Rajah 9 menunjukkan status IJT subjek mengikut kumpulan tempoh perkhidmatan. Dalam kategori kurang berat badan, subjek dengan kumpulan tempoh perkhidmatan yang lama menunjukkan prevalens kurang berat badan yang paling rendah iaitu hanya 1%. Berlainan pula dengan kategori obes di mana subjek dengan kumpulan tempoh perkhidmatan yang lebih lama iaitu 21 hingga 40 tahun menunjukkan prevalens berat badan berlebihan atau obes yang lebih tinggi (59%) berbanding kumpulan tempoh perkhidmatan 11 hingga 20 tahun (52%) dan 1 hingga 10 tahun (35%). Trend yang dapat diperhatikan ialah semakin lama tempoh perkhidmatan, prevalens kurang berat badan dan berat badan normal semakin berkurangan dengan ketara manakala prevalens berat badan berlebihan pula semakin meningkat. Terdapat perkaitan yang signifikan antara status IJT dan tempoh perkhidmatan dalam kalangan subjek ($p < 0.05$).



Rajah 7: Status IJT subjek mengikut status perkahwinan.



Rajah 8: Status IJT subjek mengikut kumpulan gaji.

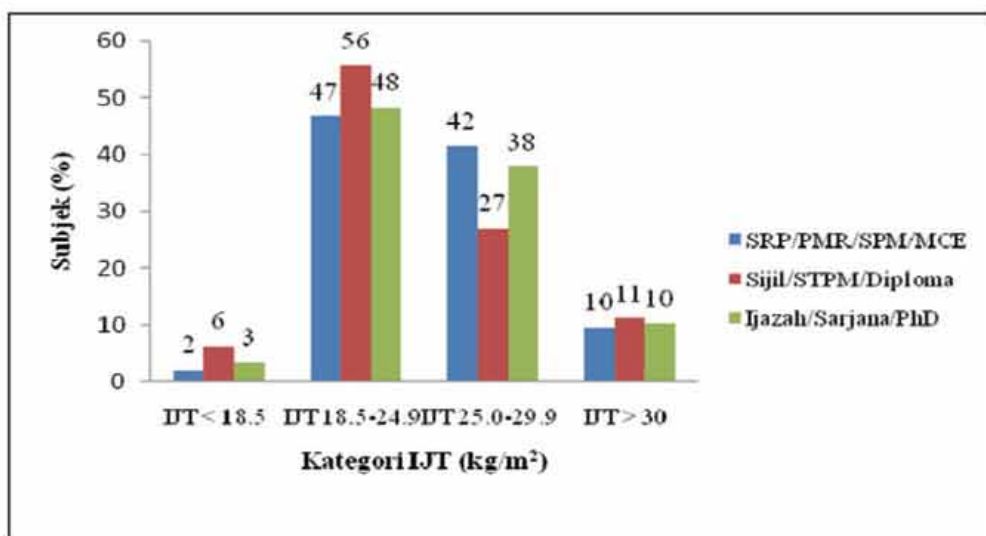


Rajah 9: Status IJT subjek mengikut kumpulan tempoh perkhidmatan.

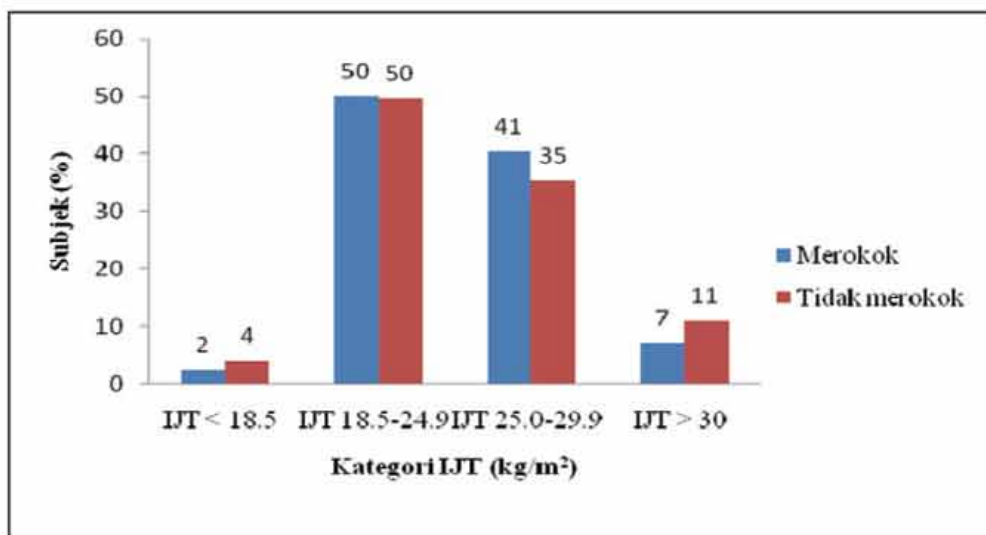
Status IJT subjek mengikut tahap pendidikan ditunjukkan dalam Rajah 10. Subjek yang berpendidikan Sijil/STPM/Diploma didapati menunjukkan prevalens yang tinggi bagi setiap kategori IJT kecuali bagi kategori berat badan berlebihan. Walaupun prevalens obes adalah sama bagi ketiga-tiga kumpulan tahap pendidikan namun subjek dengan tahap pendidikan terendah menunjukkan prevalens berat badan berlebihan yang paling tinggi (42%) berbanding subjek dengan pendidikan ijazah/sarjana/Phd (38%) dan Sijil/STPM/Diploma (27%). Berdasarkan keputusan kajian ini juga, subjek dengan pendidikan paling rendah didapati memperoleh prevalens kurang berat badan dan berat badan normal yang paling rendah iaitu 47% dan 2% masing-masing. Walau bagaimanapun kesan tahap pendidikan terhadap prevalen berat badan berlebihan tidak dapat dilihat dengan jelas dalam kajian ini. Kajian Razalee (2008) secara bandingannya mendapati bahawa anggota yang dengan tahap pendidikan terendah menunjukkan prevalens berat badan berlebihan atau obes paling tinggi manakala anggota dengan kelulusan ijazah dan keatas menunjukkan prevalens berat badan berlebihan atau obes paling rendah.

Prevalens subjek yang mengamalkan tabiat merokok dalam kajian ini ialah 19.5% di mana kesemuanya adalah terdiri daripada subjek lelaki. Peratusan ini adalah meliputi satu per tiga daripada jumlah subjek lelaki secara keseluruhan. Berpandukan Rajah 11, kumpulan subjek yang merokok dan tidak merokok menunjukkan prevalens berat badan berlebihan atau obes yang tidak jauh berbeza iaitu 48% dan 46% masing-masing dan prevalens berat badan normal yang sama iaitu 50% masing-masing. Tiada perkaitan yang signifikan antara status IJT dan status merokok ($p > 0.05$). Keputusan ini adalah tidak konsisten dengan kajian Razalee (2008) yang mendapati bahawa subjek yang merokok menunjukkan prevalens berat badan berlebihan yang lebih rendah (33%) berbanding subjek yang tidak merokok (42%).

Kajian yang dijalankan oleh Razalee (2008) ke atas anggota TLDM mendapati mendapati bahawa prevalens berat badan berlebihan didapati lebih tinggi dalam kalangan subjek dengan pangkat, umur dan pendapatan yang lebih tinggi, tempoh perkhidmatan yang panjang, tahap pendidikan yang lebih rendah dan bukan perokok di mana kesemua pembolehubah memberikan perkaitan yang signifikan dengan status berat badan. Hasil kajian yang diperolehi dalam kajian ini tidak banyak berbeza dengan kajian Razalee (2008) kecuali hanya pembolehubah umur, tempoh perkhidmatan dan status perkahwinan yang memberikan perkaitan yang signifikan dengan status berat badan.



Rajah 10: Status IJT subjek mengikut tahap pendidikan.



Rajah 11: Status IJT subjek mengikut status merokok.

4.5 Ukur Lilit Pinggang

Oleh kerana tisu adipos *abdominal* menyebabkan risiko morbiditi yang lebih tinggi dibandingkan dengan tisu adipos mengelilingi kawasan *subcutaneous hip* (NHLBI & NIDDKD, 1998), maka ukur lilit pinggang biasanya digunakan berbanding nisbah pinggang dan pinggul dalam menentukan tahap risiko. Merujuk Jadual 3, min ukur lilit pinggang subjek lelaki dan perempuan kajian ini ialah 87.2 cm dan 78.6 cm masing-masing. Perbandingan dengan kajian NHMS III mendapat min ukur lilit pinggang subjek lelaki (84.0 cm) adalah lebih rendah manakala lebih tinggi bagi subjek perempuan (80.3 cm). Berdasarkan titik tolak ukur lilit pinggang yang ditetapkan untuk populasi Asia, pengukuran ukur lilit pinggang dalam kalangan subjek kajian ini menunjukkan bahawa sejumlah 39% daripada subjek keseluruhan mempunyai ukur lilit pinggang yang dikira berisiko tinggi terhadap penyakit kardiovacular dan diabetes (Jadual 4). Perincian mengikut jantina menunjukkan bahawa peratusan subjek perempuan yang mempunyai ukur lilit pinggang yang berisiko adalah lebih tinggi (42%) berbanding subjek lelaki (37%). Razalee (2008) dalam kajiannya mendapat bahawa sejumlah 26% anggota lelaki TLDM menunjukkan obesiti *abdominal* di mana prevalensnya adalah lebih rendah berbanding subjek lelaki kajian ini. Dalam kajian NHMS III pula, prevalens subjek yang menunjukkan obesiti *abdominal* ialah 17.4% di mana prevalens lebih tinggi dalam kalangan perempuan (26%) berbanding lelaki (7.2%). Prevalens yang lebih rendah diperolehi kerana pengelasan ini adalah berdasarkan titik tolak yang disarankan oleh WHO (1998) iaitu obesiti *abdominal* bagi lelaki sekiranya ukur lilit pinggang melebihi 102 cm dan 88 cm untuk perempuan. Sekiranya pengelasan obesiti *abdominal* bagi subjek kajian ini berdasarkan titik tolak yang disarankan oleh WHO (1998), prevalens obesiti *abdominal* dalam kalangan subjek adalah lebih rendah iaitu 10.7% di mana 8.1% bagi lelaki dan 14.3% bagi perempuan. Memandangkan kaitan yang kuat antara obesiti *abdominal* dengan risiko pelbagai penyakit kronik, maka kejadian obesiti *abdominal* dalam kalangan subjek, khususnya subjek dengan berat badan berlebihan hendaklah diberi perhatian sewajarnya. Subjek berat badan berlebihan dengan ukur lilit pinggang melebihi had perlu berusaha menurunkan berat badan, kerana ia secara kategorinya meningkatkan risiko penyakit bagi setiap klas IJT (Kushner & Blatner, 2005).

Jadual 4: Prevalens ukur lilit pinggang mengikut jantina.

Ciri fizikal	Lelaki		Perempuan		Total	
	Normal	Risiko	Normal	Risiko	Normal	Risiko
Ukur lilit pinggang	63	37	58	42	61	39

4.6 Tahap Lemak Tubuh

Berpandukan kriteria BIA, TBF 300A, Jadual 5 menunjukkan dalam kalangan subjek lelaki, sejumlah 73% subjek mempunyai tahap lemak yang dikira melebihi julat yang sihat, 20% subjek mempunyai tahap lemak dalam julat yang sihat dan hanya sejumlah kecil iaitu 7% subjek mempunyai tahap lemak yang rendah (*lean*). Trend yang sama juga dapat diperhatikan dalam kalangan subjek perempuan, di mana sejumlah 90% subjek dikategorikan sebagai mempunyai tahap lemak yang tinggi, 7% dengan tahap lemak dalam julat yang sihat dan hanya 3% dengan tahap lemak yang rendah. Subjek perempuan, di samping menunjukkan peratusan bagi ukur lilit pinggang yang berisiko lebih tinggi, turut menunjukkan peratusan yang tinggi (90%) bagi tahap lemak tubuh yang tinggi berbanding subjek lelaki (73%).

Jadual 5: Tahap lemak tubuh subjek.

Jantina	Tahap lemak tubuh		
	Rendah	Optima	Tinggi
Lelaki	7	20	73
Perempuan	3	7	90
Jumlah	6	14	80

Terdapat kajian yang menjalankan pengukuran peratus lemak tubuh dengan menggunakan alat pengukuran komposisi tubuh seperti mana yang digunakan dalam kajian ini. Kajian oleh Aina Mardiah & Hazizi (2010) mendapati lebih daripada 70% kakitangan kerajaan di BPPP mempunyai tahap lemak tubuh yang tinggi dengan min $33.0 \pm 9.57\%$ manakala kajian di Kangar, Perlis pula menunjukkan 64.4% subjek mempunyai lemak tubuh yang tinggi dengan min lemak tubuh $26.44 \pm 6.61\%$ dan $37.99 \pm 11.02\%$ bagi lelaki dan perempuan masing-masing (Zahratul & Hazizi, 2010). Kajian ke atas guru di Marang, Terengganu (Nor Izzati & Rokiah, 2010) mendapati sejumlah 65.1% subjek lelaki (min $27.26 \pm 6.12\%$) dan 74.6% subjek perempuan (min $35.71 \pm 6.05\%$) mempunyai tahap lemak tubuh yang tinggi masing-masing. Perbandingan di atas menunjukkan bahawa walaupun secara keseluruhannya, peratusan subjek dengan tahap lemak tubuh yang tinggi dalam kajian ini (80%) adalah lebih tinggi namun begitu min lemak tubuh masih lebih rendah ($29.9 \pm 8.7\%$) berbanding dengan kajian oleh Aina Mardiah & Hazizi (2010) ($33.0 \pm 9.5\%$). Perbandingan antara subjek lelaki dan perempuan dalam min lemak tubuh dengan kajian Zahratul & Hazizi (2010) dan Nor Izzati & Rokiah (2010) mendapati min lemak tubuh subjek perempuan ($26 \pm 6.7\%$) dan lelaki ($35.4 \pm 8.2\%$) kajian ini adalah lebih rendah. Razalee (2008) dalam kajiannya mendapati sejumlah 51% anggota TLDM dikategorikan mempunyai tahap lemak tubuh yang tinggi di mana adalah jauh lebih rendah berbanding kajian ini (80%). Memandangkan penetapan pengelasan tahap lemak tubuh ini adalah sebagai panduan kepada subjek dalam memantau komposisi tubuh mereka, maka majoriti subjek dengan tahap lemak tubuh yang tinggi perlu berusaha mengurangkan berat lemak tubuh

dengan mengamalkan pemakanan yang seimbang, gaya hidup yang sihat serta melakukan senaman secara berterusan.

4.7 Hubungan Antara IJT dan Peratus Lemak Tubuh dengan Ciri-ciri Fizikal

Jadual 6 menunjukkan koefisien korelasi antara parameter IJT, peratus lemak tubuh, ciri-ciri fizikal dan sosio-demografi. Kesemua ciri-ciri yang diuji menunjukkan perhubungan yang signifikan dengan IJT kecuali pembolehubah ketinggian. Koefisien korelasi antara IJT dan peratus lemak tubuh dalam kalangan subjek kajian ini ialah 0.74 bagi lelaki manakala 0.81 bagi perempuan ($p < 0.001$). Keputusan ini menunjukkan bahawa IJT adalah merupakan petunjuk yang baik bagi peratus lemak tubuh. Bagi subjek lelaki, terdapat hubungan korelasi yang tinggi antara IJT dengan berat badan ($r = 0.91$, $p < 0.001$), ukur lilit pinggang ($r = 0.91$, $p < 0.01$), ukur lilit pinggul ($r = 0.89$, $p < 0.01$), berat lemak ($r = 0.87$, $p < 0.01$), peratus lemak tubuh ($r = 0.74$, $p < 0.01$) dan JTTL ($r = 0.65$, $p < 0.01$). Berlainan sedikit dengan subjek perempuan, berat badan menunjukkan hubungan korelasi yang paling tinggi ($r = 0.95$, $p < 0.001$) dengan IJT, diikuti dengan ukur lilit pinggul ($r = 0.91$, $p < 0.001$), ukur lilit pinggang ($r = 0.84$, $p < 0.001$), peratus lemak tubuh ($r = 0.81$, $p < 0.01$) berat lemak ($r = 0.81$, $p < 0.001$) dan JTTL ($r = 0.66$, $p < 0.001$). Koefisien korelasi antara IJT dengan nisbah pinggang dan pinggul menunjukkan hubungan korelasi yang sederhana tetapi signifikan bagi subjek lelaki ($r = 0.47$, $p < 0.001$) dan perempuan ($r = 0.29$, $p < 0.001$). Hubungan korelasi yang lebih tinggi ($r = 0.88$, $p < 0.001$) antara IJT dan peratus lemak tubuh diperolehi dalam kajian keatas anggota TLDM (Razalee, 2008) berbanding subjek lelaki kajian ini ($r = 0.74$, $p < 0.01$).

Jadual 6: Korelasi antara IJT dan peratus lemak tubuh dengan komposisi tubuh dan ciri-ciri fizikal.

Ciri-ciri fizikal	Indeks Jisim Tubuh			Peratus Lemak Tubuh		
	Lelaki	Perempuan	Total	Lelaki	Perempuan	Total
Peratus lemak tubuh	0.74**	0.81**	0.67**	-	-	-
Tinggi	-0.097	-0.17	-0.10	-0.14	-0.15	-0.46**
Berat badan	0.91**	0.95**	0.86**	0.64**	0.79**	0.39**
Berat lemak	0.87**	0.81**	0.89**	0.93**	0.91**	0.88**
JTTL	0.65**	0.66**	0.41**	0.12	0.28**	-0.29**
Ukur lilit pinggang	0.91**	0.84**	0.79**	0.70**	0.72**	0.33**
Ukur lilit pinggul	0.89**	0.91**	0.86**	0.68**	0.78**	0.76**
Pinggang:pinggul	0.47**	0.29**	0.23**	0.36**	0.27**	-0.25**

** $p < 0.001$

Dalam kalangan subjek lelaki, peratus lemak tubuh berkorelasi secara signifikan dengan semua pembolehubah yang diuji kecuali JTTL dan ketinggian (Jadual 4). Korelasi yang paling tinggi adalah dengan ukur lilit pinggang ($r = 0.70, p < 0.001$), ukur lilit pinggul ($r = 0.68, p < 0.001$) dan berat badan ($r = 0.64, p < 0.001$). Pembolehubah lain seperti nisbah pinggang dan pinggul memberikan hubungan korelasi yang sederhana tetapi signifikan dengan peratus lemak tubuh ($r = 0.36, p < 0.001$). Dalam kalangan subjek perempuan pula, peratus lemak tubuh berkorelasi secara signifikan dengan semua pembolehubah kecuali ketinggian dengan korelasi paling tinggi adalah dengan berat badan ($r = 0.79, p < 0.001$) diikuti ukur lilit pinggul ($r = 0.78, p < 0.001$) dan ukur lilit pinggang ($r = 0.72, p < 0.001$).

5. KESIMPULAN

Subjek yang dikaji mempunyai prevalensi berat badan berlebihan atau obes yang tinggi iaitu sejumlah 47% yang dikira boleh mendatangkan kesan kesihatan yang kurang baik. Berat badan berlebihan, ukur lilit pinggang serta peratusan lemak tubuh yang tinggi akan menyebabkan subjek berisiko tinggi terhadap masalah kesihatan seperti penyakit kardiovacular, tekanan darah tinggi dan penyakit diabetis. Kajian ini mendapati bahawa faktor sosio-demografi seperti status perkahwinan, umur dan tempoh perkhidmatan menyumbangkan secara signifikan kepada kejadian berat badan berlebihan dan obesiti dalam kalangan subjek. Secara keseluruhannya, IJT mempunyai perhubungan yang signifikan dengan kesemua ciri-ciri fizikal yang diuji ($p < 0.001$) kecuali ketinggian manakala peratus lemak tubuh menunjukkan perhubungan yang signifikan dengan kesemua ciri-ciri fizikal ($p < 0.001$).

Hasil kajian ini menunjukkan bahawa Malaysia sememangnya menghadapi masalah peningkatan berat badan berlebihan dan obesiti dalam kalangan populasi awam termasuk dalam kalangan kakitangan kerajaannya. Usaha hendaklah diambil bagi meningkatkan status pemakanan dengan mengamalkan pemakanan yang baik serta aktiviti fizikal yang berterusan khususnya bagi kumpulan sasaran yang mengalami masalah berat badan berlebihan. Hasil kajian ini diharap dapat memberi maklumat kepada STRIDE berkenaan status pemakanan terkini dalam kalangan pegawai dan kakitangannya dan sekiranya perlu, program yang bersesuaian boleh diwujudkan bagi meningkatkan status pemakanan dan tahap kesihatan dalam kalangan warganya.

PENGHARGAAN

Kajian ini dijalankan semasa penulis pertama bertugas di Institut Penyelidikan Sains & Teknologi Pertahanan (STRIDE). Penulis ingin mengucapkan terima kasih kepada warga STRIDE yang mengambil bahagian di dalam kajian ini. Kami juga menghargai sokongan kumpulan pelajar Universiti Industri Selangor (UNISEL) yang telah menjalani latihan industri di Cawangan Pemakanan & Rangsum pada tahun 2008 serta penyelaras-penyalaras bagi setiap bahagian di STRIDE yang sedia memberikan kerjasama dan bantuan dalam menjayakan kajian ini.

RUJUKAN

- Aina Mardiah, B. & Hazizi, A.S. (2010). Relationship between body weight status, attitudes and strategies for weight control behavior among government staff in Bangunan Persekutuan Pulau Pinang. Abstrak dalam buku program dan pembentangan poster di *21st Scientific Conference & Annual General Meeting*, 25-26 Mac 2010, Kuala Lumpur.
- Azmi, M.Y., Junidah, R., Siti Mariam, A., Safiah, M.Y., Fatimah, S., Norimah, A.K., Poh, B.K., Kandiah, M., Zalilah, M.S., Wan Abdul Manan, W.M., Siti Haslinda, M.D. & Tahir, A. (2009). Body mass index (BMI) of adults: findings of the Malaysian Adult Nutrition Survey (MANS). *Mal. J. Nutr.*, **15**: 97-119.
- Balkau, B., Deanfield, J.E., Despres, J.P., Bassand, J.P., Fox, K.A.A., Smith, S.C., Bater, J.P., Tan, C.E., Caal, L.E., Wittchen, H.U., Massien, C. & Haffner, S.M. (2007). International Day for the Evaluation of Abdominal Obesity (IDEA): A study of waist circumference, cardiovascular disease and diabetes mellitus in 168000 primary care patients in 63 countries. *Circulation*, **116**: 1942-1951.
- Bouchard, C., Bray, G.A. & Hubbard, V.S. (1990). Basic and clinical aspects of regional fat distribution. *Am. J. Clin. Nutr.*, **52**: 946-950.
- Deurenberg, P., Deurenberg Yap, M., Wang, J.Z., Fu, P.L. & Schmidt, G. (2000). Prediction of percentage body fat from anthropometry and bioelectrical impedance in Singaporeans and Beijing Chinese. *Asia Pacific J. Clin. Nutr.*, **9**: 93-98.
- Han, T.S., Sattar, N. & Lean, M. (2006). Assessment of obesity and its clinical implication. *Bri. Med. J.*, **333**: 695-698.
- Hankinson, S.E. (1999). Waist circumference, waist-to-hip ratio and risk of breast cancer in the nurse' health study. *Am. J. Epid.*, **150**: 1316-1324.
- Huang, Z.P., Willet, W.C., Colditz, G.A., Hunter, D.J., Manson, J.E., Rosner, B., Speizer, F.E. & Hankinson, S.E. (1999). Waist circumference, waist-to-hip ratio and risk of breast cancer in the nurse' health study. *Am. J. Epid.*, **150**: 1316-1324.
- Ismail, M.N., Zawiah, H., Chee, S.S. & Ng, K.K. (1995). Prevalence of obesity and chronic energy deficiency (CED) in adult Malaysians. *Mal. J. Nutr.*, **1**: 1-9.
- Ismail, M.N., Chee, S.S., Nawawi, H., Yusoff, K., Lim, T.O. & James, W.P.T. (2002). Obesity in Malaysia. *Obesity Rev.*, **3**: 203-208.
- James, P.T., Leach, R., Kalamara, E. & Shayeghi, M. (2001). The worldwide obesity epidemic. *Obesity Res.*, **9**: 228S-233S.
- Kee, C.C., Jamaiyah, H., Noor Safiza, M.N., Geeta, A., Khor, G.L., Suzana, S., Jamalludin, A.R., Rahmah, R., Ahmad, A.Z., Ruzita, A.T., Wong, N.F. & Ahmad Faudzi, Y. (2008). Abdominal Obesity in Malaysian Adults: National Health and Morbidity Survey III (NHMS III, 2006). *Mal. J. Nutr.*, **14**: 125-135.
- Kementerian Kesihatan Malaysia (KKM). (2008). *The Third National Health and Morbidity Survey (NHMS III): Nutritional Status*. Institut Kesihatan Umum, Kementerian Kesihatan Malaysia (KKM), Malaysia,
- Kushner, R.F. & Blatner, D.J. (2005). Risk Assessment of the overweight and obese patient. *J. Am. Diet. Assoc.*, **105**: 53-62.

- Lim, T.O., Goh, B.L., Zaki, M., Suleimann, A.B., Fatimah, H., Siti, S., Tahir, A. & Maimunah, A.H. (2000). Distribution of body weight, height, and body mass index in a national sample of Malaysian adults. *Med. J. Malaysia.* **55:** 108-128.
- NHLBI and NIDDKD. (1998). Clinical Guidelines on the Identification, Evaluation and Treatment of Overweight and Obesity in Adults the Evidence Report. *Obes Res.* **6:** S51-S210.
- Nor Izzati Aqmar, A.R. & Rokiah, M.Y. (2010). Nutritional status and health behaviours among teachers in Marang, Terengganu. Abstrak dalam buku program dan pembentangan poster di *21st Scientific Conference & Annual General Meeting*, 25-26 Mac 2010, Kuala Lumpur.
- Popkin, B.M. & Doak, C.M. (1998). The obesity epidemic is worldwide phenomenon. *Nutrition Rev.*, **56:** 106-114.
- Razalee, S. (2008). *Kajian Status Pemakanan, Keperluan Tenaga dan Kecergasan Fizikal di Kalangan Anggota Tentera Laut Diraja Malaysia*. Tesis Ijazah Doktor Falsafah, Universiti Kebangsaan Malaysia.
- The World Health Report. (2002). *Reducing Risks, Promoting Healthy Life*. World Health Organization (WHO), Geneva.
- World Health Organization (WHO) (1998). *Obesity: Preventing and Managing the Global Epidemic*. World Health Organization (WHO), Geneva.
- World Health Organization (WHO) (2000). Obesity: preventing and managing the global epidemic. Report of a WHO consultation. *WHO Tech. Rep. Ser.*, **894:** 1-253.
- World Health Organization (WHO) (2006). *Fact Sheet No. 311: WHO Global InfoBase Online*. Tersedia ada daripada http://www.who.int/ncd_surveillance/infobase. (Diakses pada September 2008)
- Baker IDI (2000). The Asia-Pacific perspective: redefining obesity and its treatment. Tersedia ada daripada <http://www.idi.org.au/home.htm>. (Diakses pada 26 March 2008).
- Zahratul Nur, K. & Hazizi, A.S. (2010). Nutritional status and stages of change in body weight management and exercise among malay government staff in Kangar, Perlis. Abstrak dalam buku program dan pembentangan poster di *21st Scientific Conference & Annual General Meeting*, 25-26 Mac 2010, Kuala Lumpur.

SISTEM PENGAWALAN SUHU DAN KELEMBAPAN SECARA BERKOMPUTER

Shaiful Bahri Zainal Abidin*, Mohd Zaidi Mohtar, Hanif Md. Saad, Mohd Razali Mat Yassin, Ahmad Faridz Abd Ghaffar, Hanafiah Hussin & Wan Salwa Wan Hassan

Bahagian Teknologi Instrumentasi dan Elektronik, Institut Penyelidikan Sains & Teknologi Pertahanan (STRIDE), Kementerian Pertahanan, Malaysia

*E-mail: shaiful1400@yahoo.com

ABSTRAK

Objektif penyelidikan ini adalah untuk membangunkan sebuah sistem pengawalan suhu dan kelembapan secara berkomputer di dalam Makmal Pengukuran Jitu STRIDE. Sistem ini perlu memenuhi kehendak dan keperluan bagi kawalan suhu dan kelembapan peralatan kalibrasi di dalam piawaian ISO 17025 (Competence of Testing and Calibration Laboratories). Daripada analisa yang dijalankan, didapati yang sistem ini dapat mampu memaksimakan kecekapan penggunaan tenaga, menurunkan kadar tenaga yang hilang, dan mengekalkan spesifikasi persekitaran yang dikehendaki. Sistem ini juga berpotensi membantu pengguna mengawal kos, kualiti, dan kebolehharapan sistem pengudaraan, pemanasan dan penyejukkan. Sistem ini juga berpotensi membantu pengguna mengawal kos, kualiti, dan kebolehharapan sistem pengudaraan, pemanasan dan penyejukkan.

Kata Kunci: *Suhu; kelembapan; penghawa dingin; penyahlempab; peralatan kalibrasi.*

1. PENGENALAN

Suhu dan kelembapan merupakan parameter penting yang mempengaruhi keadaan persekitaran. Kedua-dua menjadi tumpuan para pengkaji di dalam menyediakan keadaan yang sesuai untuk penggunaan sesuatu ruang. Dalam kerja-kerja kalibrasi, adalah mustahak untuk menetapkan suhu dan kelembapan pada piawaian tertentu kerana ia boleh menjelaskan bacaan kalibrasi Alat-alat yang sensitif kepada perubahan suhu dan kelembapan menjadi kekangan terbesar dalam mendapatkan keputusan yang persis dan konsisten. Oleh itu, suhu dan kelembapan di dalam makmal ujikaji perlu dikekalkan pada keadaan tertentu berdasarkan piawaian yang telah ditetapkan. Ketiadaan sistem pemantauan yang sistematik menyebabkan ralat perubahan keadaan persekitaran tidak dapat dihindari dan prestasi pengukuran yang tidak menentu seterusnya menyumbang kepada implikasi buruk jika penggunaan bahan melibatkan kos yang mahal, faktor manusia dan sebagainya.

Menurut Çengel & Boles (2007), sistem pemanasan, pengudaraan dan pendinginan, lebih dikenali dengan sistem HVAC (*Heating, Ventilating and Air-Conditioning*), merupakan sistem yang penting di dalam pembinaan sesebuah bangunan. Dalam

struktur bangunan yang tertutup, sistem ini memain peranan dalam menyediakan keadaan yang bersesuaian dengan kehendak dan spesifikasi yang diingini untuk keselesaan manusia, atau ketahanan alatan dan barang-barang yang sensitif. Walau bagaimanapun, sistem rekabentuk kawalan yang kurang cekap akan melibatkan pembaziran penggunaan tenaga. Oleh itu, kecekapan tenaga dalam teknologi sistem HVAC telah menjadi perhatian kebanyakan negara kerana peningkatan penggunaan tenaga sedangkan sumber penjanaan tenaga adalah amat terhad. Peningkatan tenaga yang hilang daripada proses pengudaraan dan pergerakkan udara dijangkakan akan menjadi penyebab dominan kehilangan pemanasan, dan seterusnya penyejukan, di dalam bangunan pada masa depan.

Objektif penyelidikan ini adalah untuk membangunkan sebuah sistem pengawalan suhu dan kelembapan secara berkomputer di dalam Makmal Pengukuran Jitu STRIDE. Sistem ini perlu memenuhi kehendak dan keperluan bagi kawalan suhu dan kelembapan peralatan kalibrasi di dalam piawaian ISO 17025 (*Competence of Testing and Calibration Laboratories*).

2. PRINSIP-PRINSIP ASAS

2.1 Parameter-Parameter bagi Sistem Kawalan Pemanasan, Pengudaraan dan Penyejukan

Menurut Angevine & Fair (2001), fungsi utama sistem HVAC adalah untuk mengawal suhu, kelembapan dan kualiti udara. Di dalam kajian ini, hanya suhu dan kelembapan sahaja diambil kira sebagai parameter kawalan. Walaubagaimanapun, kandungan kelembapan merupakan salah satu elemen penting di dalam mengawal kualiti udara, selain daripada faktor pencemaran yang disebabkan asap rokok, bahan organik yang mudah meruap (*volatile organic material*) dan lain-lain lagi. Suhu adalah ukuran kuantitatif yang digunakan untuk menunjukkan darjah kepanasan dan kesejukan. Di dalam ruang yang tertutup, suhu udara disukat dengan menggunakan penderia suhu dari jenis termokopel (*thermocouple*) atau pengesan rintangan suhu (*resistance temperature detector-RTD*). Udara yang tidak mempunyai kandungan wap air ialah udara kering, manakala udara yang tepu terjadi apabila kuantiti wap air dalam udara mencapai tahap maksimum, di mana jika wap air ditambah ke dalam udara tersebut, udara itu akan terkondensasi.

2.2 Kesan Suhu dan Kelembapan kepada Prestasi Pengukuran Alat Kalibrasi

Kebanyakan alat-alat kalibrasi yang digunakan untuk kerja-kerja pengukuran adalah sensitif kepada perubahan suhu dan kelembapan nisbi, ia boleh mengganggu bacaan sebenar peralatan yang dikalibrasi. Ketidakpastian kalibrasi (*calibration uncertainties*) bergantung pada pengekalan suhu dan kelembapan nisbi pada toleransi tertentu(I-Hai-Lin & Broberg, 2002). Sisihan yang melebihi had toleransi akan menyebabkan nilai ketidakpastian menjadi besar dan kegagalan dalam kerja-kerja kalibrasi (Walker, 2006). Selalunya di dalam buku panduan peralatan kalibrasi akan dinyatakan had operasi suhu dan kelembapan, dan juga lain-lain faktor penghad.

2.3 Suhu dan Kelembapan untuk Kerja-Kerja Kalibrasi

Bagi kerja-kerja kalibrasi melibatkan pengukuran suhu, suhu dan kelembapan nisbi mestilah dikekalkan di antara julat $\pm 2^{\circ}\text{C}$ dan $\pm 15\%$, manakala bagi pengukuran jisim dan dimensi, toleransi persekitaran lebih ketat dikenakan, iaitu $\pm 0.25^{\circ}\text{C}$ dan $\pm 5\%$ (Walker, 2006). Menurut piawaian NCSL-RP14 (*Guide to Selecting Standards-Laboratory Environment*), pemilihan suhu dan kelembapan bergantung pada jenis kalibrasi dan peringkat ketepatan yang diingini seperti di dalam Jadual 1 dan 2. Oleh itu, nilai suhu dan kelembapan yang ingin dikekalkan untuk bilik instrumentasi perlu memenuhi syarat julat dan toleransi yang telah ditetapkan.

**Jadual 1: Suhu dan kelembapan nisbi makmal kalibrasi untuk penggunaan umum.
(Diadaptasikan dari Bucher (2004))**

Jenis Pengukuran	Suhu ($^{\circ}\text{C}$)	Kestabilan dan pengekalan ($^{\circ}\text{C}$ per jam)	Kelembapan Nisbi (%)
Dimensi, Optikal	20 ± 1	± 0.3	20 – 45
Elektrik, Elektronik	20 ± 2	± 2.0	20 – 60
Fizikal, Mekanikal	20 ± 2	± 2.0	20 – 60

**Jadual 2: Suhu dan kelembapan nisbi makmal kalibrasi untuk ketepatan tinggi.
(Diadaptasikan dari Bucher (2004))**

Jenis Pengukuran	Suhu ($^{\circ}\text{C}$)	Kestabilan dan pengekalan ($^{\circ}\text{C}$ per jam)	Kelembapan Nisbi (%)
Dimensi, Optikal	20 ± 0.3	± 0.1	20 – 45
Elektrik, Elektronik	20 ± 1.0	± 1.0	35 – 55
Fizikal, Mekanikal	20 ± 1.5	± 1.5	35 – 55

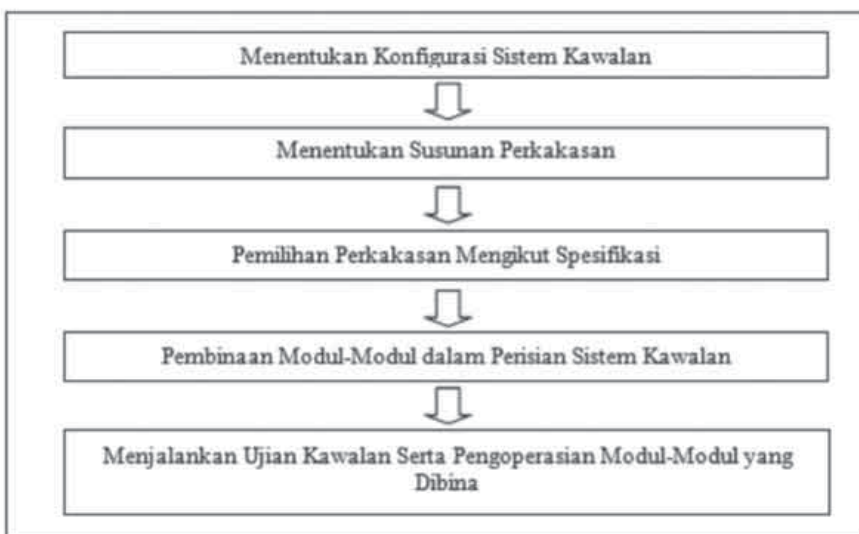
3. METODOLOGI

Sistem kawalan yang dibangunkan adalah terdiri daripada terdiri daripada gabungan perkakasan (*hardware*) dan perisian (*software*) yang memerlukan panduan terperinci. Kaedah yang akan digunakan adalah seperti di Rajah 1.

3.1 Konfigurasi Sistem Kawalan Suhu Dan Kelembapan

Teknik kawalan suhu dan kelembapan di dalam kajian ini menggunakan teknik Buka-Tutup atau lebih dikenali sebagai Kawalan *Bang-Bang* (*Bang-Bang Controller*) (Pang & Mesbah, 1998). Kawalan PID (*proportional-integral-derivative*) tidak dapat dilakukan untuk sistem ini kerana penghawa dingin dan penyahlembap hanya mampu dikawal secara tutup dan buka sahaja. Namun,

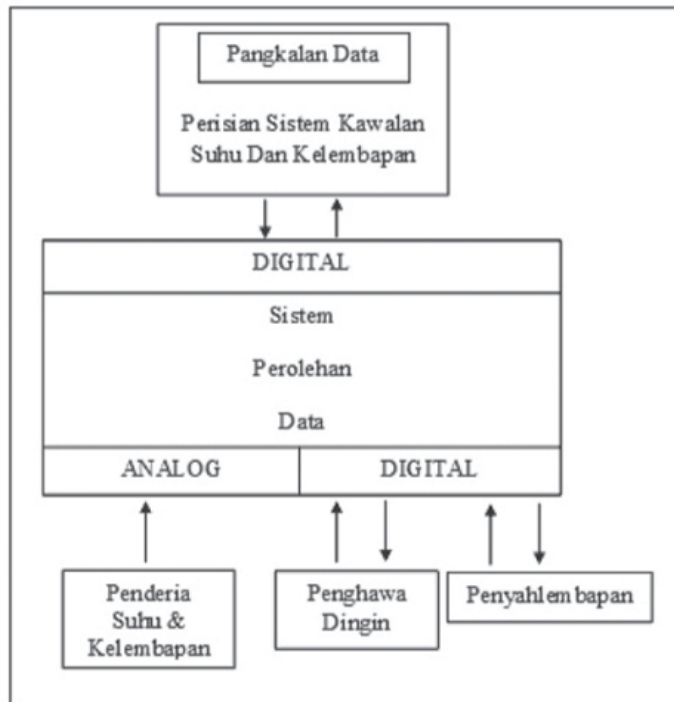
kawalan Buka-Tutup boleh digunakan untuk mengawal suhu dan kelembapan bilik jika konfigurasi sistem disusun dan spesifikasi perkakasan dipilih dengan betul.



Rajah 1: Kaedah merekabentuk sistem kawalan suhu dan kelembapan.

Untuk mengawal suhu dan kelembapan nisbi bilik, penghawa dingin dan penyahlembap akan dibuka dan ditutup mengikut arahan yang diberikan oleh di dalam sistem kawalan suhu dan kelembapan. Arahan ini berdasarkan kepada bacaan purata semasa dan nilai yang dikendaki yang dimasukkan oleh pengguna. Untuk mengelakkan suhu dan kelembapan nisbi melebihi nilai yang dikehendaki dan berada dalam julat yang ditetapkan, sebaik sahaja suhu purata dan kelembapan melebihi atau kurang daripada nilai yang dikehendaki, arahan akan segera diberikan diberikan oleh sistem ini kepada penghawa dingin dan penyahlembap agar suhu dan kelembapan dikawal.

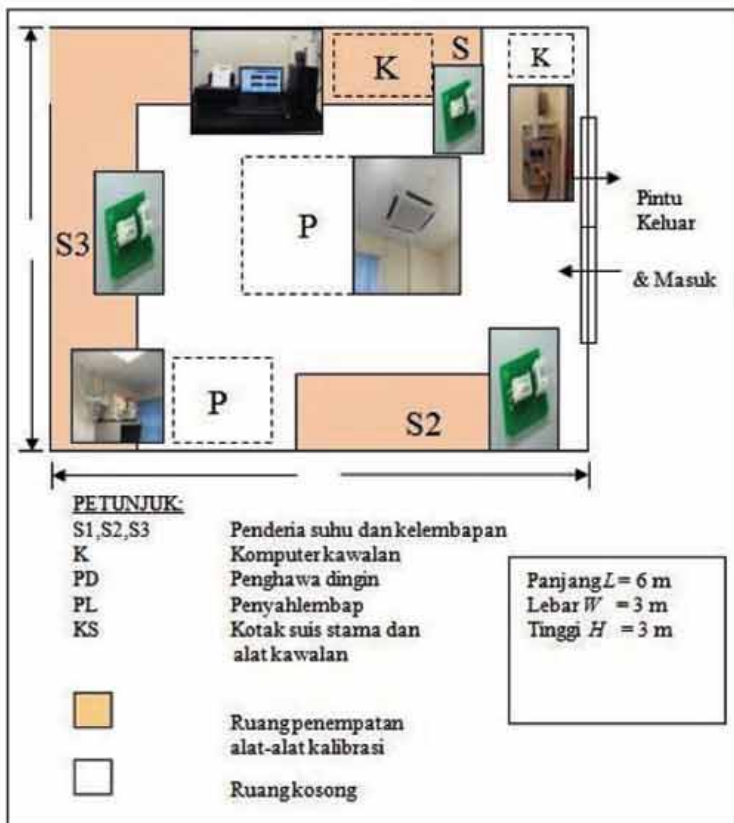
Sistem kawalan suhu dan kelembapan beroperasi seperti di dalam Rajah 2. Konfigurasi sistem akan memberitahu pengguna bagaimana sesuatu sistem kawalan berfungsi. Bagi rekabentuk di dalam kajian ini, penderia akan menentukan suhu dan kelembapan semasa. Kemudian, isyarat dalam bentuk voltan akan dihantar ke sistem perolehan data untuk ditukar ke isyarat digital. Perisian akan mentafsir isyarat digital dan menyimpan data dalam pangkalan data. Berdasarkan isyarat yang dihantar, perisian akan menghantar isyarat tindakan kawalan ke penghawa dingin dan penyahlembap. Proses kawalan boleh ditukar kepada kawalan dengan perisian, kawalan secara sendiri (*manual*) atau kawalan automatik (*automatic*) dengan menggunakan kekotak suis utama.



Rajah 2: Konfigurasi sistem kawalan suhu dan kelembapan.

3.2 Penentuan Susunan Perkakasan di dalam Makmal Pengukuran Jitu STRIDE

Apabila konfigurasi sistem telah diketahui, kedudukan perkakasan seperti penyahlembap, penghawa dingin dan penderia ditentukan. Perkakasan akan disusun berdasarkan kedudukan yang paling strategik di dalam meningkatkan prestasi kawalan serta berdasarkan fungsi perkakasan dalam sistem kawalan. Penderia yang berfungsi dalam menyukat suhu dan kelembapan nisbi akan diletak pada tiga lokasi di dalam bilik ujikaji bagi mendapatkan bacaan purata, manakala penghawa dingin akan diletakkan di tengah makmal untuk menyeragamkan proses penyejukkan. Penyahlembap juga perlu diletakkan di bahagian tengah ruang kawalan bagi kawalan yang optimum tetapi tidak dapat dilaksanakan atas sebab keadaan struktur asal makmal ini tidak mengizinkan alat penyahlembap ini diletakkan pada kedudukan tengah. Gambarajah skematik dan peralatan yang digunakan adalah seperti di dalam Rajah 3.



Rajah 3: Gambarajah skematik ruang kajian, kotak suis utama, alat kawalan penghawa dingin dan alat kawalan penyahlembap di dalam Makmal Pengukuran Jitu STRIDE.

3.3 Pengujian Bagi Keberkesanan Sistem Yang Dibangunkan

Terdapat tiga ujian telah dilaksanakan bagi membuktikan bahawa sistem ini dapat mengawal kelembapan dan suhu dengan baik. Ujian yang digunakan adalah untuk perbandingan kestabilan nilai suhu dan kelembapan tanpa menggunakan sistem kawalan suhu dan kelembapan, dan kestabilan nilai suhu dan kelembapan sekiranya menggunakan sistem kawalan suhu dan kelembapan yang dibangunkan. Sistem kawalan suhu dan kelembapan yang dibina mempunyai aplikasi penyelesaian ralat, sebagai contoh pada suhu 20°C , ralat $\pm 2^\circ\text{C}$ diaktifkan bagi memberi fleksibiliti kepada sistem penghawa dingin agar ia boleh menyesuaikan diri dengan keadaan suhu persekitaran.

Ujian A: Menguji Kawalan Suhu oleh Penghawa Dingin Tanpa Sistem Kawalan

Seperti yang diketahui, penghawa dingin telah dibina dengan sistem kawalan suhunya sendiri. Namun, keberkesanannya dalam mengawal suhu bilik pada suhu yang ditetapkan masih tidak diketahui. Oleh itu, ujian bertujuan untuk melihat kawalan suhu yang dibina dalam penghawa dingin itu sendiri tanpa menggunakan sistem kawalan. Prosedur ujian adalah seperti berikut:

- a. Tetapkan suhu pada alat kawalan penghawa dingin pada 20°C .
- b. Mulakan sistem kawalan hanya menggunakan pilihan kawalan kelembapan sahaja yang ditetapkan pada $55 \pm 5\%$ dengan pilihan kawalan suhu pada sistem kawalan suhu dan kelembapan yang dibina dimatikan.
- c. Lakukan ujian selama 30 minit.
- d. Selepas 30 minit, ulang langkah di atas dengan menetapkan suhu pada 18°C .
- e. Apabila sistem telah stabil, buka pintu dan tingkap selama 15 minit dan tutup selepas 15 minit (ujian gangguan kepada kestabilan sistem).
- f. Biarkan sistem selama 30 minit.

Ujian B: Menguji Kawalan Kelembapan oleh Penyahlembap Tanpa Sistem Kawalan

Ujian ini adalah sama seperti Ujian A, di mana ujian ini dilakukan untuk menguji sistem kawalan yang terbina dalam penyahlembap. Prosedur ujian adalah seperti berikut:

- a. Tetapkan kelembapan nisbi pada alat kawalan penyahlembap pada 55% .
- b. Mulakan sistem kawalan hanya menggunakan pilihan kawalan suhu yang ditetapkan pada $20 \pm 2^{\circ}\text{C}$ sahaja dengan pilihan kawalan kelembapan dimatikan.
- c. Lakukan ujian selama 30 minit.
- d. Selepas 30 minit, ulang langkah di atas dengan menetapkan kelembapan nisbi pada 45% .
- e. Apabila sistem telah stabil, buka pintu dan tingkap selama 15 minit dan tutup selepas 15 minit (ujian gangguan kepada kestabilan sistem).
- f. Biarkan selama 30 minit.

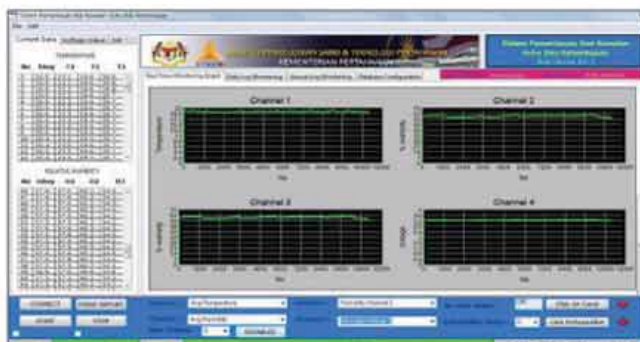
Ujian C: Menguji Kawalan Suhu dan Kelembapan dengan Sistem Kawalan

Ujian ini bertujuan untuk menguji keberkesanan sistem kawalan suhu dan kelembapan yang dibangunkan untuk dibandingkan dengan Ujian A dan B. Prosedur ujian adalah seperti berikut:

- Tetapkan suhu dan kelembapan nisbi pada perisian sistem kawalan suhu dan kelembapan masing-masing pada 20 ± 2 °C dan 58 ± 2 %. Nilai kelembapan yang tinggi dipilih bagi mengelakkan alat penyahlembap berada dalam keadaan buka terlalu lama.
- Mulakan sistem kawalan.
- Apabila suhu dan kelembapan telah stabil, buka pintu dan tingkap selama 15 minit dan tutup selepas 15 minit.
- Biarkan selama 15 minit.

4. KEPUTUSAN DAN KESIMPULAN

Modul-modul yang dibina merupakan keperluan yang perlu ada di dalam sistem kawalan suhu dan kelembapan. Dengan adanya modul-modul ini, sebuah sistem kawalan yang lengkap telah dibina, iaitu proses kawalan, menyimpan, mendapat dan mengekspot data, persemaahan data dalam bentuk grafik, dan menghasilkan laporan kawalan. Antaramuka perisian sistem kawalan suhu dan kelembapan adalah seperti di dalam Rajah 4-6.



Rajah 4: Paparan grafik dengan empat graf bagi setiap bacaan alat penderia dan bacaan purata



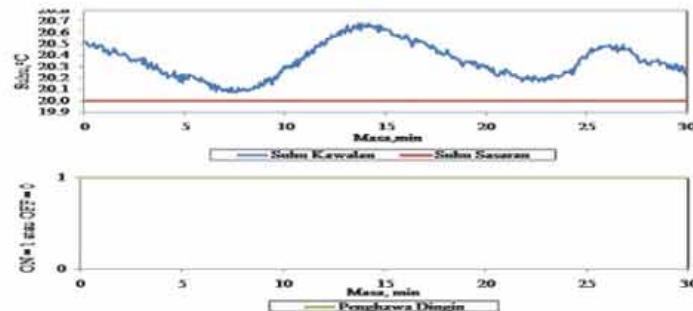
Rajah 5: Paparan grafik perolehan data.



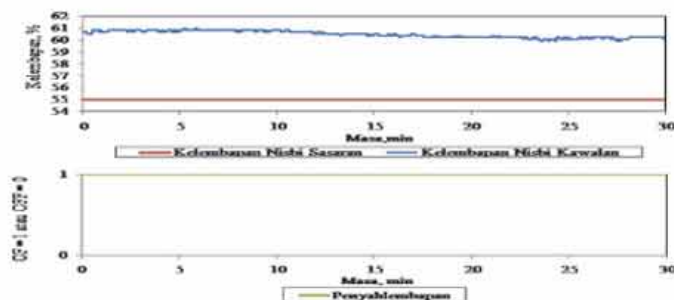
Rajah 6: Paparan grafik cetakan laporan kawalan.

4.1 Keputusan Ujian A

Ujian A adalah bertujuan untuk menguji keberkesanan kawalan suhu yang terbina di dalam penghawa dingin itu sendiri. Rajah 7 dan 8 merupakan hasil keputusan ujian apabila suhu ditetapkan pada 20°C . Selepas 30 minit, didapati bahawa suhu masih tidak dapat mencapai suhu sasaran. Ini menunjukkan bahawa sistem kawalan yang terbina di dalam penghawa dingin kurang berkesan di dalam mengawal suhu bilik. Hal ini adalah kerana sistem penderia termistor pada penghawa dingin hanya menyukat suhu bebuli kering udara yang masuk ke dalam penghawa dingin sahaja. Suhu udara yang masuk ke dalam penghawa dingin adalah dipengaruhi oleh udara sejuk di persekitaran. Oleh itu, udara kering akan mengalami perubahan suhu apabila mengalir menghampiri penghawa dingin. Persekutuan berdekatan penghawa dingin adalah lebih sejuk berbanding suhu yang berjauhan. Mengikut graf yang di peroleh, alat penghawa dingin ini tidak dapat mencapai suhu 20°C yang ditetapkan, ini menunjukkan alat penghawa dingin tidak memberikan bacaan tepat seperti yang dikehendaki oleh pengguna.



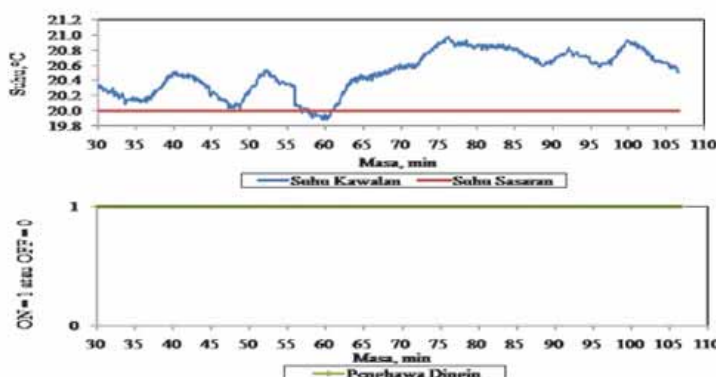
Rajah 7: Graf suhu bagi Ujian A dengan suhu ditetapkan pada 20 °C.



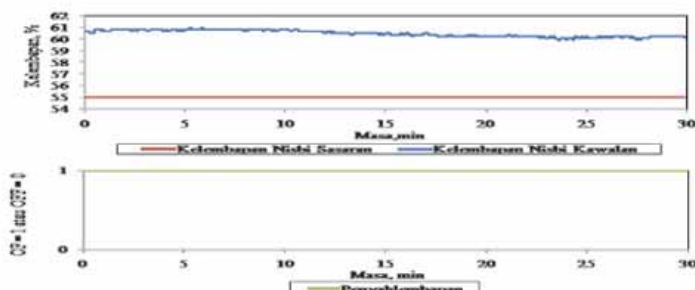
Rajah 8: Graf kelembapan nisbi bagi Ujian A dengan suhu ditetapkan pada 20 °C.

Untuk kawalan kelembapan, didapati yang nilai kelembapan nisbi menurun dengan pertambahan masa, dan pada minit yang ke-23, kelembapan nisbi mencapai nilai maksimum kelembapan nisbi yang dikehendaki, iaitu 60 % ($55 \pm 5\%$). Bagi ujian ini, kelembapan nisbi bilik dikawal dengan perisian, didapati graf kelembapan semakin menurun untuk mencapai sasaran nilai kelembapan pada 55 %.

Untuk ketetapan suhu pada 18 °C (Rajah 9 dan 10), ujian adalah bertujuan untuk memastikan keupayaan sistem penghawa dingin sedia ada apabila suhu ditetapkan lebih rendah dari 20 °C. Selain dari itu, dalam ujikaji ini juga, gangguan turut dikenakan pada sistem penghawa dingin sedia ada untuk mengenalpasti keupayaannya untuk mengekalkan suhu sasaran pada masa gangguan dikenakan. Oleh itu, perilaku ini perlu dikaji samada suhu dapat dikawal selepas gangguan dikenakan.



Rajah 9: Graf suhu bagi Ujian A dengan suhu ditetapkan pada 18 °C.



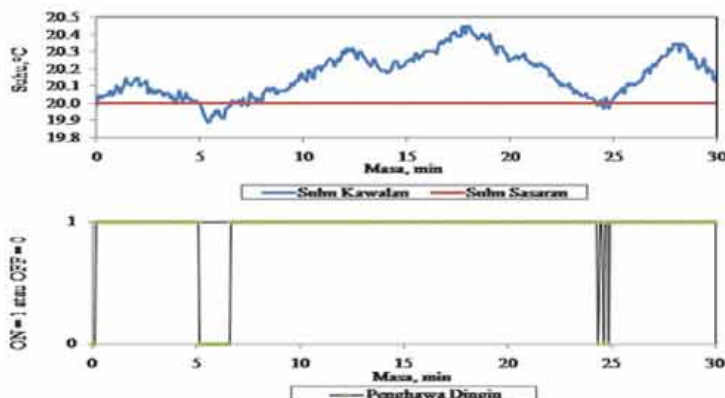
Rajah 10: Graf kelembapan nisbi bagi Ujian A dengan suhu ditetapkan pada 18°C.

Apabila suhu ditetapkan pada 18 °C, suhu sasaran dapat dicapai pada minit yang ke-57. Tempoh masa diambil untuk mencapai suhu sasaran adalah 27 minit. Suhu berayun pada suhu maksimum 20.5 °C dari minit ke-37 hingga ke-54. Selepas 15 minit gangguan dikenakan pada sistem, didapati yang suhu tidak dapat dikembalikan kepada suhu sasaran. Suhu berayun pada suhu ayunan minimum 20.6 °C walaupun setelah 30 minit sistem dibiarkan. Ini adalah kerana penghawa dingin mengesan suhu berhampirannya sahaja tetapi tidak mengesan purata suhu bilik.

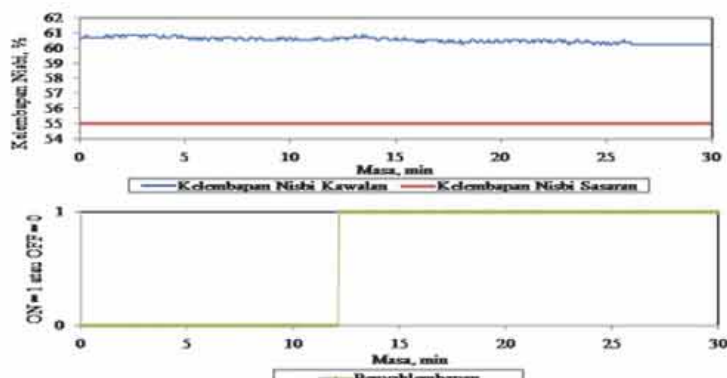
4.2 Keputusan Ujian B

Ujian B adalah bertujuan untuk menguji keberkesanan tindakbalas sistem kawalan terbina bagi penyahlembap tanpa dibantu oleh sistem kawalan suhu dan kelembapan yang dibina. Di dalam ujian pertama, kawalan kelembapan nisbi pada alat penyahlembap telah ditetapkan pada 55 % (Rajah 11 dan 12). Walaupun kelembapan nisbi bilik telah melebihi paras maksimum, penyahlembap masih tidak bertindak sehingga minit yang ke-12. Hal ini menunjukkan yang sistem kawalan penderia terbina lambat dalam menentukan nilai kelembapan nisbi semasa. Nilai

suhu telah ditetapkan menggunakan sistem kawalan suhu dan kelembapan yang dibangunkan tidak mempunyai nilai ayunan maksimum yang besar, iaitu 20.3°C . Ini menunjukkan yang suhu dapat dikawal dengan baik sekiranya menggunakan sistem kawalan suhu dan kelembapan yang dibangunkan.



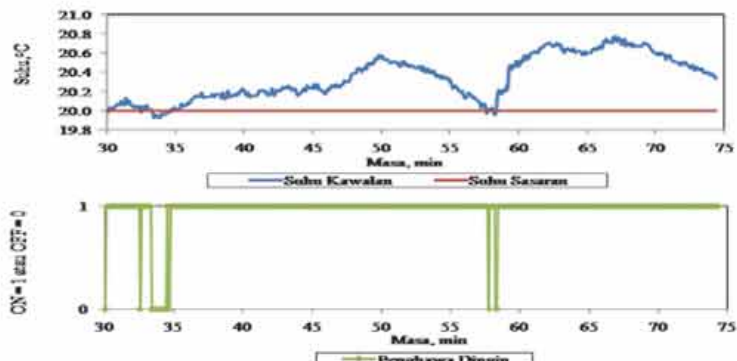
Rajah 11: Graf suhu bagi Ujian B dengan kelembapan nisbi ditetapkan pada 55%.



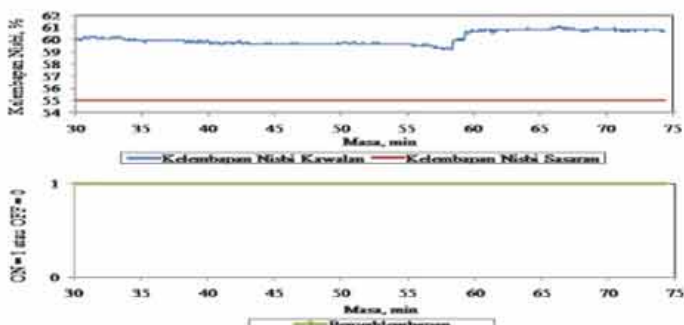
Rajah 12: Graf kelembapan nisbi bagi Ujian B dengan kelembapan nisbi ditetapkan pada 55%.

Untuk ujian kedua, iaitu kelembapan nisbi ditetapkan pada 45% menggunakan alat penyahlembap sedia ada, keputusan yang diperoleh menunjukkan alat penyahlembap tersebut lambat memberi tindak balas mengikut ketetapan yang dipilih oleh pengguna. Ini menunjukkan bahawa alat penyahlembap yang sedia ada perlu diubahsuai agar ia dapat bertindak balas dengan lebih cepat apabila ketetapan nilai kelembapan diubah oleh pengguna. Di dalam ujian ini juga, gangguan dikenakan pada minit ke-35, nilai kelembapan menurun dengan pertambahan masa

disebabkan oleh udara yang lebih kering masuk ke dalam bilik ujian dan menyebabkan bacaan kelembapan menurun. Didapati bahawa nilai suhu masih dapat dikawal dengan baik oleh sistem sistem kawalan suhu dan kelembapan yang dibangunkan tetapi nilai kelembapan tidak dikawal dengan baik oleh alat penyahlembap sedia ada, kerana alat pengesan pada alat penyahlembap hanya mengesan kelembapan pada alat tersebut sahaja dan tidak mengambil nilai kelembapan purata pada bilik tersebut.



Rajah 13: Graf suhu bagi Ujian B dengan kelembapan nisbi ditetapkan pada 45 %.

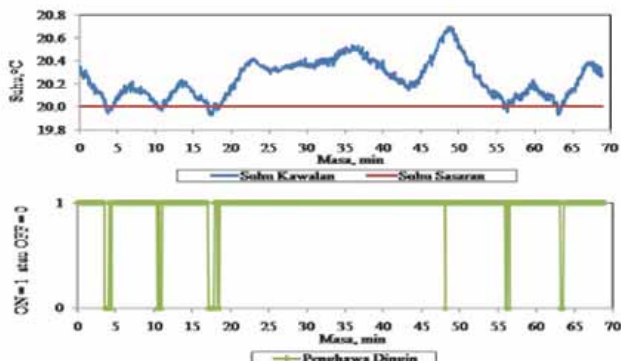


Rajah 14: Graf kelembapan nisbi bagi Ujian B dengan kelembapan nisbi ditetapkan pada 45 %.

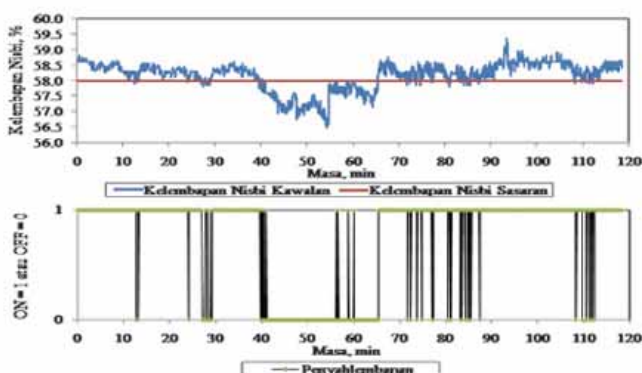
4.3 Keputusan Ujian C

Bagi Ujian C pula, seperti di dalam Rajah 15 dan 16, suhu dan kelembapan bilik dikawal dengan menggunakan sistem kawalan suhu dan kelembapan. Keputusan yang diperolehi menunjukkan keputusan yang positif, di mana suhu purata bilik mampu mencapai suhu sasaran yang dikendaki. Suhu sasaran dapat dicapai pada minit yang ke-4 selepas sistem kawalan dimulakan. Profil suhu selepas minit ke-4 hingga ke minit yang ke-17 menunjukkan ayunan suhu maksimum pada 20.2°C . Jika kawalan dibiarkan dengan lebih lama, nilai ambang boleh dikurangkan sehingga 0.1°C dari suhu sasaran. Gangguan diperkenalkan pada minit ke-18. Suhu

bilik menaik dengan mendadak sehingga pada minit ke-48. Nilai kadar kenaikan suhu adalah kurang berbanding kadar kenaikan suhu pada Ujian A. Pada minit ke-57, suhu sasaran dapat dicapai dan sistem berayun dengan seragam. Bagi ujian kelembapan pula, nilai kelembapan yang diperoleh adalah dalam julat yang dijangka iaitu kurang dari 60%, ini menunjukkan sistem yang di bina mampu memberikan hasil yang di inginkan.



Rajah 15: Graf suhu bagi Ujian C.



Graf 16: Graf kelembapan nisbi bagi suhu $20^\circ \pm 2^\circ\text{C}$ dan kelembapan nisbi $58 \pm 2\%$.

4.4 Analisis Sistem Kawalan Suhu dan Kelembapan

Berdasarkan keputusan di atas, dapat disimpulkan bagi kesemua ujian yang dilakukan, apabila gangguan dikenakan pada sistem, kelembapan nisbi akan menurun dan sebaliknya suhu akan meningkat. Tanpa penggunaan perisian sistem kawalan suhu dan kelembapan, didapati suhu terus berayun dengan ambang yang besar selepas 30 minit sistem dibiarkan, manakala kelembapan nisbi juga melebihi daripada nilai maksimum yang dibenarkan. Ini menunjukkan bahawa kawalan melalui perisian sistem kawalan suhu dan kelembapan adalah lebih baik daripada kawalan terbina dalam penghawa dingin dan penyahlembap. Berikut merupakan ringkasan analisis kawalan melalui perisian:

- a. Suhu sasaran dapat dicapai dengan pantas dan suhu berayun pada julat yang telah ditetapkan, iaitu kurang daripada 1°C .
- b. Suhu dan kelembapan nisbi masing-masing dapat dikekalkan pada julat yang telah ditetapkan iaitu $20 \pm 2^{\circ}\text{C}$ dan $55 \pm 5\%$.
- c. Suhu dan kelembapan dapat dikembalikan ke dalam julat yang dibenarkan selepas gangguan dikenakan pada sistem.

Ketetapan nilai kelembapan nisbi pada nilai kestabilan 55% tidak digalakkan, ini kerana untuk mengekalkan nilai kelembapan yang rendah, penyahlembap akan berada dalam keadaan terbuka sepanjang masa tanpa berhenti. Jangka hayat penyahlembap akan berkurang dan mudah rosak. Oleh itu, nilai kelembapan nisbi yang perlu ditetapkan perlu ditingkatkan. Nilai yang dicadangkan adalah 58 % iaitu separuh daripada nilai julat yang telah ditetapkan. Ini akan melanjutkan jangka hayat alat penyahlembap.

5. KESIMPULAN

Sistem kawalan suhu dan kelembapan yang dibina di dalam kertas kerja ini boleh digunakan di ruang jenis lain yang sama saiz. Namun, sistem ini juga boleh digunakan pada ruang yang bersaiz lebih besar dengan menggantikan penghawa dingin dan penyahlembap pada kapasiti yang bersesuaian dengan keperluan.

Untuk kajian lanjutan, kawalan buka-tutup boleh diperbaiki dengan menggunakan kawalan hibrid dengan gabungan kawalan secara prediktif di mana suhu dan kelembapan pada masa depan dapat ditentukan. Dengan ini, penyahlembap dan penghawa dingin ditutup dan dibuka berdasarkan pengiraan masa prediktif. Oleh itu, masalah pada kekerapan peralatan dibuka dan ditutup dapat diselesaikan.

RUJUKAN

- Angevine, E.N. & Fair, J.S. (2001). HVAC systems. In Turner, W.C. & Doty, S. (Eds.), *Energy Management Handbook*. The Fairmont Press, Lilburn, Georgia.
- Bucher, J.L. (2004). *The Metrology Handbook*. American Society of Qualities (ASQ), USA.
- I-hai Lin, P. & Broberg, H.L. (2002). Internet-Based Monitoring and Controls for HVAC Applications. *IEEE Ind. Appl. Mag.*, **8**: 49-54.
- Walker, R. (2006). Temperature and humidity calibration system. *2006 NCSL International Workshop and Symposium*, 3-5 Ogos 2006, Orlando, Florida.
- Pang, G.K.H. & Mesbah, S.A. (1998). Design of Bang-bang controller based on a fuzzy-neuro approach: Application to a heating system. *J. Intell. Robot. Syst.*, **22**: 51 - 85
- Cengel, Y.A. & Boles, M.A.. (2007). *Thermodynamics: An Engineering Approach*. McGraw-Hill Higher Education, Boston.